Fault Estimation Schemes of Wireless Networked Control Systems for Real-Time Industrial Applications

Von der Fakultät für Ingenieurwissenschaften
Abteilung Elektrotechnik und Informationstechnik

der

Universität Duisburg-Essen

zur Erlangung des akademischen Grades

Doktors der Ingenieurwissenschaften (Dr.-Ing.)

genehmigte Dissertation

von

Ying Wang

aus

Zhangjiakou, VR China

1. Gutachter: Prof. Dr.-Ing. Steven X. Ding
2. Gutachter: Prof. Dr. Zidong Wang

Tag der mündlichen Prüfung: 27.3.2014

Acknowledgements

This thesis was written while the author was with the Institute for Automatic Control and Complex Systems (AKS) in the Faculty of Engineering at the University of Duisburg-Essen, Germany. I would like to give the most sincere thanks to my respectful mentor Prof. Dr.-Ing. Steven X. Ding, the head of the institute, for his constant guidance, understanding and patience in preparation of this thesis. I could not imagine having a better advisor and mentor for my Ph.D study. I am also grateful to Prof. Zidong Wang, my second supervisor, for his valuable suggestions about my dissertation and great support for my doctoral examination. His words inspired me to keep reflecting on myself.

Many thanks to my wonderful colleagues of AKS, who always offered great help during the days in Duisburg. Special thanks to Prof. Dr. Bo Shen for his valuable help and discussion. I consider it a great honor to work with him. My sincere appreciation must also go to Prof. Dr. Hongli Dong and Dr. -Ing. Birgit Kppen-Seliger for their helpful suggestions of this work. I have extensively worked with Prof. Dr. Bo Shen, M. Sc. Dongmei Xu and Dr. -Ing. Ionut Chihaia. I would like to acknowledge the help from them for their great supports. My special thanks go to M. Sc. Dongmei Xu for the sleepless nights working together before deadlines and the encouragement. I would also like to thank the support of China Scholarship Council (CSC) gratefully during my study.

Finally, I would like to express my gratitude to my family, especially to my parents and husband, for their constant patience and support.

Duisburg, 1 April 2014
Ying Wang

II

Contents

List of Figures

Notation and symbols

Abbreviations

Abbreviation	Expansion
FD	fault diagnosis
FE	fault estimation
FTC	fault tolerant control
LTI	linear time invariant
LP	linear periodic
NCSs	networked control systems
W-NCSs	wireless networked control systems
QoS	quality of service
QoC	quality of control
MCU	main control unit
CS	control station
CL	control loop
MAC	medium access control
TDMA	time division multiple access
CSMA/CA	carrier sense multiple access/collision avoidance
CSMA/CD	carrier sense multiple access/collision detection
W-LANs	wireless local area networks
LMIs	linear matrix inequalities
ACK	acknowledge
GCD	greatest common divisor
LCM	least common multiple
RTS/CTS	request to send/clear to send
GUI	graphic user interface
PI	proportional integral
EDF	earliest deadline first
LSTF	least slack time first
SP	shortest path
PF	particle filter
PCA	principle component analysis

MJSs	Markov jumping systems
CW	contention window
OPP	optimal pointer placement

Mathematical symbols

Symbol	Description
$\| \ \|$	2-norm
$\| \ \|_\infty$	∞-norm
$\hat{\mathbf{a}}$	estimate of $\mathbf{a}$
$\tilde{\mathbf{a}}$	estimate error of $\mathbf{a}$
$\bar{\mathbf{a}}$	$\mathbf{a}$ in the integrated model
$\mathbf{a}_k$	$\mathbf{a}$ in Krein space
$\mathbf{A}^T$	transpose of $\mathbf{A}$
$\mathbf{A}^{-1}$	inverse of $\mathbf{A}$
$\mathcal{R}$	set of real numbers
$\mathcal{R}^m$	set of m-dimensional real vectors
$\mathcal{R}^{l\times m}$	set of $l \times m$ dimensional real matrices
$\mathbf{I}_m$	$m \times m$ identity matrix
$\mathbf{O}_{l\times m}$	$l \times m$ zero matrix
$\in$	belong to
max(min)	maximum(minimum)
sup(inf)	supremum(infimum)

Control theoretical symbols

Symbol	Description
N	number of sub-systems
i	sub-system indicator
T_{period}	main period of periodic system
$T_{cyc,i}$	sampling period of i-th sub-system
T_{slot}	interval of one time slot
k	discrete main period sample of periodic system
j	discrete time segment in one main period
ς_j	time instant of j-th segment in one main period
θ	number of segments in one main period
I_{ς_j}	set of updated sub-systems at ς_j
$\mathbf{A}$	system matrix of plant model
$\mathbf{B}$	input matrix of plant model

$\mathbf{C}$	output matrix of plant model
$\mathbf{B}_d$	disturbance matrix of plant model
$\mathbf{E}_f$	actuator fault distribution matrix of plant model
$\mathbf{F}_f$	sensor fault distribution matrix of plant model
$\mathbf{A}_s$	system matrix of scheduler model
$\mathbf{B}_{sy}$	measurement input matrix of scheduler model
$\mathbf{B}_{su}$	command input matrix of scheduler model
$\mathbf{C}_{sy}$	measurement output matrix of scheduler model
$\mathbf{D}_{sy}$	measurement feed-through matrix of scheduler model
$\mathbf{C}_{su}$	command output matrix of scheduler model
$\mathbf{D}_{su}$	command feed-through matrix of scheduler model
$\mathbf{L}$	observer gain
$\mathbf{V}$	post-filter matrix
n_i	sub-system order
q_i	number of inputs for i-th sub-system
m_i	number of outputs for i-th sub-system
n	plant model order
$q_s(j)$	number of inputs for plant model
$m(j)$	number of outputs for plant model
l	number of driving disturbances for plant model
s	number of faults for plant model
n_s	scheduler model order
q	number of command inputs for scheduler model
$m_s(j)$	number of measurement outputs for scheduler model
$\mathbf{x}$	state variable vector of plant model
$\mathbf{u}_s$	input signal vector of plant model
$\mathbf{y}$	output signal vector
$\mathbf{d}$	unknown driving disturbance vector
$\mathbf{v}$	unknown measurement disturbance vector
$\mathbf{f}$	fault signal vector
$\mathbf{x}_s$	state variable vector of scheduler model
$\mathbf{u}$	command input signal vector of scheduler model
$\mathbf{y}$	measurement input signal vector of scheduler model
$\mathbf{u}_s$	command output signal vector of scheduler model
$\mathbf{y}_s$	measurement output signal vector of scheduler model
$\mathbf{r}$	residual signal vector
$\mathbf{e}$	error signal vector
$\mathbf{G}(z)$	transfer function of discrete-time system

$(\mathbf{A}, \mathbf{B}, \mathbf{C}, \mathbf{D})$ shorthand for $\mathbf{D} + \mathbf{C}(z\mathbf{I} - \mathbf{A})^{-1}\mathbf{B}$

Symbols for three-tank system

Symbol	Description	Unit
S	cross section area of tanks	$[\mathrm{m}^2]$
s_n	cross section area of pipes	$[\mathrm{m}^2]$
u_{1max}	maximal flow rate of pump 1	$[\mathrm{m}^3/\mathrm{s}]$
u_{2max}	maximal flow rate of pump 2	$[\mathrm{m}^3/\mathrm{s}]$
a_1	outflow coefficient of tank 1	$[-]$
a_2	outflow coefficient of tank 2	$[-]$
a_3	outflow coefficient of tank 3	$[-]$
K_p	proportional gain of PI controller	$[-]$
K_i	integral gain of PI controller	$[-]$

Abstract

With the rapid growth of microelectronics, information and communication technologies, much attention has been paid on the research of wireless networked control systems (W-NCSs). The development of W-NCSs raises new challenges in fault estimation (FE) technology regarding to the imperfect data transmission, such as transmission delay, packet loss, jitter and so on. To ensure the system safety and reliability, an effective FE approach over networks is of prime importance to be developed.

On the other hand, aiming for the applications on real-time industrial automation, the specific characteristics of network should be properly considered. Since the transmission tasks of measurements and control commands are normally deterministic over a period of time, a deterministic transmission mechanism and the relevant FE scheme should be proposed. Motivated by the widespread popularity of centralized and decentralized structures for industrial processes, development of both centralized and decentralized FE schemes for W-NCSs, which can be applied on industrial automation, is the primary objective of this thesis.

This thesis is first dedicated to the modeling of communication and process. For the communication modeling, time division multiple access (TDMA) based medium access control (MAC) protocol is modified to guarantee the real-time performance. The process model is built considering multirate sampling based on the hierarchical structure of W-NCSs. By observing the uncertainty of networks and effects of faults, a linear periodic (LP) system model, which is the integration of communication model and process model, is presented as a basis for the later developments.

The further study focuses on the development of FE schemes for both centralized and decentralized W-NCSs. To reach an enhanced robustness against unknown disturbance and initial state estimate error, the centralized FE approach is proposed with the help of stochastic model in Krein space. For decentralized FE, the algorithm is implemented by every sub-system, and the coupling relations between sub-systems should be properly considered. Based on it, the FE approaches are presented with two kinds of residual

signals, i.e., non-shared residuals and shared residuals, respectively.

To illustrate the effectiveness of the derived FE approaches, an industrial platform WiNC integrated with three-tank system is utilized in this thesis. The FE algorithms have been verified for three data transmission cases, i.e., sampling-based, delay and packet loss, so that the robustness against imperfect communication is demonstrated. Moreover, the performances of sensor and actuator FE have also been tested well on WiNC platform.

Chapter 1

Introduction

This chapter briefly introduces the motivation and objective of this thesis. The outline and contributions of the thesis will also be presented at the end of this chapter.

1.1 Motivation

The thesis deals with the fault estimation (FE) of NCSs for real-time industrial application, where FE is regarded as a branch of fault diagnosis (FD). The motivation of this thesis will be addressed from the views of the importance of FD, especially FE, for networked control systems (NCSs) and its application on industrial field, the necessity of exploring FE approach on centralized and decentralized systems, and the advantages of developing the network protocol to fit for real-time industrial applications. Those points will be addressed in this section consecutively.

1.1.1 FE of NCSs and its industry application

With the development of microelectronics, information and communication technologies, much attention has been paid on the research of NCSs in recent decades. NCSs are feedback control systems, where the control loops are connected via network [3]. Compared with conventional control systems with point-to-point connections, the data transmission uncertainties caused by network properties, such as transmission delay, packet loss rate, jitter, bit error rate and so on, can degrade the system performance. So the design and performance characteristics of the data transmission network, which are expressed in terms of quality of service (QoS) parameters, should be defined in advance to guarantee the network ability of delivering predictable results.

It's still a new challenge to deal with the effects of network on system performance with the restriction of QoS. With the increasing complexity of NCSs, faults or abnormal changes of network components, e.g., actuators, sensors and controllers, may occur and result in economic loss, system damage or even catastrophic failures. This drives researchers to develop FD technique over network with the objectives of guaranteeing system safety and reliability.

Recently, rich research results on FD have been reported aiming at solving uncertainties caused by network-induced delay and other characteristics of network [54, 69, 71, 52, 57, 84]. Those fruitful theoretical results have been fully integrated into many industrial applications [87, 20, 74], e.g., power system [34, 83, 5], vehicle and transport control system [98, 78], process control [59]. A field of FD technology focuses on the research of FE and filtering, which extracts the needed information about the faults of interest from the residual signals [16, 75, 2, 91, 96]. However the applications on industrial control system based on FE technology is still rare.

The schematic description of model-based FE/filtering including residual generation is shown in Fig. 1.1, where a process model is running in parallel with process. The process model is developed based on the physical and mathematical knowledge of the process into the form of state-space equations, and is driven by the same input of physical process as well as the output. The model output is the estimate of the process output. The difference between the process output and its estimate is called residual, and this procedure is called residual generation. In fault-free cases, if the process model is perfect and there is no disturbance in the physical process, the residual should be zero; when fault and disturbance exist, the value of residual varies and it carries important messages about fault of interest, unknown disturbance and model uncertainties. Hence the residual generation is critical for the development of FE. Then the information of fault is extracted from the residual signals by means of a post-filtering of the residual. From the 70s, the observer-based and Kalman filter-based approaches for residual generator have been widely developed to estimate the process output [23], and some other approaches based on parity relation can be found in [33, 86]. In the last three decades, tremendous research results in the field of FD technology have been developed based on those approaches [26, 32, 47].

FE/filtering approach is considered as a branch of FD technology, and the academic research on it has attracted a surge of research interests [39, 59, 42, 18]. In [58], an fault filter has been designed over networks with bounded packet losses under the assumption that the packet loss process is arbitrary or Markovian. In [82], an auxiliary H_∞ filtering problem is figured out for a class of nonlinear NCSs, which are represented by a unified model including four kinds of imperfect measurements, i.e., access constraints, time

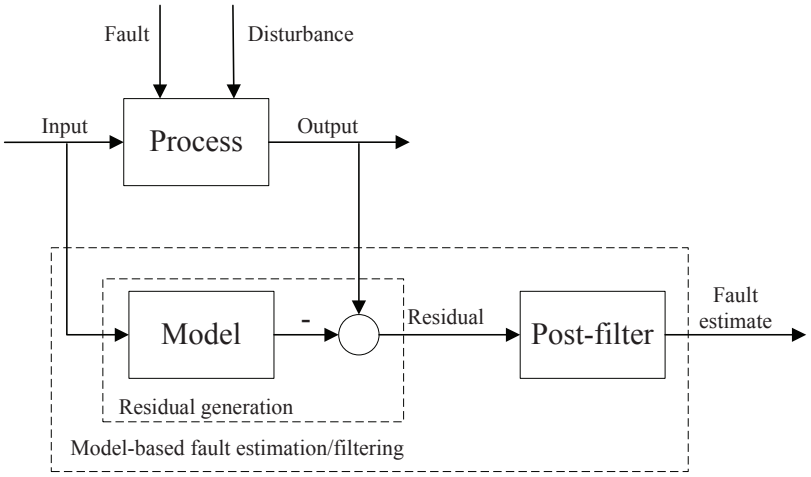

Figure 1.1: Schematic description of model-based fault estimation

delay, packet dropout and quantization. In [70], by introducing an index η_k, which describes the non-ideal QoS parameters, and supposing that the possibility of switching between different η_k is Markovian, NCSs, which are involved with η_k, are developed into the Markov jumping systems (MJSs), and an H_∞ observer-based fault filter is established in terms of linear matrix inequalities (LMIs). An FD filtering approach is put forward in [40] to deal with NCSs with random communication delay and stochastic packet losses.

Some FE schemes have already applied on industrial field, such as process control [59], power system [34, 83], aerospace area [94] and vehicle control system [36]. However, the development of industrial application for FE over network are still not so sufficient, and we are inspired to focus on this concern in this thesis.

Both in the research and industrial application domains, wireless network is regarded as a further-oriented trend in automatic control [11, 13]. Since the cabling and maintaining of wired industrial network are very time-consuming and expensive, and cables are frequent sources of failures due to the harsh environment in factory and may cause additional costs by production outage, the adoption of wireless NCSs (W-NCSs) can eliminate cable issues and also perform well in cases of mobility and equipment modification. The major efforts of W-NCSs in the industry automation are devoted to the development of the standards and protocols [46, 65, 48]. Due to the advantages of W-NCSs, wireless network will be regarded as the background of FE approach in this thesis.

1.1.2 FE of centralized and decentralized NCSs

The centralized and decentralized structures are both widely applied on the industrial automotive applications. Each structure has its good points. For example, the centralized form is beneficial to achieve a global optimization of system performance, while the decentralized form is superior at the system flexibility and robustness against severe faults. The choice of centralized or decentralized infrastructure is based on the requirements of application from the view of offering a good balance of flexibility, availability, reliability and cost. For example, when the system is complicated, and the costs of communication and computation are too high to meet the system real-time demand, decentralized solution will be a right choice; when the system has a high requirement on the reliability, it needs a greater autonomy of some key executive components to react quickly in the emergency case and keep the system safe, the decentralized structure should be chosen, since it supports multiple intelligent control units to implement urgent reactions; when the system asks for a global optimization, centralized infrastructure is thus preferred.

The concept of centralized NCSs is normally mentioned, when comparing with decentralized. The centralized NCSs mean that all the decision making is completed by an exclusive controller in the whole system, where the measurements and information of decision are transmitted over the network. The research achievements of FE technique summarized in the last subsection can also be applied for the centralized NCSs, where the control input and measurement output are fused data all over the system.

While in recent decades, with the fast development of industrial automation, especially for the real-time applications, the limitation of the plant-wide centralized control approach is more and more evident. First, since main control unit (MCU) needs all information over the whole plant, the cost of information communication could be very high and the network building is very complex. It makes the communication as a potential frequent source of failures and may cause additional expenses by production outage. Second, with the increasing dimensionality, the interaction or coupling between system units can be very complicated. It requires a very high computing capability of MCU and the computing delay may affect greatly the real-time performance. Third, the decentralized solutions is robust enough to operate in harsh environments, and the system stability condition can still be satisfied even in the case of one or more sub-systems malfunction. All these points lead to the research based on decentralized controller/observer structure. To be specific, the development of the FE approach on decentralized structure has attracted more and more attentions.

Unlike the design of centralized systems, one of the key challenges in the research of coordinated decentralized systems, also named interconnected decentralized systems is to deal with the couplings caused by the interconnections. Most of the works have been done from two respects. One is to relax the interconnection requirements by assuming the boundary of the interconnections. For example, the interconnections are assumed to be uniformly Lipschitz [97], unknown and bounded [21] and so on [73]. The other one is to approximate the unknown interconnections or the effects of interconnections by extracting the information of interest from residual signals. In [22], the interconnections are assumed to be unknown, whose effects on state estimation are approximately learned by recursive calculation with the information of the output of neighboring sub-systems. [61] estimates the unknown conjunction together with system state in one fused vector, and the decentralized filtering can be approached based on Kalman filter.

When considering the relevance between centralized and decentralized design issues, some concerns have been considered. One is to decompose and modeling the whole system into decentralized form. To partition the whole system reasonably into several sub-systems, a component analysis (PCA) based process decomposition principle is proposed in [35] and it has been proved that the PCA-based decomposition performs better that the topology-based plant decomposition. An overlapping decompositions of large-scale system is put forward in [22], and it can make more than one sub-observer estimate the fault based on a shared variable. In [1], the whole system is transformed into an equivalent distributed system, in which FE and control approaches are presented. While another concern is to consider the decentralized design issues dealing with the problems of centralized systems or the systems with centralized data [50, 49, 31, 60]. [49] deals with the decentralized implementation problem of the system with centralized controller, which can make the decentralized control performance close to the performance of centralized one. This kind of researches can be considered as the extension of design issues for centralized structure on the decentralized structure. While in some cases, the decentralized system model can be directly built based on the well acquainted knowledge about the physical system and the conjunctive relations, so local FE decision can be made based on the knowledge of local and coupled sub-systems.

Focusing on the FE and filtering problems for decentralized systems, [4] presented a reduced-order filter with the purpose of saving system computation resources. An hierarchical filter is developed based on the measurement subspace of each sub-system in order to provide the optimal performance and saved calculation time [64]. In [14], the decentralized particle filter (PF) is recreated by decomposing the state space, and it has been approved that the

new decentralized PF can run faster than the regular PF under the requirement of same performance criterion. In [88], a decentralized FE strategy is proposed using a sliding mode observer, which can further be exploited for the structure with uncertainty.

The application research of centralized and decentralized FE/filtering on the industrial automation are still lacking. In [62] the decentralized FE scheme has been applied on a network of unmanned vehicles. Considering the applicability of FE on the industrial applications, the centralized approach will be designed as well as the decentralized approach.

1.1.3 Network protocol for real-time industrial applications

The research of NCSs lies in the intersection of control and communication theories, so to design the communication scheme and protocol for real-time industrial applications is also a key point in this thesis. Nowadays more and more network protocols have been developed as standard solutions supporting various industrial automotive plants with different characteristics, such as EtherNet/IP, Modbus, Profinet, Profibus, HART and so on. With the increasing scale and complexity of industrial process, an unique industrial network solution is no longer applicable, an hybrid protocol is thus be employed. For example, EtherNet/IP is an excellent solution for industrial network communications and is widely adopted since it is an open, cost-effective, world-wide standard [8]. However, due to the carrier sense multiple access/collision detection (CSMA/CD) principle employed in data link layer, Ethernet has an inherent non-determinism, which makes the EtherNet/IP protocol not be reliable enough for critical real-time applications. Therefore, although there are already many developed industrial network protocols, the specific protocol should be further developed for concrete applications based on the existing protocol or the combination of protocols [7, 79, 66, 68].

A critical design issue of NCSs with increasing complexity is to ensure the system safety and reliability, in the mean while guarantee high system performance. This thesis is going to focus on the communication protocol development for the real-time applications in the industrial automatic domain. In [27], the simplified ISO/OSI three-layer model, including physical layer, data link layer and application layer, is introduced for industrial control system. The physical layer is standardized regarding to the hardware and operating system. Hence, at this layer no design freedom is available for the users. Differently, at the data link layer, also called media access control (MAC) layer, and at the application layer, the user is able to implement a

protocol modification, which fits for specific applications.

In this thesis, the adequate MAC behaviors will be developed to support those application domains correspondingly. Since the transmission tasks of measurements and control commands are normally deterministic over a period of time for industrial applications and the network load only varies in case of faults with a rare probability, the MAC protocol should be designed to support deterministic transmission behavior on one hand. On the other hand, to meet the critical real-time requirement of industrial applications, it should also guarantee QoS. As seen from the literatures, those QoS parameters are generally supposed to be stochastic [90, 85, 53] or bounded [51, 89, 19], which are independent of the network protocols. Actually QoS parameters depend greatly on the parameters and schemes defined in the network protocol. For example, the length of contention window (CW) defined in carrier sense multiple access/collision avoidance (CSMA/CA), which is used for most local area networks (LANs), affects greatly on the average packet accessing time, in other words, on the packet delay when many nodes have packets to send; meanwhile, when the maximal value of retry counter is reached, it will lead to packet losses, so the setting of retry counter has a great impact on packet loss rate.

Those two requirements motivate us to develop a deterministic transmission mechanism, which is able to guarantee system QoS demands. Thus time division multiple access (TDMA) based MAC protocol, which allows several users to share the same frequency channel by allocating the transmission of signals into different time slots, is selected as a feasible solution. In TDMA mechanism, the network resource is shared according to the schedule, which is a sequence of the packets' medium access time, and the control and measurement signals can be transmitted in the dedicated time slots without collisions so that the network induced delay can be potentially reduced and real-time performance can be satisfied.

Generally, network scheduling is implemented off-line with the objectives of utilizing network bandwidth efficiently and supporting QoS parameters [56, 44, 92]. For dynamic systems with variable network load, online scheduling is adopted to reallocate network resources [43, 72, 77]. Real-time scheduling algorithms, no matter off-line or online scheduling, assign the network resources according to tasks priorities, task deadline or some other constraints, e.g., earliest deadline first (EDF) [56], least slack time first (LSTF) [44], shortest path (SP) for multi-hop network [92].

Since adopting real-time scheduling can effectively reduce the control period, which will lead to better Quality of Control (QoC), but more network resource consumption, a tradeoff has to be made to balance network load and control performance. Only a few literatures have designed the real-time

scheduling algorithms with the objective of optimizing system control performance. In [9, 80, 81], the control periods and controller gains are adjusted considering an optimal control performance index subject to a number of processor consumption constraints. In [10], considering the varying capacity of wireless networks caused by multipath fading and mobility, a robust scheduling algorithm is proposed with the purpose of keeping the queue length in the network close to an operating point. In [28, 30, 29], the optimal integrated control and scheduling under limited network bandwidth condition is addressed. An optimal pointer placement (OPP) scheduling algorithm is proposed to improve the control performance on one hand, and to reduce the requirements on computing on the other hand.

Although, there are rich achievements with network scheduling, the network induced delay and packet losses still can't be avoided even with deterministic network behavior, when the network is under heavy load. Since the incomplete information can degrade the system performance and in some cases can even destabilize the system, the integrated design of scheduling, control and FD is capable of optimizing the system performance. This motivates us to represent the scheduler in a mathematical way and further develop the integrated model of W-NCSs with scheduler, so that the FE technology is adaptive for the NCSs with deterministic imperfect transmission.

1.2 Objective

The development on industrial automotive W-NCSs with increasing complexity and scale have been considered as a future-oriented technology, and it drives us to develop a comprehensive framework to standardize the process model and communication scheme with the consideration of system reliability, security, comprehensiveness and expansibility. Based on this framework, the advanced FE approaches should be proposed, which is the main objective of this thesis. More specifically, the goals of this thesis are stated as follows

- Modeling of process and communication scheme based on the hierarchical framework of centralized and decentralized W-NCSs, respectively. The coupling relation within W-NCSs and multi-rate sampling should be considered in the modeling procedure;

- Parameterizing of deterministic communication scheduler and formulating it into state-space equations. The transmission delay, packet loss should also be represented by the state-space equations of scheduler;

- Developing FE approaches of centralized and decentralized W-NCSs,

respectively, which satisfy H_∞ performance indices with robustness against unknown input;

- Demonstrating the validity of FE approaches on the WiNC platform.

1.3 Outline and major contributions

The thesis consists of seven chapters organized as shown in Fig. 1.2 . Chapter 2 introduces the preliminary of FE technology. The residual generation, which is an important part of FE, will be presented from two aspects, i.e., observer-based and parameter identification-based. Those two kinds of residual generation methods are both of interest for this thesis. The basic knowledge of FE for linear time-invariant (LTI) systems will be illustrated step by step, that is, the system modeling, observer-based residual generation and post-filtering will be explored, respectively. FE approach will further be extended for linear periodic (LP) systems, which serve as fundamental basis in forthcoming chapters.

In Chapter 3, the hierarchical centralized and decentralized structures of fault tolerant W-NCSs are proposed. The process model and communication scheme corresponding with centralized and decentralized structures are subsequently built. To parameterize the deterministic transmission scheduling, the communication scheme is further formulated into mathematical equation, which can express the transmission delay, packet loss and such kind of network-induced imperfect transmission. At last, an integrated model of the process and communication are developed, which serves as a basic model in the entire thesis.

In Chapter 4, the fault estimation problem of centralized W-NCSs based on the integrated periodic model of process and schedule, proposed in the last chapter, will be solved. An H_∞ performance criterion will be proposed with the help of Krein space, in which the parameter estimation can be achieved based on the recursive computation. Parameter identification-based residual generation will be utilized in FE approach, in which the inner product of the state estimate is regarded as the parameter estimate.

Followed the objectives in the last section, Chapter 5 discusses FE scheme of decentralized W-NCSs based on the integrated periodic model, which is proposed in Chapter 3. LMI-based approaches for characterizing the solution of FE will be addressed with the consideration of sensor and actuator faults, respectively. Note that the FE problem is considered for two kinds of residual structures, i.e., non-shared and shared residuals.

As the implementation of developed FE approaches, Chapter 6 will be

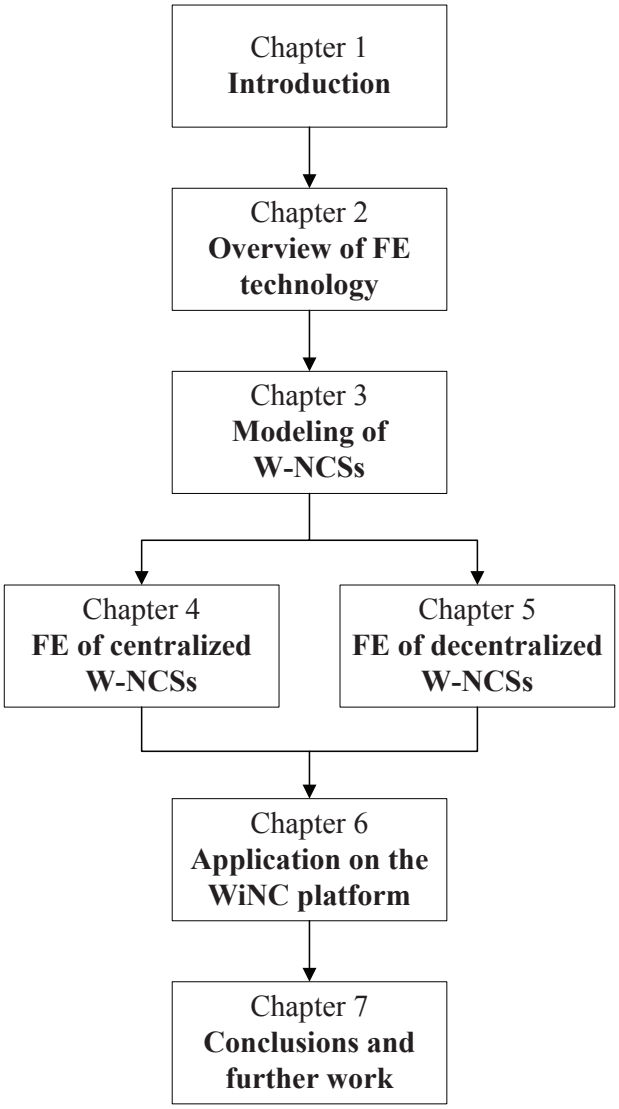

Figure 1.2: Organization of chapters

presented. The algorithms are demonstrated on WiNC platform, which is integrated with three-tank system and embedded wireless network. The system and communication scheme will be first modeled and parameterized into periodic form in according with the modeling methods in Chapter 3. Second, centralized FE algorithm will be verified on WiNC with three schedulers, i.e., sampling-based scheduler, scheduler with transmission delay, scheduler with packet loss, respectively. Similarly, the algorithms for decentralized systems will also be demonstrated on WiNC platform for the system with sensor and

actuator faults, respectively. This thesis ends with the conclusions and the discussion about future works.

The contributions of this thesis can be summarized in the following points

- Propose general centralized and decentralized W-NCSs structures for the real-time industrial automatic applications, and formulate those two kinds of W-NCSs into periodic systems considering the coupling relations and multi-rate sampling;
- Explore the deterministic transmission mechanism for real-time industrial automatic applications, and build the model of medium access behavior, i.e., communication scheduler, into the form of periodic state-space equation, which can also depict the imperfect transmission behaviors, such as deterministic delay, packet loss and so on;
- Develop FE approach by means of recursive calculation on Krein space for periodic centralized W-NCSs. The FE algorithm is applicable for the system with arbitrary input;
- Propose the structures of observer gain and post-filter on the restriction of coupling relations for decentralized W-NCSs, and develop the decentralized FE approaches with non-shared and shared residuals, respectively.
- Demonstrate all the developed FE approaches on the WiNC platform as practical applications, which haven't realized to the author's best of knowledge.

Chapter 2

Overview of FE technology

The objective of this chapter is to introduce the FE theoretical background for LTI systems and LP systems. Since FE is included in FD technology, an overview of the basic principles of model-based FD technology will be first presented. The technical systems will be represented by the input-output description and the state-space model. The state-space model will be further reformulated considering the driving disturbance, measurement disturbance and fault. The most important part of the FE technology, i.e., residual generation, is also formulated mathematically. The principle of designing robust post-filter as well as observer will be finally discussed, which plays an important role in the whole thesis.

2.1 Principles of FD

The FD technology is used to detect and isolate faults and assess their significance of a system, which is achieved by using analytical or functional information of the system being monitored. The tasks of FD include the following three different types or levels

- *Fault detection:* to make a logic decision of the occurrence of faults, either that one or several components are faulty or that everything is under normal condition;

- *Fault isolation:* to determine the location or classification of faults, e.g., to find out which component(s) is(are) faulty;

- *Fault identification:* to determine the type, magnitude and cause of the fault(s).

Apparently, FE technique, which extracts the value of fault from information of systems, belongs to the fault identification level.

The fault is defined as a permanent interruption of a system's ability to perform a required function under specified operating conditions, which can be classified as follows

- *Sensor fault:* these faults influence directly on the process measurement;
- *Actuator fault:* these faults cause changes of the actuator input;
- *Component fault:* these faults are used to indicate malfunctions within the process.

The faults can also be classified into additive faults and multiplicative faults according with the way of how these faults affect the system dynamics. The multiplicative fault is a function of the state or input variables, so in this case the system stability will be affected.

FD technique can be implemented, when the current system behavior is compared with the nominal one. It drives the researchers to build the system model and compare the model behavior online with the system behavior, which is called model-based FD. Generally, the difference between the system output y and the system output estimate $\hat{y}$, which is calculated by the system model, can indicate the information of fault, and the difference r, which is called residual, can be represented by $r = y - \hat{y}$. This process is the residual generation, which can refer to Fig. 1.1. The residual generation plays a very important role for model-based FD, which will be illustrated in detail in the next section.

2.2 Residual generation approaches

To improve the robustness of FD approach against disturbances and model uncertainty, three kinds of residual generation schemes have been proposed, i.e., observer-based approach, parity space approach and parameter identification approach [16, 6]. The parity space approach can be structurally equivalent to the observer-based one, so the observer-based and parameter identification methods will be discussed and compared in the following.

2.2.1 Observer-based residual generation

The observer-based residual generation is most commonly applied for the model-based FD [12, 25, 16]. Comparing with the model-based FE in Fig.

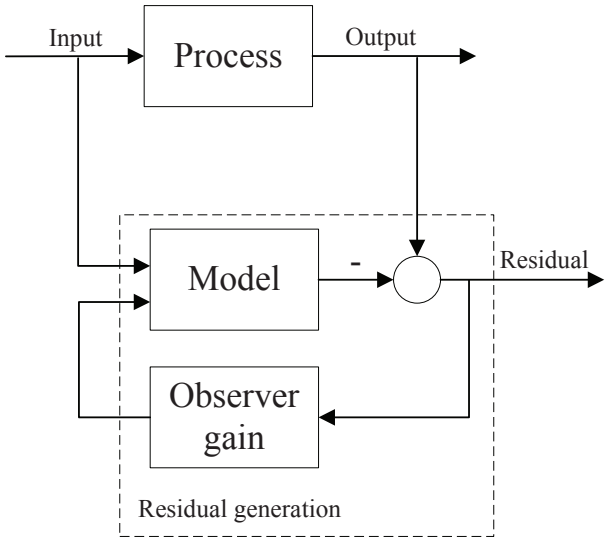

Figure 2.1: Schematic description of observer-based FD scheme

1.1, the system model is replaced by a model with observer, which is shown in Fig. 2.1. The residual signal is the difference between the system output and its estimate generated by the observer, and this resulted residual is fed back to the system model through the observer gain.

Note that the observers may be different according to the usages. For FD purpose, the observer is based on the estimation of the system output. While for control purpose, the system state, which is unmeasurable, is estimated. The observer-based residual generation scheme can be applies for both FD and control purpose.

The model-based FD works under the condition that the model can depict the system process perfectly. Actually in the practical process, unknown disturbances, noise and model simplifications are commonly existed, which will cause the model inaccuracy and degrade the model-based FD performance. Therefore the observer-based residual generation is developed to achieve the robustness against unknown disturbances, noise and model uncertainty.

2.2.2 Parameter identification based residual generation

The parameter is estimated through online recursive calculation, and the residual is generated by comparing the parameter estimate and the corresponding actual process parameter. Fig. 2.2 shows the schematic description

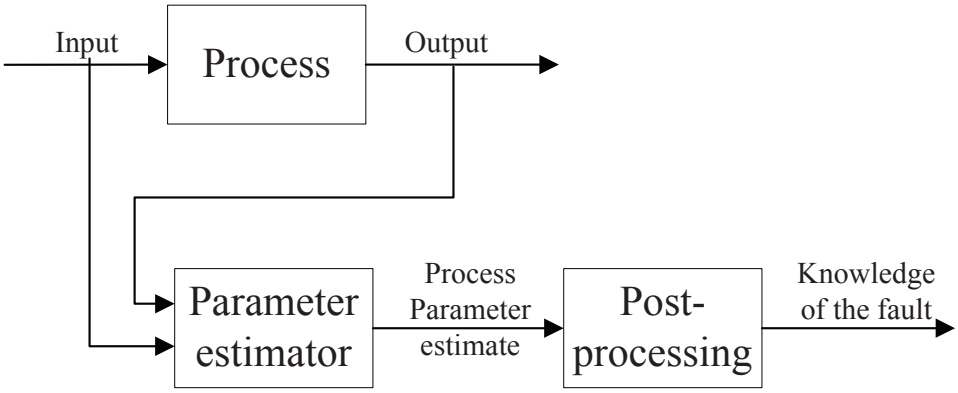

Figure 2.2: Schematic description of parameter identification method

of parameter identification-based residual generation. There are several approaches for parameter identification, e.g., least square-based (LS), extended least square-based (ELS) and recursive least square-based (RLS) [47].

Generally, the parameter identification-based residual generation is more flexible that the observer-based one, since several parameters can be estimated simultaneously using the information of process input and output, and more details of the internal process variables can be discovered. In the meanwhile, because of the flexibility of parameter estimation, this residual generation method is applicable for not only sensor and actuator faults, but also component fault.

In the recent decades, the well-developed adaptive observer design is based on the combination of the observer-based and parameter identification-based residual generation schemes. In the following, the system modeling, residual generation and filtering for observer-based FE approaches, which are the key points of this thesis, will be described.

2.3 FE of LTI systems

According to the process dynamics and modeling objectives, technical processes can be described by different system model types, among which LTI systems are most commonly used. The observer-based FE of LTI systems will be presented in the following.

2.3.1 Modeling of LTI systems

The standard form of the state-space description of discrete-time LTI systems is given by

$$\begin{aligned}\mathbf{x}(k+1) =& \mathbf{A}\mathbf{x}(k) + \mathbf{B}\mathbf{u}(k),\ \mathbf{x}(0) = \mathbf{x}_0 \\ \mathbf{y}(k) =& \mathbf{C}\mathbf{x}(k) + \mathbf{D}\mathbf{u}(k)\end{aligned} \tag{2.1}$$

where $\mathbf{x} \in \mathcal{R}^n$ is the state vector, $\mathbf{x}_0$ is the initial state, $\mathbf{u} \in \mathcal{R}^q$ is the input vector and $\mathbf{y} \in \mathcal{R}^m$ is the output vector. System matrices $\mathbf{A}$, $\mathbf{B}$, $\mathbf{C}$ and $\mathbf{D}$ are real constant matrices with appropriate dimensions.

In order to describe the inevitable deterministic disturbances, an unknown input vector $\mathbf{d} \in \mathcal{R}^l$ is added to (2.1) as follows

$$\begin{aligned}\mathbf{x}(k+1) =& \mathbf{A}\mathbf{x}(k) + \mathbf{B}\mathbf{u}(k) + \mathbf{B}_d\mathbf{d}(k) \\ \mathbf{y}(k) =& \mathbf{C}\mathbf{x}(k) + \mathbf{D}\mathbf{u}(k) + \mathbf{D}_d\mathbf{d}(k)\end{aligned} \tag{2.2}$$

where $\mathbf{B}_d$ and $\mathbf{D}_d$ are disturbance distribution matrices with compatible dimensions.

In some literatures, assume that the process is corrupted by deterministic unknown driving disturbance and measurement disturbance. The state-space representation is reformulated into

$$\begin{aligned}\mathbf{x}(k+1) =& \mathbf{A}\mathbf{x}(k) + \mathbf{B}\mathbf{u}(k) + \mathbf{B}_d\mathbf{d}(k) \\ \mathbf{y}(k) =& \mathbf{C}\mathbf{x}(k) + \mathbf{D}\mathbf{u}(k) + \mathbf{v}(k)\end{aligned} \tag{2.3}$$

where $\mathbf{d} \in \mathcal{R}^l$, $\mathbf{v} \in \mathcal{R}^m$ are driving disturbance and measurement disturbance, respectively. $\mathbf{B}_d$ is disturbance matrix with appropriate dimension.

Suppose $\mathbf{x}_0 = \mathbf{0}$, this model can equivalently be represented by the following input-output form

$$\mathbf{y}(z) = \mathbf{G}_{yu}(z)\mathbf{u}(z) + \mathbf{G}_{yd}(z)\mathbf{d}(z) + \mathbf{G}_{yv}(z)\mathbf{v}(z)$$

with

$$\begin{aligned}\mathbf{G}_{yu}(z) &= \mathbf{D} + \mathbf{C}\left(z\mathbf{I} - \mathbf{A}\right)^{-1}\mathbf{B} \\ \mathbf{G}_{yd}(z) &= \mathbf{C}\left(z\mathbf{I} - \mathbf{A}\right)^{-1}\mathbf{B}_d \\ \mathbf{G}_{yv}(z) &= \mathbf{I}\end{aligned}$$

where $\mathbf{G}_{yu}(z)$ is the transfer function from $\mathbf{u}$ to $\mathbf{y}$, $\mathbf{G}_{yd}(z)$ is the driving disturbance transfer matrix, and $\mathbf{G}_{yv}(z)$ is the transfer function from $\mathbf{v}$ to $\mathbf{y}$.

In order to model the faults in technical systems, the system model in (2.3) can further be extended to

$$\begin{aligned}\mathbf{x}(k+1) =& \mathbf{A}\mathbf{x}(k) + \mathbf{B}\mathbf{u}(k) + \mathbf{B}_d\mathbf{d}(k) + \mathbf{E}_f\mathbf{f}(k)\\ \mathbf{y}(k) =& \mathbf{C}\mathbf{x}(k) + \mathbf{D}\mathbf{u}(k) + \mathbf{v}(k) + \mathbf{F}_f\mathbf{f}(k)\end{aligned} \tag{2.4}$$

where $\mathbf{f} \in \mathcal{R}^s$ is the unknown fault vector to be estimated and $\mathbf{E}_f$, $\mathbf{F}_f$ are fault distribution matrices with appropriate dimensions.

2.3.2 Residual generation

To illustrate the system observer structure according to (2.4) [16], $\hat{\mathbf{x}}(k) \in \mathcal{R}^n$ is first introduced, which is an estimate of $\mathbf{x}(k)$ delivered by the observer. The full order state observer is described by

$$\begin{aligned}\hat{\mathbf{x}}(k+1) &= \mathbf{A}\hat{\mathbf{x}}(k) + \mathbf{B}\mathbf{u}(k) + \mathbf{L}\mathbf{r}(k)\\ \hat{\mathbf{y}}(k) &= \mathbf{C}\hat{\mathbf{x}}(k) + \mathbf{D}\mathbf{u}(k)\\ \mathbf{r}(k) &= \mathbf{y}(k) - \hat{\mathbf{y}}(k)\end{aligned} \tag{2.5}$$

where $\mathbf{r} \in \mathcal{R}^m$ is the residual signal, $\hat{\mathbf{y}} \in \mathcal{R}^m$ is output estimate and $\mathbf{L} \in \mathcal{R}^{n\times m}$ is the so-called observer gain matrix. By introducing the estimation error $\mathbf{e}(k)$, where $\mathbf{e}(k) = \mathbf{x}(k) - \hat{\mathbf{x}}(k)$, the system dynamics is governed by

$$\begin{aligned}\mathbf{e}(k+1) &= (\mathbf{A} - \mathbf{L}\mathbf{C})\mathbf{e}(k) + (\mathbf{E}_f - \mathbf{L}\mathbf{F}_f)\mathbf{f}(k) + \mathbf{B}_d\mathbf{d}(k) - \mathbf{L}\mathbf{v}(k)\\ \mathbf{r}(k) &= \mathbf{C}\mathbf{e}(k) + \mathbf{F}_f\mathbf{f}(k) + \mathbf{v}(k)\end{aligned} \tag{2.6}$$

The above equation can also be represented by the input-output form

$$\mathbf{r}(k) = \mathbf{G}_{rd}(z)\mathbf{d}(k) + \mathbf{G}_{rv}(z)\mathbf{v}(k) + \mathbf{G}_{rf}(z)\mathbf{f}(k) \tag{2.7}$$

where

$$\begin{aligned}\mathbf{G}_{rd}(z) =& (\mathbf{A} - \mathbf{L}\mathbf{C}, \mathbf{B}_d, \mathbf{C}, \mathbf{0})\\ \mathbf{G}_{rv}(z) =& (\mathbf{A} - \mathbf{L}\mathbf{C}, -\mathbf{L}, \mathbf{C}, \mathbf{I})\\ \mathbf{G}_{rf}(z) =& (\mathbf{A} - \mathbf{L}\mathbf{C}, \mathbf{E}_f - \mathbf{L}\mathbf{F}_f, \mathbf{C}, \mathbf{F}_f)\end{aligned} \tag{2.8}$$

The observer gain matrix $\mathbf{L}$ is properly chosen such that $\mathbf{A}-\mathbf{L}\mathbf{C}$ is stable, i.e., the estimation error asymptotically goes to zero. The selection of $\mathbf{L}$ is crucial to improve the performance of estimation, which can be achieved by utilizing different performance indices according to the design purposes.

The procedure from observer design until now is called residual generation, which is shown in a dashed line box of Fig. 1.1. This residual signal

includes very important information about the system, and can be explored for many FD purposes, such as fault identification, unknown input evaluation, fault of interest estimation and so on.

The choice of $\mathbf{L}$ may result in complicated computation, when the design is based on the full-order state observer, which isn't really necessary in some cases. The diagnostic observer (DO) is one of the solutions [41, 45, 63], which can support a reduced-order observer design.

2.3.3 Post-filter design

When considering the robustness of FE against unknown disturbance, a post-filter of residual is needed to be designed besides the observer gain $\mathbf{L}$ to extract the significant characteristics of fault of interest. The residual generator in (2.6) can thus be reformulated into

$$\mathbf{r}(k) = \mathbf{V}\left(\mathbf{y}(k) - \hat{\mathbf{y}}(k)\right) \tag{2.9}$$

where $\mathbf{V}$ is the so-called post-filter and, by a suitable selection, is helpful to obtain significant characteristics of faults. Obviously, the transfer functions from unknown disturbances and fault to the residual can thus be described by

$$\begin{aligned}
\mathbf{G}_{rd}(z) &= \mathbf{VC}(z\mathbf{I} - \mathbf{A} + \mathbf{LC})^{-1}\mathbf{B}_d \\
\mathbf{G}_{rv}(z) &= -\mathbf{VC}(z\mathbf{I} - \mathbf{A} + \mathbf{LC})^{-1}\mathbf{L} + \mathbf{I} \\
\mathbf{G}_{rf}(z) &= \mathbf{VC}(z\mathbf{I} - \mathbf{A} + \mathbf{LC})^{-1}(\mathbf{E}_f - \mathbf{LF}_f) + \mathbf{F}_f
\end{aligned} \tag{2.10}$$

The observer gain $\mathbf{L}$ and post-filter $\mathbf{V}$ are both design parameters. Generally, $\mathbf{L}$ is constant for LTI systems and it should be selected to guarantee the stability of the system dynamics (2.6), while the post-filter is arbitrarily selectable and it can either be constant or dynamic. The selection of $\mathbf{V}$ is independent of the selection of $\mathbf{L}$, and $\mathbf{V}$ can be decided by solving the perfect fault identification (PFI) problem, which is stated by

$$\mathbf{G}_{rd}(z) = \mathbf{0},\ \mathbf{G}_{rv}(z) = \mathbf{0},\ \mathbf{G}_{rf}(z) = \mathbf{I}$$

PFI problem isn't achievable in most cases due to the strict existence conditions. In practice, FE is considered as an optimal problem aiming at achieving the trade-off between robustness against unknown disturbances and the sensitivity to faults, and the problem is stated in the following

$$\|\mathbf{G}_{rd}(z)\|_\infty < \alpha_1,\ \|\mathbf{G}_{rv}(z)\|_\infty < \alpha_2,\ \|\mathbf{I} - \mathbf{G}_{rf}(z)\|_\infty < \beta$$

where the operator norm $\|\mathbf{G}_{r\eta}(z)\|_\infty$ with η standing for $\mathbf{d}$, $\mathbf{v}$, $\mathbf{f}$ is defined in terms of the norms of input and output signals in (2.6) as follows

$$\|\mathbf{G}_{r\eta}(z)\|_\infty = \sup_{\eta \neq 0} \frac{\|\mathbf{r}\|}{\|\eta\|}$$

and the l_2 norms of vector-valued signals $\mathbf{r}(k)$ and $\eta(k)$ are defined by

$$\|\mathbf{r}\| = \left(\sum_{k=0}^{\infty} \mathbf{r}^T(k)\mathbf{r}(k) \right)^{1/2}$$
$$\|\eta\| = \left(\sum_{k=0}^{\infty} \eta^T(k)\eta(k) \right)^{1/2}$$

It is obvious that the optimal performance can be reached, when the observer gain matrix $\mathbf{L}$ and the post-filter $\mathbf{V}$ are selected simultaneously with the objective of minimizing β under the given α_1 and α_2. There are already many literatures focusing on the optimal design of the robust residual generator [25, 24, 55], which have considered both the influence of disturbances and faults on the residual signals simultaneously.

2.4 FE of LP systems

With the increasing complexity of industrial process, the requirement on the sampling rates of components or sub-systems may vary due to the different functionalities or locations. By employing the multirate sampling, the processing efficiency can be greatly increased and it leads to a periodic system representation. Although LP systems have encountered in many different industrial automotive fields, e.g., power supply [37], electronics [93], the research on LP systems should be paid more and more attentions. In this section, the modeling and standard FE schemes of LP systems will be presented.

Compared with the model (2.1) of LTI systems, LP systems are formulated by the following state-space description

$$\begin{aligned} \mathbf{x}(k+1) =& \mathbf{A}(k)\mathbf{x}(k) + \mathbf{B}(k)\mathbf{u}(k) \\ \mathbf{y}(k) =& \mathbf{C}(k)\mathbf{x}(k) + \mathbf{D}(k)\mathbf{u}(k) \end{aligned} \tag{2.11}$$

where $\mathbf{x} \in \mathcal{R}^{n(t)}$, $\mathbf{u} \in \mathcal{R}^{q(t)}$ and $\mathbf{y} \in \mathcal{R}^{m(t)}$ are the system state, input and output with time-varying dimensions, respectively. $\mathbf{A}(k)$, $\mathbf{B}(k)$, $\mathbf{C}(k)$ and

$\mathbf{D}(k)$ are appropriately dimensioned real periodic matrices satisfying

$$\begin{aligned}\mathbf{A}(k) = \mathbf{A}(k+\theta),\ \mathbf{B}(k) = \mathbf{B}(k+\theta),\\ \mathbf{C}(k) = \mathbf{C}(k+\theta),\ \mathbf{D}(k) = \mathbf{D}(k+\theta).\end{aligned}$$

where θ is a positive constant integer, which can reflect the system discrete period.

To clearly distinguish the system period from the fragment within the period, (2.11) can further be formulated into

$$\begin{aligned}\mathbf{x}(k, j+1) =& \mathbf{A}(j)\mathbf{x}(k, j) + \mathbf{B}(j)\mathbf{u}(k, j)\\ \mathbf{y}(k, j) =& \mathbf{C}(j)\mathbf{x}(k, j) + \mathbf{D}(j)\mathbf{u}(k, j)\end{aligned} \tag{2.12}$$

where k represents the system discrete time period and $j,\ j = 0, 1, \cdots, \theta - 1$ is the number of fragments in one period. This representation will continue to be used in the following parts of this thesis.

When the disturbances and the additive fault are considered, (2.12) can be extended to

$$\begin{aligned}\mathbf{x}(k, j+1) &= \mathbf{A}(j)\mathbf{x}(k, j) + \mathbf{B}(j)\mathbf{u}(k, j) + \mathbf{B}_d(j)\mathbf{d}(k, j) + \mathbf{E}_f(j)\mathbf{f}(k, j)\\ \mathbf{y}(k, j) &= \mathbf{C}(j)\mathbf{x}(k, j) + \mathbf{D}(j)\mathbf{u}(k, j) + \mathbf{v}(k, j) + \mathbf{F}_f(j)\mathbf{f}(k, j)\end{aligned} \tag{2.13}$$

where $\mathbf{d} \in \mathcal{R}^{l(t)}$, $\mathbf{v} \in \mathcal{R}^{m(t)}$ and $\mathbf{f} \in \mathcal{R}^{s(t)}$ are deterministic unknown driving disturbance, measurement disturbance and fault, respectively. $\mathbf{B}_d(j)$, $\mathbf{E}_f(j)$ and $\mathbf{F}_f(j)$ are appropriately dimensioned real matrices satisfying periodic properties with the period of θ.

The general observer-based residual generator with post-filter of LP systems can be constructed as follows

$$\begin{aligned}\hat{\mathbf{x}}(k, j+1) &= \mathbf{A}(j)\hat{\mathbf{x}}(k, j) + \mathbf{B}(j)\mathbf{u}(k, j) + \mathbf{L}(j)\mathbf{r}(k, j)\\ \hat{\mathbf{y}}(k, j) &= \mathbf{C}(j)\hat{\mathbf{x}}(k, j) + \mathbf{D}(j)\mathbf{u}(k, j)\\ \mathbf{r}(k, j) &= \mathbf{V}(j)(\mathbf{y}(k, j) - \hat{\mathbf{y}}(k, j))\end{aligned} \tag{2.14}$$

Similarly as for LTI systems, the system dynamics can be governed by

$$\begin{aligned}\mathbf{e}(k, j+1) =& (\mathbf{A}(j) - \mathbf{L}(j)\mathbf{C}(j))\mathbf{e}(k, j) + (\mathbf{E}_f(j) - \mathbf{L}(j)\mathbf{F}_f(j))\mathbf{f}(k, j)\\ &+ \mathbf{B}_d(j)\mathbf{d}(k, j) - \mathbf{L}(j)\mathbf{v}(k, j)\\ \mathbf{r}(k, j) =& \mathbf{V}(j)(\mathbf{C}(j)\mathbf{e}(k, j) + \mathbf{F}_f(j)\mathbf{f}(k, j) + \mathbf{v}(k, j))\end{aligned} \tag{2.15}$$

The corresponding input-output representation is

$$\mathbf{r}(k, j) = \mathbf{G}_{rd,j}(z)\mathbf{d}(k, j) + \mathbf{G}_{rv,j}(z)\mathbf{v}(k, j) + \mathbf{G}_{rf,j}(z)\mathbf{f}(k, j) \tag{2.16}$$

where $\mathbf{G}_{rd,j}(z)$ is the transfer function from $\mathbf{d}$ to $\mathbf{r}$ at the j-th discrete segment. The meanings of $\mathbf{G}_{rv,j}(z)$ and $\mathbf{G}_{rf,j}(z)$ can easily be understood.

The optimal design of LP systems is to find $\mathbf{L}(j)$ and $\mathbf{V}(j)$ such that

$$\|\mathbf{G}_{rd,j}(z)\|_\infty < \alpha_{1j},\ \|\mathbf{G}_{rv,j}(z)\|_\infty < \alpha_{2j},\ \|\mathbf{I} - \mathbf{G}_{rf,j}(z)\|_\infty < \beta_j$$

for all $j = 0, 1, \cdots, \theta - 1$.

Suppose that

$$\alpha_1 = \max_{j=0,1,\cdots,\theta-1} \alpha_{1j},\ \alpha_2 = \max_{j=0,1,\cdots,\theta-1} \alpha_{2j},\ \beta = \max_{j=0,1,\cdots,\theta-1} \beta_j$$

the optimal performance indices can be relaxed to

$$\|\mathbf{G}_{rd,j}(z)\|_\infty < \alpha_1,\ \|\mathbf{G}_{rv,j}(z)\|_\infty < \alpha_2,\ \|\mathbf{I} - \mathbf{G}_{rf,j}(z)\|_\infty < \beta$$

for all $j = 0, 1, \cdots, \theta - 1$.

Similarly, the H_∞ norm of transfer functions is defined by

$$\|\mathbf{G}_{r\eta,j}(z)\|_\infty = \sup_{\eta \neq 0,\ k \in [0,\infty]} \frac{\|\mathbf{r}_j\|}{\|\eta_j\|}$$

where η stands for $\mathbf{d}$, $\mathbf{v}$ and $\mathbf{f}$. $\mathbf{r}_j$ is the residual vector at the j-th segment in every period, and η_j is the signal of $\mathbf{d}$, $\mathbf{v}$ or $\mathbf{f}$ at the j-th segment in every period.

The l_2 norms of signals $\mathbf{r}_j$ and η_j are defined by

$$\|\mathbf{r}_j\| = \left(\sum_{k=0}^{\infty} \mathbf{r}_j^T \mathbf{r}_j \right)^{1/2}$$
$$\|\eta_j\| = \left(\sum_{k=0}^{\infty} \eta_j^T \eta_j \right)^{1/2}$$

From the l_2 norm definition, the periodic signals of LP systems can be measured by the energy as follows

$$\|\mathbf{r}(k,j)\| = \left(\sum_{k=0}^{\infty} \sum_{j=0}^{\theta-1} \mathbf{r}(k,j)^T \mathbf{r}(k,j) \right)^{1/2}$$
$$\|\eta(k,j)\| = \left(\sum_{k=0}^{\infty} \sum_{j=0}^{\theta-1} \eta(k,j)^T \eta(k,j) \right)^{1/2}$$

and the generalized H_∞ norm of LP systems (2.15) is the induced norm with the input signals, i.e., $\mathbf{d}$, $\mathbf{v}$ and $\mathbf{f}$, and residual signal all measured by energy, which is presented by

$$\|\mathbf{G}_{r\eta}(z)\|_\infty = \sup_{\eta\neq 0,\, k\in[0,\infty],\, j=0,1,\cdots,\theta-1} \frac{\|\mathbf{r}(k,j)\|}{\|\eta(k,j)\|}$$

It is worth pointing out that the periodicity makes system norm and further the performance index different from those of LTI systems. It also brings new challenges for FE approach design with an optimal performance index, which will be the main concern in this thesis.

2.5 Summary

This chapter serves as a preliminary of the FD technologies, especially for FE, which act as a branch of FD technique. The principles of FD has been first addressed and the residual generation schemes have been depicted from two aspects, i.e., observer-based and parameter identification-based. The existence conditions of perfect FE of LTI systems have been derived. Due to the strict conditions, FE has been developed into solving an optimal problem, which can achieve the robustness against unknown disturbances. Furthermore, LP systems are modeled and the observer-based FE approaches have been studied. The preliminary of FE approaches for LP systems will be the groundwork of the whole dissertation.

Chapter 3

Modeling of W-NCSs

The major objective of this chapter is the mathematical modeling of W-NCSs from the point of view of applications to industrial automatic control systems. We consider the systems are large-scale interconnected, which are composed of several sub-systems interconnected in symmetrical fashion. In this way, the complexity of large-scale system and time consumption can be greatly reduced.

The partition of systems is generally based on the functionalities, locations, hierarchies or other elements, which can make the sub-systems perform as independent units. The difference between sub-systems may lead to the multi-sampling measuring, e.g., the sampling time of sub-system with temperature measurements is usually tens of times more than the sampling time with measurements of movement parameters, such as velocity, acceleration, force and so on. So in this chapter, the modeling of large-scale systems, which are composed of sub-systems with a variety of sampling rates, will be built.

As mentioned in Chapter 1, the modeling will be concerned with both centralized and decentralized system infrastructures from the aspects of process modeling and communication scheme modeling. The modeling procedure of centralized NCSs will be illustrated at first.

3.1 Problem formulation of centralized W-NCSs

Considering the centralized control system, which consists of several sub-systems, the W-NCS structure based on it in hierarchical architecture is proposed in Fig. 3.1, which can be described by

- *Execution layer:* At this layer, sensors are time-driven components to observe process parameters, while actuators are event-driven by network coordinator at the upper layer. The sampling cycles of sensors and the actions of actuators are all decided by upper layer's coordinator.

- *Coordination layer:* This layer consists of N network coordinators. Each sub-system has one exclusive coordinator and a number of sensors and actuators at the execution layer. The coordinator is responsible for packet routing between the upper layer and the lower layer. By employing proper coordination algorithm, the components at execution layer of all N sub-systems can thus work in parallel, therefore network resource can be used more efficiently.

- *Supervision and management layer:* At this layer, the centralized control and FD algorithm are implemented by MCU based on the information of overall system. The algorithms will be activated every time when any sub-system has an update of measurement. To optimize the system resource usage, especially when one or several components are faulty, the resource management and fault tolerant control (FTC) schemes can realize the online reconfiguration of the controller, FD and the communication protocols of the whole system. The research of this layer is still under way.

The communication structure corresponding to this W-NCSs framework can be classified as:

- communications in a sub-system, which will operate in a master-slave mode with the coordinator operating as a master.

- communications between the sub-systems and the centralized controller MCU, which serve as synchronization and execution of the control, monitoring and communication actions, and the activation and execution of the resource re-allocation and FTC algorithms in the faulty case. The data exchanges at this layer also work using a master-slave protocol, while the centralized controller (MCU) acts as a master in this case.

Apparently, the communication of entire system is under a hierarchical master-slave architecture. In the following, the system modeling and communication parameterization based on this centralized W-NCSs framework will be built.

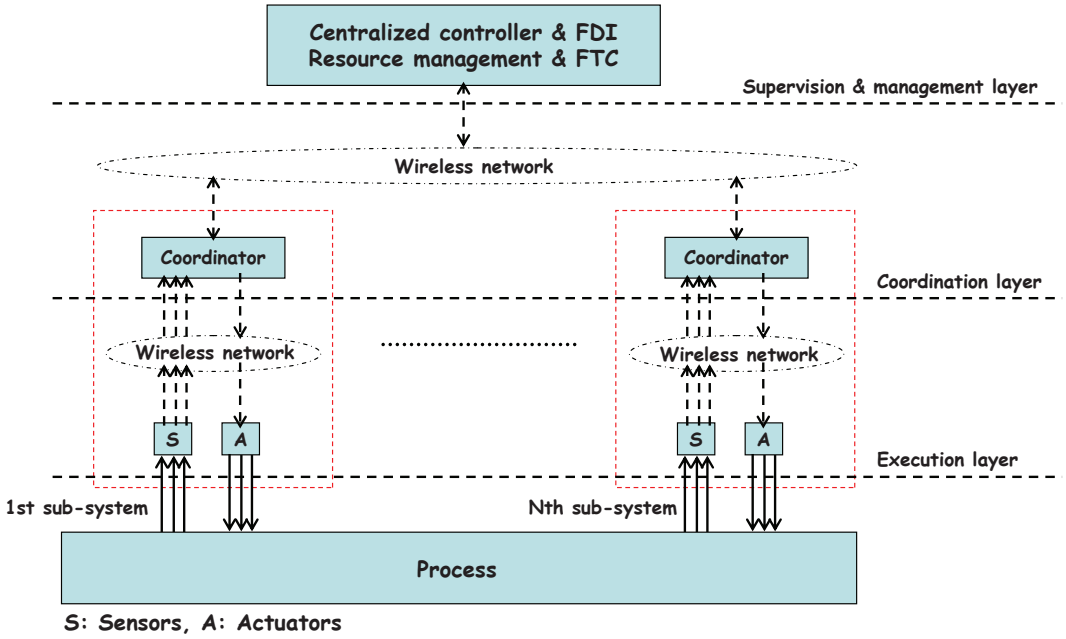

Figure 3.1: Fault tolerant centralized W-NCSs structure

3.1.1 Modeling of communication schemes

As depicted in the centralized W-NCSs structure, the communication scheme is hierarchical, in which the communications are carried out between the execution layer and the coordination layer, and between the coordination layer and the supervision and management layer. Therefore the modeling in the way of scheduler will be built correspondingly, which is based on the TDMA medium access technology.

Communication modeling in a sub-system

Following the TDMA mechanism, the data transmissions within one sub-system are periodic. The measurements from sensors are transmitted to coordinator sequentially, then the coordinator will repack those measurements into one or several larger packet(s); after receiving the control commands from MCU, the coordinator will broadcast those control commands to all actuators under the purpose of utilizing the network resource efficiently and optimizing real-time communication performance.

Let $\bar{T}_{slot}$ be the maximum data transmission time (including physical transmission time and software computation time) between any two nodes within the i-th sub-system. Define a time slot $T_{slot} \geq \bar{T}_{slot}$. Let $T_{cyc,i}$ be the

cyclic time of the i-th sub-system. In this cycle, a number of time slots are reserved for (a) transmission of sensor data with $\gamma_{i,s}$ time slots (b) transmission of control commands with $\gamma_{i,c}$ time slots (c) implementation of the communication strategy with $\gamma_{i,com}$ time slots. $T_{cyc,i}$ holds

$$T_{cyc,i} = (\gamma_{i,s} + \gamma_{i,c} + \gamma_{i,com})\, T_{slot} \tag{3.1}$$

Set $T_{cyc,i}$ smaller than the critical sampling time $T_{cri,i}$, where $T_{cri,i}$ is the decided by the system real-time behavior. Note that the parameter T_p defined by

$$T_p = \frac{T_{cyc,i}}{\gamma_{i,s} + \gamma_{i,c} + \gamma_{i,com}} \leq \frac{T_{cri,i}}{\gamma_{i,s} + \gamma_{i,c} + \gamma_{i,com}} \tag{3.2}$$

should be larger than $\bar{T}_{slot}$. As a result, the data throughput of the i-th subsystem is partly determined by T_p. $\gamma_{i,c} = 1$ in this structure, because of the broadcast communication of control commands. It is evident that reducing $\gamma_{i,s}$ will relax the technical requirements on the network.

$\gamma_{i,com}$ time slots are reserved for those communication actions like special coding schemes, acknowledgement (ACK) of receiving data, asking for repeating sending, sending synchronization signals etc. From the communication viewpoint, $\gamma_{i,com}$ is a design parameter for setting the CoS of the data transmissions within the i-th sub-system and thus determines the network reliability. For the W-NCSs, all these communication actions can considerably and efficiently improve the network reliability.

Denote M_i as the number of sensors of the i-th sub-system, the cycle of i-th sub-system $T_{cyc,i}$ from (3.1) holds for

$$T_{cyc,i} = (M_i + 1 + h_i)\, T_{slot},\ \gamma_{i,s} = M_i,\ \gamma_{i,c} = 1 \tag{3.3}$$

where h_i is the number of reserved time slots which is decided by the scheduling algorithm.

The scheduler for the local wireless transmission of i-th sub-system is schematically shown in Fig. 3.2, where $C_i,\ i = 1, \cdots, N$, represents the i-th coordinator and $S_j,\ j = 1, \cdots, M_i$, represents the j-th sensor of i-th sub-system. It is straightforward that sensor detection and command transmission are operated periodically based on this schedule. The measurements of sensors are sent slot by slot to the coordinator from the beginning of period. After certain reserved time slots, which are designed for the retransmission of measurements and other network management packets, the control commands are broadcasted by the i-th coordinator to all actuators belonging to the i-th sub-system. Some time slots are also reserved after data collection to guarantee the accuracy rate of successful transmission. The length of reserved time slots is chosen considering system real-time demand in one hand,

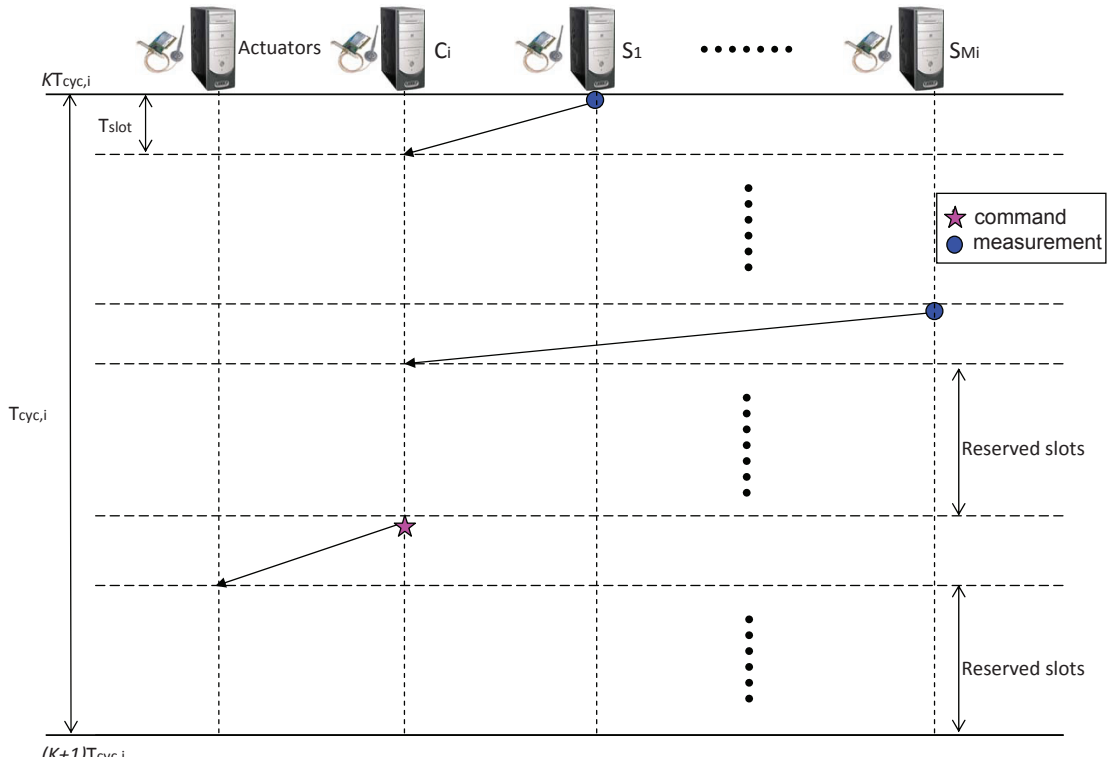

Figure 3.2: Scheduler for the i-th sub-system of centralized W-NCSs

and the network performance in the other hand. Since the shorter the length of reserved time slots is, the higher the real-time performance is, but in the same time, it may lead to the degradation of network performance. So it's a trade-off to design the reserved time slots' length considering both system real-time and network performances.

Note that, to improve the efficiency of network usage, in the network protocol the active ACK packets sent by the receiving station (destination) will not be used instead of asking for retransmission. When the packets are lost or incorrect, after a period of time, the receiving station will send a retransmission message to the source station actively.

Taking the example of scheduler in Fig. 3.2 to illustrate, the coordinator will not send back an ACK packet to the sensor after the receipt of any recognizable packet. Instead, after the scheduled time slots of all sensors, the coordinator will send a retransmission command, if there is one or several sensors transmission are failed in the broadcasting. In this way, the occupied slots of ACK can be saved and the number of reserved time slots can be reduced.

Communication modeling between sub-systems and MCU

The basic idea behind the schedule approach between sub-systems and MCU is to perform the transmission of measurements with multi-sampling rates from coordinators and the transmission of control commands from MCU. The communication between sub-systems and MCU also operates in a master-slave mode. But different from the master-slave mode of communication in a sub-system, coordinator acts as sending station (source) when sending out measurements, as well as receiving station (destination) when receiving control commands. Assume that $T_{cyc,i},\ i = 1, \cdots, N$, is the sampling period of i-th sub-system, which can be expressed by

$$T_{cyc,i} = l_i T_{cyc,\min},\ l_i \text{ is some integer} \tag{3.4}$$

Let h, T_{period} be

$$\begin{aligned} h &= \min\left\{ l \,\middle|\, \frac{l}{l_i} = \text{integer},\ i = 1, \cdots, N \right\}, \\ T_{period} &= hT_{cyc,\min} \end{aligned} \tag{3.5}$$

In the time interval $[kT_{period}, (k+1)T_{period})$, the i-th coordinator, $i = 1, \cdots, N$, will send the repacked measurements of i-th sub-system to MCU periodically based on $T_{cyc,i}$ at the time instants $kT_{period}, kT_{period} + T_{cyc,i}, \cdots, kT_{period} + (h/l_i - 1)T_{cyc,i}$. It is evident that this scheduler is a periodic one with the period time equal to T_{period}. Fig. 3.3 shows an example of such a scheduler with $N = 3,\ l_1 = 2,\ l_2 = 3,\ l_3 = 6$ and $T_{cyc,\min} = T_{cyc,1},\ T_{period} = 6T_{cyc,\min}$. $T_{cyc,min}$ is the greatest common divisor (GCD) of sensors' sampling cycles and is treated as basic process unit. Any process unit with transmission of measurements will be treated as an arithmetic unit. It means that in every process unit when MCU receives any update of measurements from sub-systems, the operation of control and FD algorithms will be activated, then calculated command, such as control input and fault warning signal, will be broadcasted to all coordinators.

Notice that in every arithmetic unit, when more than one coordinators would like to send measurement packets simultaneously, a priority-based transmission sequence is organized in the protocol to avoid the collision. With regard to the connection of the two schedule schemes, i.e., the schedule within sub-system shown in Fig. 3.2 and the schedule between sub-systems and MCU shown in Fig. 3.3, the coordinator plays an important role. Take the coordinator of i-th sub-system, namely C_i, for example. C_i waits until all measurements from sensors have been received, then repacks those packets and further transmits to MCU. MCU calculates and broadcasts the control

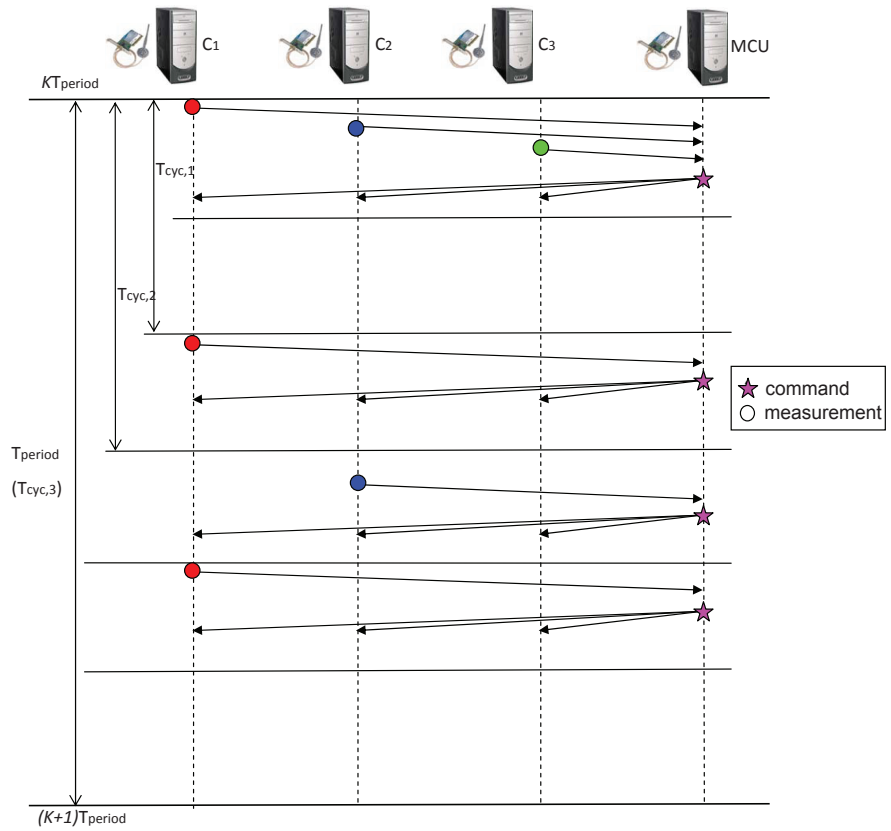

Figure 3.3: An example of scheduler between MCU and sub-systems

command every arithmetic unit when all scheduled coordinators in this period have finished the transmission with MCU successfully. Until now, C_i will execute as a relay and broadcast the control command to actuators belonging to the i-th sub-system. So considering the connection of the two communication schemes, the reserved time slots after the transmission of measurements within the i-th sub-system in Fig. 3.2 should be at least enough for transmission of scheduled coordinators with MCU and broadcasting of control command from MCU.

To denote the time instants of arithmetic units, which play an important role for the study forward, the following definition is given

Definition 1 *Denote all the time instants,* $jT_{cyc,i},\ j = 0, 1, \cdots, h/l_i - 1,\ i = 1, \cdots, N,$ *by* $\varsigma_1, \cdots, \varsigma_\theta,\ \theta \leq \sum_{i=1}^{N} h/l_i,$ *and order them as* $\varsigma_j < \varsigma_{j+1},\ j = 0, \cdots, \theta - 1.$

3.1.2 Modeling of centralized W-NCSs

Modeling of a sub-system

The i-th sub-system coupling with other sub-systems can be modeled by

$$\begin{aligned}\dot{\mathbf{x}}_i(t) =&\mathbf{A}_{ii}\mathbf{x}_i(t) + \mathbf{B}_i\mathbf{u}_i(t) + \sum_{j\neq i}^{N}\mathbf{A}_{ij}\mathbf{x}_j(t)\\ \mathbf{y}_i(t) =&\mathbf{C}_i\mathbf{x}_i(t),\ i = 1, 2, \cdots, N\end{aligned} \tag{3.6}$$

where $\mathbf{x}_i(t) \in \mathcal{R}^{n_i}$, $\mathbf{u}_i(t) \in \mathcal{R}^{q_i}$ and $\mathbf{y}_i(t) \in \mathcal{R}^{m_i}$ denote the state vector, the control input and the measurement output of i-th sub-system, respectively. $\mathbf{A}_{ii}$, $\mathbf{A}_{ij}$, $\mathbf{B}_i$ and $\mathbf{C}_i$ are known matrices of appropriate dimensions.

Since the sampling period of the i-th sub-system is $T_{cyc,i}$, the continuous-time model described by (3.6) can be discretized as follows

$$\begin{aligned}\mathbf{x}_i\left((k+1)T_{cyc,i}\right) =&\mathbf{A}_{d,ii}\mathbf{x}_i(kT_{cyc,i}) + \mathbf{B}_{d,i}\mathbf{u}_i(kT_{cyc,i})\\ &+\sum_{j\neq i}^{N}\mathbf{A}_{d,ij}(kT_{cyc,i})\bar{\mathbf{x}}_j(kT_{cyc,i})\\ \mathbf{y}_i\left(kT_{cyc,i}\right) =&\mathbf{C}_{d,i}\mathbf{x}_i(kT_{cyc,i})\end{aligned} \tag{3.7}$$

where $\mathbf{A}_{d,ii} = e^{\mathbf{A}_{ii}T_{cyc,i}}$, $\mathbf{B}_{d,i} = \int_0^{T_{cyc,i}} e^{\mathbf{A}_{ii}(T_{cyc,i}-\tau)}\mathbf{B}_i d\tau$ and $\mathbf{C}_{d,i} = \mathbf{C}_i$. Suppose that in the time interval $[kT_{cyc,i}, (k+1)T_{cyc,i})$ updates in the j-th sub-system are realized at the time instants $kT_{cyc,i} + t_{ij,1}(kT_{cyc,i}),\ \cdots,\ kT_{cyc,i} + t_{ij,\kappa}(kT_{cyc,i})$. Assuming that $\mathbf{x}_j(\tau) \approx \mathbf{x}_j(kT_{cyc,i})$ for $\tau \in [kT_{cyc,j}, kT_{cyc,i} + t_{ij,1}(kT_{cyc,i}))$, $\cdots$, $\mathbf{x}_j(\tau) \approx \mathbf{x}_j(kT_{cyc,i} + t_{ij,\kappa}(kT_{cyc,i}))$ for $\tau \in [kT_{cyc,j} + t_{ij,\kappa}(kT_{cyc,i}), (k+1)T_{cyc,i})$, $\mathbf{A}_{d,ij}(kT_{cyc,i})$ and $\bar{\mathbf{x}}_j(kT_{cyc,i})$ can be written into (3.8) and (3.9), respectively.

Note that $\zeta_{ij}(kT_{cyc,i})$ represents the last time instant, at which an update of the j-th sub-system is realized before the time instant $kT_{cyc,i}$.

Modeling of overall W-NCSs

The modeling of the overall W-NCSs is based on the discrete-time models of sub-system (3.9) and the scheduler for the communications between the sub-systems and MCU, which are periodic with the period time $T_{period} = hT_{cyc,\min}$.

Based on the scheduler and Definition 1, the state vectors $x_i,\ i = 1, \cdots, N$, in the time intervals $[kT_{period} + \varsigma_j, (k+1)T_{period} + \varsigma_j)$ for $j = 1, \cdots, \theta$ are lifted into a vector denoted by $\mathbf{x}(k, j)$ as follows

$$\mathbf{A}_{d,ij}(kT_{cyc,i}) = \begin{cases} \int_0^{T_{cyc,i}} e^{\mathbf{A}_{ii}(T_{cyc,i}-\tau)}\mathbf{A}_{ij}d\tau, \text{ no update of } j\text{-th sub-system in} \\ \qquad [kT_{cyc,i}, (k+1)T_{cyc,i}); \\ \left[\int_0^{t_{ij,1}(k)} e^{\mathbf{A}_{ii}(T_{cyc,i}-\tau)}\mathbf{A}_{ij}d\tau, \quad \cdots, \quad \int_{t_{ij,\kappa}(k)}^{T_{cyc,i}} e^{\mathbf{A}_{ii}(T_{cyc,i}-\tau)}\mathbf{A}_{ij}d\tau \right], \\ \text{update(s) of } j\text{-th sub-system in } [kT_{cyc,i}, (k+1)T_{cyc,i}) \end{cases} \tag{3.8}$$

$$\bar{\mathbf{x}}_j(kT_{cyc,i}) = \begin{cases} \mathbf{x}_j(\zeta_{ij}(kT_{cyc,i})), \text{ no update of } j\text{-th sub-system in} \\ \qquad [kT_{cyc,i}, (k+1)T_{cyc,i}); \\ \begin{bmatrix} \mathbf{x}_j(\zeta_{ij}(kT_{cyc,i})) \\ \mathbf{x}_j(kT_{cyc,i} + t_{ij,1}(k)) \\ \vdots \\ \mathbf{x}_j(kT_{cyc,i} + t_{ij,\kappa}(k)) \end{bmatrix}, \text{update(s) of } j\text{-th sub-system in} \\ \qquad [kT_{cyc,i}, (k+1)T_{cyc,i}) \end{cases} \tag{3.9}$$

To model the overall NCS, we introduce the following vector

$$\mathbf{x}(k,j) = \begin{bmatrix} \bar{\mathbf{x}}_j(kT_{period} + \varsigma_j) \\ \vdots \\ \bar{\mathbf{x}}_\theta\left(kT_{period} + \varsigma_\theta\right) \\ \bar{\mathbf{x}}_1((k+1)T_{period} + \varsigma_1) \\ \vdots \\ \bar{\mathbf{x}}_{j-1}((k+1)T_{period} + \varsigma_{j-1}) \end{bmatrix} \tag{3.10}$$

where $\bar{\mathbf{x}}_j(kT_{period} + \varsigma_j)$ denotes the vector consisting of all those state variables that have an update at the time instant $kT_{period} + \varsigma_j$. In other words, $\mathbf{x}(k,j)$, $j = 1, \cdots, \theta$ represents the vector of the whole process state variables with all their updates in the time interval $[kT_{period} + \varsigma_j,\ (k+1)T_{period} + \varsigma_j)$. For the sake of simple notation, I_{ς_j} is used to denote the set of all those sub-systems, which have an update at the time instant $kT_{period} + \varsigma_j$.

Similarly $\mathbf{u}(k,j)$ is used to denote all input variables of whole system in

the time interval $[kT_{period}+\varsigma_j,\ (k+1)T_{period}+\varsigma_j)$ as follows

$$\mathbf{u}(k,j)=\begin{bmatrix} \bar{\mathbf{u}}_j(kT_{period}+\varsigma_j) \\ \vdots \\ \bar{\mathbf{u}}_\theta\left(kT_{period}+\varsigma_\theta\right) \\ \bar{\mathbf{u}}_1((k+1)T_{period}+\varsigma_1) \\ \vdots \\ \bar{\mathbf{u}}_{j-1}((k+1)T_{period}+\varsigma_{j-1}) \end{bmatrix} \tag{3.11}$$

where $\bar{\mathbf{u}}_j(kT_{period}+\varsigma_j)$ represents the vector consisting of all those input signals from the set of sub-systems I_{ς_j}.

Comparing the change of lifted state vectors $\mathbf{x}(k,j)$ with j ranging from 1 to θ, which are listed

$$\mathbf{x}(k,1)=\begin{bmatrix} \bar{\mathbf{x}}_1(kT_{period}+\varsigma_1) \\ \bar{\mathbf{x}}_2(kT_{period}+\varsigma_2) \\ \vdots \\ \bar{\mathbf{x}}_\theta\left(kT_{period}+\varsigma_\theta\right) \end{bmatrix},\ \cdots,$$

$$\mathbf{x}(k,j)=\begin{bmatrix} \bar{\mathbf{x}}_j(kT_{period}+\varsigma_j) \\ \vdots \\ \bar{\mathbf{x}}_\theta\left(kT_{period}+\varsigma_\theta\right) \\ \bar{\mathbf{x}}_1((k+1)T_{period}+\varsigma_1) \\ \vdots \\ \bar{\mathbf{x}}_{j-1}((k+1)T_{period}+\varsigma_{j-1}) \end{bmatrix},\ \cdots,$$

$$\mathbf{x}(k,\theta)=\begin{bmatrix} \bar{\mathbf{x}}_\theta\left(kT_{period}+\varsigma_\theta\right) \\ \bar{\mathbf{x}}_1((k+1)T_{period}+\varsigma_1) \\ \vdots \\ \bar{\mathbf{x}}_{\theta-1}\left((k+1)T_{period}+\varsigma_{\theta-1}\right) \end{bmatrix},$$

it is clear that $\mathbf{x}(k,j)$ works like a buffer, in which all state variables in the time interval $[kT_{period}+\varsigma_j,(k+1)T_{period}+\varsigma_j)$ are saved. In the next time instant $kT_{period}+\varsigma_{j+1}$, the state variables at the time instant $kT_{period}+\varsigma_j$ are removed from the buffer and those at the time instant $(k+1)T_{period}+\varsigma_j$ are added. As a result, $\mathbf{x}(k,j+1)$ is formed, which includes all state variables in the time interval $[kT_{period}+\varsigma_{j+1},(k+1)T_{period}+\varsigma_{j+1})$. This procedure can be modeled by

$$\begin{aligned} \mathbf{x}(k,j+1)&=\mathbf{A}(j)\mathbf{x}(k,j)+\mathbf{B}(j)\mathbf{u}(k,j) \\ \mathbf{y}(k,j)&=\mathbf{C}(j)\mathbf{x}(k,j) \end{aligned} \tag{3.12}$$

where

$$\mathbf{A}(j) = \begin{bmatrix} \mathbf{0} & \mathbf{I} \\ \bar{\mathbf{A}}_{21}(j) & \bar{\mathbf{A}}_{22}(j) \end{bmatrix},\ \mathbf{B}(j) = \begin{bmatrix} \mathbf{0} \\ \bar{\mathbf{B}}_2(j) \end{bmatrix},\ \mathbf{C}(j) = \bar{\mathbf{C}}_2(j)$$

and

$$\bar{\mathbf{x}}_j((k+1)T_{period} + \varsigma_j) = \begin{bmatrix} \bar{\mathbf{A}}_{21}(j) & \bar{\mathbf{A}}_{22}(j) \end{bmatrix} \mathbf{x}(k,j) + \bar{\mathbf{B}}_2(j)\mathbf{u}(k,j) \quad (3.13)$$

Note that $\bar{\mathbf{x}}_j((k+1)T_{period} + \varsigma_j)$ is the last row block of $\mathbf{x}(k, j+1)$, as defined in (3.10). $\mathbf{y}(k,j)$ is composed of all output in the time interval $[(k+1)T_{period} + \varsigma_{j-1}, (k+1)T_{period} + \varsigma_j)$ and is only related with $\bar{\mathbf{x}}_{j-1}((k+1)T_{period} + \varsigma_{j-1})$. Suppose that $\mathbf{x}(k,j) \in \mathcal{R}^n$, $\mathbf{u}(k,j) \in \mathcal{R}^q$ and $\mathbf{y}(k,j) \in \mathcal{R}^{m(j)}$. Recall the dimensions of $\mathbf{x}_i(t)$, $\mathbf{u}_i(t)$ and $\mathbf{y}_i(t)$ for the i-th sub-system, it is easy to obtain that $n = \sum_{i=1}^{N} n_i l_i$, $q = \sum_{i=1}^{N} q_i l_i$ and $m(j) = \sum_{i \in I_{\varsigma_j}} m_i$.

For the purpose of determining matrices $\bar{\mathbf{A}}_{21}(j)$, $\bar{\mathbf{A}}_{22}(j)$, $\bar{\mathbf{B}}_2(j)$, $\bar{\mathbf{C}}(j)$, the sub-system model (3.7) is used. Assume that the i-th sub-system belongs to I_{ς_j}, i.e., $\mathbf{x}_i((k+1)T_{period} + \varsigma_j)$ is included in $\bar{\mathbf{x}}_j((k+1)T_{period} + \varsigma_j)$ and $\mathbf{y}_i((k+1)T_{period} + \varsigma_j - T_{cyc,i})$ is in $\mathbf{y}(k,j)$. It follows from (3.7) that

$$\begin{aligned}
&\mathbf{x}_i((k+1)T_{period} + \varsigma_j) \\
&= \mathbf{A}_{d,ii}\mathbf{x}_i\left((k+1)T_{period} + \varsigma_j - T_{cyc,i}\right) + \mathbf{B}_{d,i}\mathbf{u}_i((k+1)T_{period} + \varsigma_j - T_{cyc,i}) \\
&+ \sum_{l \neq i}^{N} \mathbf{A}_{d,il}((k+1)T_{period} + \varsigma_j - T_{cyc,i})\bar{\mathbf{x}}_l((k+1)T_{period} + \varsigma_j - T_{cyc,i}) \\
&\mathbf{y}_i((k+1)T_{period} + \varsigma_j - T_{cyc,i}) = \mathbf{C}_{d,i}\mathbf{x}_i((k+1)T_{period} + \varsigma_j - T_{cyc,i}) \qquad (3.14)
\end{aligned}$$

Since $\mathbf{x}_i\left((k+1)T_{period} + \varsigma_j - T_{cyc,i}\right)$, $\mathbf{x}_l((k+1)T_{period} + \varsigma_j - T_{cyc,i})$ are included in $\bar{\mathbf{x}}(k,j)$, $\mathbf{u}_i((k+1)T_{period} + \varsigma_j - T_{cyc,i})$ in $\mathbf{u}(k,j)$, the above equation can be further written into

$$\begin{aligned}
&\mathbf{x}_i((k+1)T_{period} + \varsigma_j) = \begin{bmatrix} \bar{\mathbf{A}}_{21,i}(j) & \bar{\mathbf{A}}_{22,i}(j) \end{bmatrix} \mathbf{x}(k,j) + \bar{\mathbf{B}}_{2,i}(j)\mathbf{u}(k,j) \\
&\mathbf{y}_i((k+1)T_{period} + \varsigma_j - T_{cyc,i}) = \bar{\mathbf{C}}_{2,i}(j)\mathbf{x}(k,j) \qquad (3.15)
\end{aligned}$$

where $\bar{\mathbf{A}}_{21,i}(j)$, $\bar{\mathbf{A}}_{22,i}(j)$, $\bar{\mathbf{B}}_{2,i}(j)$, $\bar{\mathbf{C}}_{2,i}(j)$ respectively consist of $\mathbf{A}_{d,ii}$, $\mathbf{A}_{d,il}((k+1)T_{period} + \varsigma_j - T_{cyc,i})$, $l \neq i$, $\mathbf{B}_{d,i}$, $\mathbf{C}_{d,i}$ and some zero matrices. Repeat this procedure for all state vectors included in $\bar{\mathbf{x}}_j((k+1)T_{period} + \varsigma_j)$ and all output

in $\mathbf{y}(k,j)$, it is obtained

$$\underbrace{\begin{bmatrix} \vdots \\ \mathbf{x}_i((k+1)T_{period}+\varsigma_j) \\ \vdots \end{bmatrix}}_{\bar{\mathbf{x}}_j((k+1)T_{period}+\varsigma_j)} = \underbrace{\begin{bmatrix} \vdots & \vdots \\ \bar{\mathbf{A}}_{21,i}(j) & \bar{\mathbf{A}}_{22,i}(j) \\ \vdots & \vdots \end{bmatrix}}_{\begin{bmatrix} \bar{\mathbf{A}}_{21}(j) & \bar{\mathbf{A}}_{22}(j) \end{bmatrix}} \mathbf{x}(k,j) + \underbrace{\begin{bmatrix} \vdots \\ \bar{\mathbf{B}}_{2,i}(j) \\ \vdots \end{bmatrix}}_{\bar{\mathbf{B}}_2(j)} \mathbf{u}(k,j)$$

$$\underbrace{\begin{bmatrix} \vdots \\ \mathbf{y}_i((k+1)T_{period}+\varsigma_j-T_{cyc,i}) \\ \vdots \end{bmatrix}}_{\mathbf{y}(k,j)} = \underbrace{\begin{bmatrix} \vdots \\ \bar{\mathbf{C}}_{2,i}(j) \\ \vdots \end{bmatrix}}_{\bar{\mathbf{C}}_2(j)} \mathbf{x}(k,j) \tag{3.16}$$

In this way, $\bar{\mathbf{A}}_{21}(j)$, $\bar{\mathbf{A}}_{22}(j)$, $\bar{\mathbf{B}}_2(j)$, $\bar{\mathbf{C}}_2(j)$ can be determined. It is clear that (3.12) is an LP system.

3.2 Problem formulation of decentralized W-NCSs

In order to achieve high reliability in one hand, and expand the system feasibility for industrial application domains as much as possible in the other hand, the decentralized W-NCSs structure [17], which is able to depict large-scale system with coupling between sub-systems, sketched in Fig. 3.4 is proposed. The structure also consists of three layers as centralized structure in Fig. 3.1, which can be described by

- *Execution layer:* In this layer to increase the system autonomy, the local controllers with the embedded sensors and actuators are introduced, which are integrated into (local) feedback CLs for three purposes: (a) ensure the system stability in the totally decentralized mode, i.e., in case of the communications failure between the CSs and CLs, (b) meet the real-time requirements and distributed synchronization, and (c) allow an early and simple FD in the local CLs.

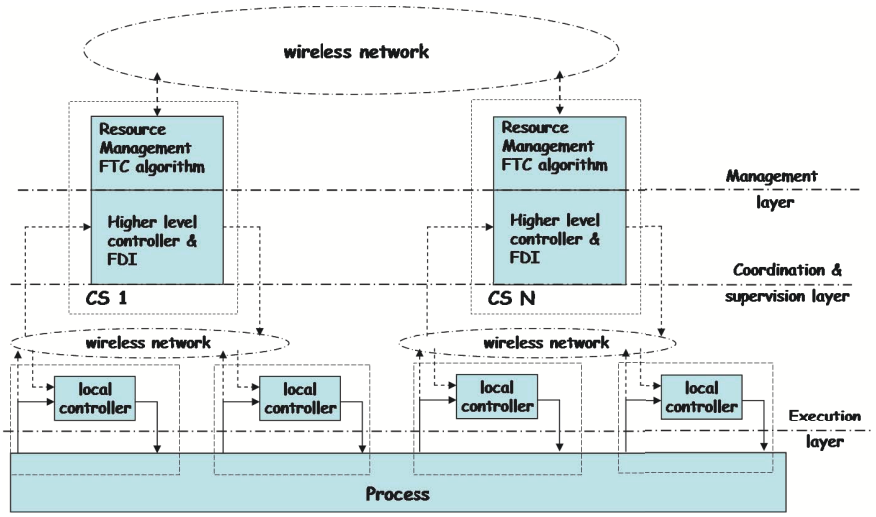

Figure 3.4: Fault tolerant decentralized W-NCSs structure

- *Coordination and supervision layer:* This layer consists of N CSs. A sub-system is consist of one CS and a number of (local) feedback CLs under the supervision of CS at the execution layer. Comparing with the coordinators in centralized structure, CSs work not only as routers, but also as controllers and observers. As routers, the N CSs will coordinate and synchronize the overall NCS aiming at sharing information, while as controllers and observers, CSs can execute advanced control and fault diagnosis by comprehensive control and FD algorithms.

- *Management layer:* In this layer, FTC is implemented in the context of resource management [67, 15]. The resource management scheme and the associated FTC algorithms are realized in a distributed manner and integrated into CSs. When a fault is alarmed by the diagnosis algorithm, a reconfiguration of the controllers, FD units and the communication protocols will be activated. The research of this layer is still under way.

The communication structure corresponding to this W-NCSs framework can be classified as:

- communications in a sub-system, which will operate in a master-slave mode with CS operating as a master.

- communications between the CSs, which serves as synchronization, new sub-system state broadcasting, and in case of fault, fault warning and

the activation and execution of FTC algorithms. The data exchanges at this layer are periodic and regulated by a protocol in the token passing mechanism.

Compared with the centralized system structure presented in Fig. 3.1, the main differences are that distributed system includes autonomous units (CLs) and distributed controllers, which also lead to the differences of communication scheme, especially the scheme between CSs. In the following, the description of modeling on communication scheme and system will focus mainly on the differences.

3.2.1 Modeling of communication schemes

According to the two kinds of communication forms, namely in a sub-system and between sub-systems, the approaches of communication scheduling scheme using TDMA mechanism are proposed separately. Due to the adoption of autonomous units (CLs) and distributed controllers, the autonomy, flexibility and expendability of the decentralized communication scheme can be greatly enforce comparing with the centralized one.

Communication modeling in a sub-system

Due to the adoption of autonomous units (CLs), the measurement packet is usually composed of more than one sensor's information. Assume that the length of each transmission signal doesn't exceed the packet maximal length, which is defined by protocol, so the transmission of every packet can be completed in one time slot. Under this assumption, the algorithm of deciding the cyclic time $T_{cyc,i}$ of i-th sub-system in (3.3) is still applicable for the sub-system of decentralized system. We have to point out that in this case M_i is the number of CLs in the i-th sub-system and the control command is also broadcasted by the i-th CS to the relative CLs.

The periodic scheduler for the local wireless data transmission is schematically shown in Fig. 3.5. The measurements are collected from CLs to the i-th CS at first. After certain reserved time slots, CS will broadcast the calculated control command to all CLs of i-th sub-system. Some time slots are again reserved after command transmission to guarantee the accuracy rate of transmission. The modification of use ACK packet fits also for the decentralized system, which is described in the modeling of communication scheme for centralized W-NCSs. Note that CL as s autonomous unit works as a sender as well as a receiver in the decentralized communication infrastructure.

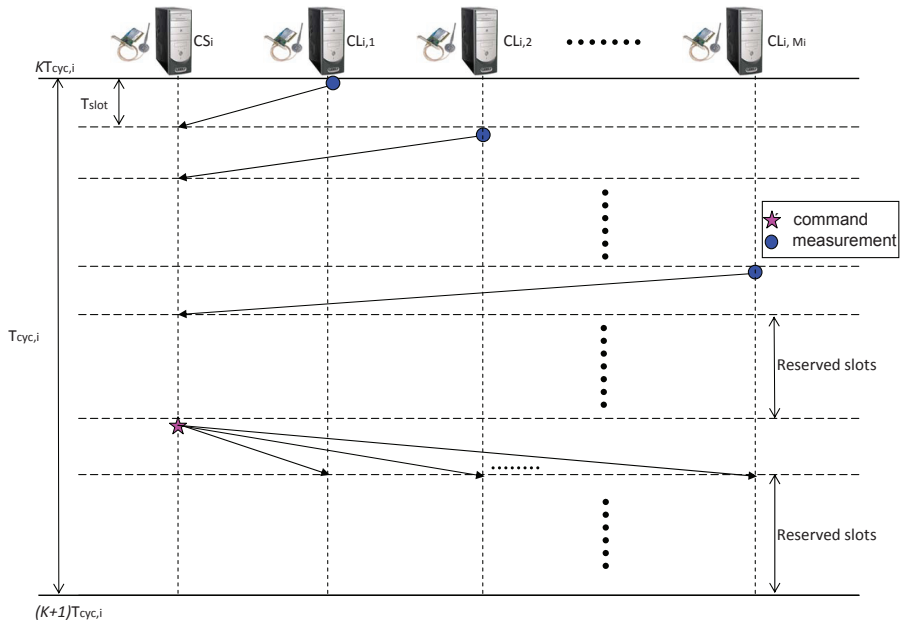

Figure 3.5: Scheduler for the i-th sub-system of decentralized W-NCSs

Communication modeling between sub-systems

The basic idea behind the scheduler between CSs is to ensure that each CS has sufficient knowledge of the state changes in all the other CSs, so the scheduler is proposed based on the principle that the i-th CS broadcasts its new state to all the other CSs every $T_{cyc,i}$. The period of whole distributed system T_{period} is the least common multiple (LCM) of sub-systems' sampling cycles, which accords with (3.5).

In the time interval $[kT_{period}, (k+1)T_{period})$, the i-th CS, $i = 1, \cdots, N$, will, in the broadcast mode, send the estimate for x_i to all other CSs at the time instants kT_{period}, $kT_{period} + T_{cyc,i}$, $\cdots$, $kT_{period} + (h/l_i - 1)T_{cyc,i}$. Fig. 3.6 shows an example of such a scheduler with $N = 3$, $l_1 = 2$, $l_2 = 3$, $l_3 = 6$ and $T_{period} = 6T_{cyc,\min}$.

Notice that at the time instants when the i-th CS broadcasts the updated state to all the other CSs, the control command is also broadcasted to local CLs of i-th sub-system simultaneously in the form of state, which isn't shown in Fig. 3.6. Assume that the state feedback control is employed. The value of control command can be calculated by local CLs using preset parameters. The schedule of specified time slots for control command can thus be canceled, which is beneficial for real-time purpose. When there are

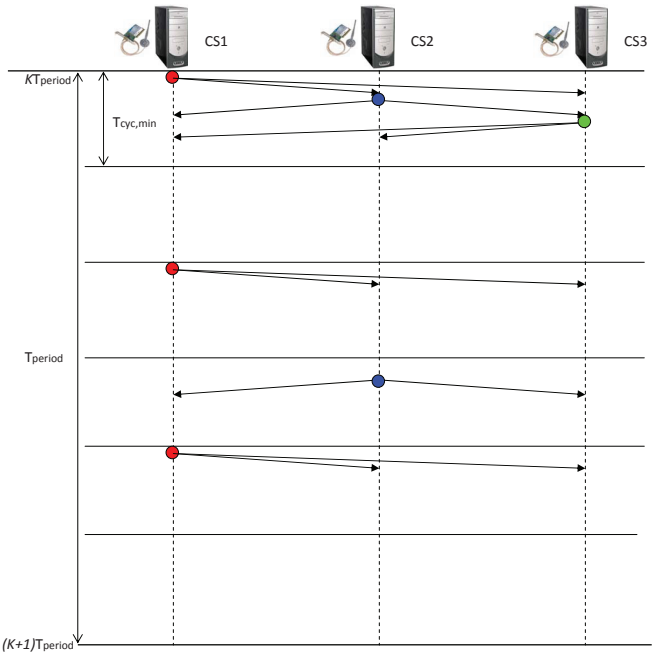

Figure 3.6: An example of scheduler between CSs

several updates in the same $T_{cyc,\min}$, the transmission sequence is decided by sub-system's priority. The control and fault diagnosis algorithm is activated in every arithmetic unit after the successful transmission of all scheduled CSs in this period.

3.2.2 Modeling of decentralized W-NCSs

Modeling of a sub-system

The main difference of the modeling for the i-th sub-system exists on the dimensions of variables. In (3.6), n_i, q_i and m_i are the dimensions of state, control input and measurement output, respectively. q_i and m_i are also the numbers of actuators and sensors in the i-th sub-system. While in the decentralized structure, the i-th CS communicates directly with CLs, so the control input and measurement output related with M_i, which is the number of CL in this sub-system, can be expressed by

$$\mathbf{u}_i = \begin{bmatrix} u_{i1} \\ \vdots \\ u_{iM_i} \end{bmatrix}, \; u_{ij} \in \mathcal{R}^{q_{ij}}, \; \sum_{j=1}^{M_i} q_{ij} = q_i \; , i = 1, \cdots, N$$

and

$$\mathbf{y}_i = \begin{bmatrix} y_{i1} \\ \vdots \\ y_{iM_i} \end{bmatrix},\ y_{ij} \in \mathcal{R}^{m_{ij}},\ \sum_{j=1}^{M_i} m_{ij} = m_i$$

The matrix $\mathbf{B}_i$ can be further expressed into

$$\mathbf{B}_i = \begin{bmatrix} B_{i1} & \cdots & B_{iM_i} \end{bmatrix}$$

in according with the structure of u_i, and the output equation can also be reformulated from the view of independent CLs into

$$y_{ij}(t) = \mathbf{C}_{ij}\mathbf{x}_i(t),\ i = 1, \cdots, N,\ j = 1, \cdots, M_i$$

where u_{ij}, y_{ij} denote the actuator and sensor signals embedded in the j-th control loop of the i-th sub-system.

After noticing the dimension differences caused by the employment of CLs, the model of the i-th sub-system can still described by (3.6), since $\mathbf{u}_i$ and $\mathbf{y}_i$ are treated as elementary variables, and the internal structure of the variables won't effect the modeling of sub-system. For the same reason, the sub-system's model can also be discretized by (3.7).

Modeling of overall W-NCSs

Based on the model of sub-system in (3.7) and the coupling relations between sub-systems, the lifted vector of states during one T_{period} is first introduced as in (3.10), and the model of overall W-NCSs is formulated into (3.12), which is exactly the same as for the centralized case. Notice that the overall system modeling approach in this chapter is developed to describe the system composed of several coupling sub-systems with multirate sampling. The coupling relations and milti-sampling scheme make no difference between centralized and decentralized system, so the model isn't affected by the system structure, decentralized or centralized. Hence the modeling process for the decentralized W-NCS is the same as for the centralized W-NCS.

Remark 1 *When designing the system observer, the system model will be slightly reformulated to be fit for the design issues. For example, the definition of* $\mathbf{y}(k, j)$ *in (3.16) is influenced by the observer's structure. From (3.16), it is easy to obtained that the definition of* $\mathbf{y}(k, j)$ *depends on the setting of* $\bar{\mathbf{C}}_2(j)$*. When* $\mathbf{y}(k, j)$ *is composed of all output in the time interval* $[(k+1)T_{period} + \varsigma_{j-1}, (k+1)T_{period} + \varsigma_j)$*,* $\bar{\mathbf{C}}_2(j) \in \mathcal{R}^{m(j)\times n}$*. The dimension of* $\mathbf{y}(k, j)$ *is varying in this case. When* $\mathbf{y}(k, j)$ *includes all output in the time interval* $[kT_{period} + \varsigma_j, (k+1)T_{period} + \varsigma_j)$*,* $\bar{\mathbf{C}}_2(j) \in \mathcal{R}^{m\times n}$ *with invariant*

dimension, where $m = \sum_{i=1}^{N} m_i l_i$. *This structure of* $\mathbf{y}(k,j)$, *which can store all output in the last* T_{period}, *is very important to design the system observer with shared residual, which will be discussed in the following chapter.*

Example 1 *To illustrate the model (3.12) and the determination of* $\bar{\mathbf{A}}_{21}(j)$, $\bar{\mathbf{A}}_{22}(j), \bar{\mathbf{B}}_2(j), \bar{\mathbf{C}}_2(j)$, *the example given in Fig. 3.6, where* $N = 3$, $l_1 = 2$, $l_2 = 3$, $l_3 = 6$, *is again considered. It holds for Definition 1 that,*

$$\begin{aligned}
&\theta = 4,\ \varsigma_1 = 0,\ \varsigma_2 = 2T_{cyc,\min},\\
&\varsigma_3 = 3T_{cyc,\min},\ \varsigma_4 = 4T_{cyc,\min},\\
&I_{\varsigma_1} = \{1,2,3\},\ I_{\varsigma_2} = \{1\},\\
&I_{\varsigma_3} = \{2\},\ I_{\varsigma_4} = \{1\}
\end{aligned}$$

As a result, the following state variables are lifted into a vector

$$\begin{aligned}
\bar{\mathbf{x}}_1((k+1)T_{period} + \varsigma_1) &= \begin{bmatrix} \mathbf{x}_1((k+1)T_{period}) \\ \mathbf{x}_2((k+1)T_{period}) \\ \mathbf{x}_3((k+1)T_{period}) \end{bmatrix},\\
\bar{\mathbf{x}}_2((k+1)T_{period} + \varsigma_2) &= \mathbf{x}_1((k+1)T_{period} + 2T_{cyc,\min}),\\
\bar{\mathbf{x}}_3((k+1)T_{period} + \varsigma_3) &= \mathbf{x}_2((k+1)T_{period} + 3T_{cyc,\min}),\\
\bar{\mathbf{x}}_4((k+1)T_{period} + \varsigma_4) &= \mathbf{x}_1((k+1)T_{period} + 4T_{cyc,\min})
\end{aligned}$$

and output variables corresponding to (3.12) for $j = 1, \cdots, 4$,

$$\begin{aligned}
\bar{\mathbf{y}}_4(kT_{period} + \varsigma_4) &= \begin{bmatrix} \mathbf{y}_1(kT_{period} + 4T_{cyc,\min}) \\ \mathbf{y}_2(kT_{period} + 4T_{cyc,\min}) \\ \mathbf{y}_3(kT_{period} + 4T_{cyc,\min}) \end{bmatrix},\\
\bar{\mathbf{y}}_1((k+1)T_{period} + \varsigma_1) &= \mathbf{y}_1((k+1)T_{period}),\\
\bar{\mathbf{y}}_2((k+1)T_{period} + \varsigma_2) &= \mathbf{y}_2((k+1)T_{period} + 2T_{cyc,\min}),\\
\bar{\mathbf{y}}_3((k+1)T_{period} + \varsigma_3) &= \mathbf{y}_1((k+1)T_{period} + 3T_{cyc,\min}).
\end{aligned}$$

Let $\tau = (k+1)T_{period}$, $\gamma = kT_{period}$, *the state equations of every sub-system at each discrete time during one overall period are obtained*

$$\begin{aligned}
&\mathbf{x}_1(\tau + \varsigma_1)\\
&= \mathbf{A}_{d,11}\mathbf{x}_1(\gamma + \varsigma_4) + \mathbf{B}_{d,1}\mathbf{u}_1(\gamma + \varsigma_4)\\
&\quad + \mathbf{A}_{d,12}(\tau + \varsigma_1)\mathbf{x}_2(\gamma + \varsigma_3) + \mathbf{A}_{d,13}(\tau + \varsigma_1)\mathbf{x}_3(\gamma + \varsigma_1),\\
&\mathbf{x}_1(\tau + \varsigma_2)\\
&= \mathbf{A}_{d,11}\mathbf{x}_1(\tau + \varsigma_1) + \mathbf{B}_{d,1}\mathbf{u}_1(\tau + \varsigma_1)\\
&\quad + \mathbf{A}_{d,12}(\tau + \varsigma_2)\mathbf{x}_2(\tau + \varsigma_1) + \mathbf{A}_{d,13}(\tau + \varsigma_2)\mathbf{x}_3(\tau + \varsigma_1),
\end{aligned}$$

$$
\begin{aligned}
&\mathbf{x}_1(\tau+\varsigma_4)\\
&=\mathbf{A}_{d,11}\mathbf{x}_1(\tau+\varsigma_2)+\mathbf{B}_{d,1}\mathbf{u}_1(\tau+\varsigma_2)\\
&\quad+\mathbf{A}_{d,12}\left(\tau+\varsigma_4\right)\left[\begin{array}{c}\mathbf{x}_2\left(\tau+\varsigma_1\right)\\ \mathbf{x}_2(\tau+\varsigma_3)\end{array}\right]+\mathbf{A}_{d,13}(\tau+\varsigma_4)\mathbf{x}_3(\tau+\varsigma_1),\\
&\mathbf{x}_2(\tau+\varsigma_1)\\
&=\mathbf{A}_{d,22}\mathbf{x}_2(\gamma+\varsigma_3)+\mathbf{B}_{d,2}\mathbf{u}_2(\gamma+\varsigma_3)\\
&\quad+\mathbf{A}_{d,21}(\tau+\varsigma_1)\left[\begin{array}{c}\mathbf{x}_1(\gamma+\varsigma_2)\\ \mathbf{x}_1(\gamma+\varsigma_4)\end{array}\right]+\mathbf{A}_{d,23}(\tau+\varsigma_1)\mathbf{x}_3(\gamma+\varsigma_1),\\
&\mathbf{x}_2(\tau+\varsigma_3)\\
&=\mathbf{A}_{d,22}\mathbf{x}_2(\tau+\varsigma_1)+\mathbf{B}_{d,2}\mathbf{u}_2(\tau+\varsigma_1)\\
&\quad+\mathbf{A}_{d,21}(\tau+\varsigma_3)\left[\begin{array}{c}\mathbf{x}_1(\tau+\varsigma_1)\\ \mathbf{x}_1(\tau+\varsigma_2)\end{array}\right]+\mathbf{A}_{d,23}(\tau+\varsigma_3)\mathbf{x}_3(\tau+\varsigma_1),\\
&\mathbf{x}_3(\tau+\varsigma_1)\\
&=\mathbf{A}_{d,33}\mathbf{x}_3(\gamma+\varsigma_1)+\mathbf{B}_{d,3}\mathbf{u}_3(\gamma+\varsigma_1)\\
&\quad+\mathbf{A}_{d,31}(\tau+\varsigma_1)\left[\begin{array}{c}\mathbf{x}_1(\gamma+\varsigma_1)\\ \mathbf{x}_1(\gamma+\varsigma_2)\\ \mathbf{x}_1(\gamma+\varsigma_4)\end{array}\right]+\mathbf{A}_{d,32}(\tau+\varsigma_1)\left[\begin{array}{c}\mathbf{x}_2(\gamma+\varsigma_1)\\ \mathbf{x}_2(\gamma+\varsigma_3)\end{array}\right],
\end{aligned}
$$

where

$$
\begin{aligned}
&\mathbf{A}_{d,12}\left(\tau+\varsigma_1\right)=\mathbf{A}_{d,12}\left(\tau+\varsigma_2\right)=\mathbf{A}_{d,120},\\
&\mathbf{A}_{d,12}\left(\tau+\varsigma_4\right)=\left[\begin{array}{cc}\mathbf{A}_{d,121} & \mathbf{A}_{d,122}\end{array}\right],\\
&\mathbf{A}_{d,13}(\tau+\varsigma_1)=\mathbf{A}_{d,13}(\tau+\varsigma_2)=\mathbf{A}_{d,13}(\tau+\varsigma_4)=\mathbf{A}_{d,13},\\
&\mathbf{A}_{d,21}(\tau+\varsigma_1)=\left[\begin{array}{cc}\mathbf{A}_{d,211} & \mathbf{A}_{d,212}\end{array}\right],\\
&\mathbf{A}_{d,21}(\tau+\varsigma_3)=\left[\begin{array}{cc}\mathbf{A}_{d,212} & \mathbf{A}_{d,211}\end{array}\right],\\
&\mathbf{A}_{d,23}(\tau+\varsigma_1)=\mathbf{A}_{d,23}(\tau+\varsigma_3)=\mathbf{A}_{d,23}\\
&\mathbf{A}_{d,31}(\tau+\varsigma_1)=\left[\begin{array}{ccc}\mathbf{A}_{d,311} & \mathbf{A}_{d,312} & \mathbf{A}_{d,313}\end{array}\right],\\
&\mathbf{A}_{d,32}(\tau+\varsigma_1)=\left[\begin{array}{cc}\mathbf{A}_{d,321} & \mathbf{A}_{d,322}\end{array}\right].
\end{aligned}
$$

According to the definition of parameters in (3.8), it is easy to obtain

$$
\mathbf{A}_{d,120}=\int_0^{T_{cyc,1}} e^{\mathbf{A}_{11}(T_{cyc,1}-\tau)}\mathbf{A}_{12}d\tau,
$$

$$
\mathbf{A}_{d,121}=\mathbf{A}_{d,122}=\int_0^{T_{cyc,\min}} e^{\mathbf{A}_{11}(T_{cyc,1}-\tau)}\mathbf{A}_{12}d\tau,
$$

$$\mathbf{A}_{d,13} = \int_0^{T_{cyc,1}} e^{\mathbf{A}_{11}(T_{cyc,1}-\tau)}\mathbf{A}_{13}d\tau,$$

$$\mathbf{A}_{d,211} = \int_0^{T_{cyc,\min}} e^{\mathbf{A}_{22}(T_{cyc,2}-\tau)}\mathbf{A}_{21}d\tau,$$

$$\mathbf{A}_{d,212} = \int_0^{2T_{cyc,\min}} e^{\mathbf{A}_{22}(T_{cyc,2}-\tau)}\mathbf{A}_{21}d\tau,$$

$$\mathbf{A}_{d,23} = \int_0^{T_{cyc,2}} e^{\mathbf{A}_{22}(T_{cyc,2}-\tau)}\mathbf{A}_{23}d\tau,$$

$$\mathbf{A}_{d,311} = \mathbf{A}_{d,312} = \mathbf{A}_{d,313} = \int_0^{T_{cyc,1}} e^{\mathbf{A}_{33}(T_{cyc,3}-\tau)}\mathbf{A}_{31}d\tau,$$

$$\mathbf{A}_{d,321} = \mathbf{A}_{d,322} = \int_0^{T_{cyc,2}} e^{\mathbf{A}_{33}(T_{cyc,3}-\tau)}\mathbf{A}_{32}d\tau$$

The parameters of (3.16) are shown in the following

$$\begin{bmatrix} \bar{\mathbf{A}}_{21}(1) & \bar{\mathbf{A}}_{22}(1) \end{bmatrix} = \begin{bmatrix} \mathbf{0} & \mathbf{0} & \mathbf{A}_{d,13} & \mathbf{0} & \mathbf{A}_{d,120} & \mathbf{A}_{d,11} \\ \mathbf{0} & \mathbf{0} & \mathbf{A}_{d,23} & \mathbf{A}_{d,211} & \mathbf{A}_{d,22} & \mathbf{A}_{d,212} \\ \mathbf{A}_{d,311} & \mathbf{A}_{d,321} & \mathbf{A}_{d,33} & \mathbf{A}_{d,312} & \mathbf{A}_{d,322} & \mathbf{A}_{d,313} \end{bmatrix},$$

$$\begin{bmatrix} \bar{\mathbf{A}}_{21}(2) & \bar{\mathbf{A}}_{22}(2) \end{bmatrix} = \begin{bmatrix} \mathbf{0} & \mathbf{0} & \mathbf{0} & \mathbf{A}_{d,11} & \mathbf{A}_{d,120} & \mathbf{A}_{d,13} \end{bmatrix},$$

$$\begin{bmatrix} \bar{\mathbf{A}}_{21}(3) & \bar{\mathbf{A}}_{22}(3) \end{bmatrix} = \begin{bmatrix} \mathbf{0} & \mathbf{0} & \mathbf{A}_{d,212} & \mathbf{A}_{d,22} & \mathbf{A}_{d,23} & \mathbf{A}_{d,211} \end{bmatrix},$$

$$\begin{bmatrix} \bar{\mathbf{A}}_{21}(4) & \bar{\mathbf{A}}_{22}(4) \end{bmatrix} = \begin{bmatrix} \mathbf{0} & \mathbf{0} & \mathbf{A}_{d,121} & \mathbf{A}_{d,13} & \mathbf{A}_{d,11} & \mathbf{A}_{d,122} \end{bmatrix},$$

$$\bar{\mathbf{B}}_2(1) = \begin{bmatrix} \mathbf{0} & \mathbf{0} & \mathbf{0} & \mathbf{0} & \mathbf{0} & \mathbf{B}_{d,1} \\ \mathbf{0} & \mathbf{0} & \mathbf{0} & \mathbf{0} & \mathbf{B}_{d,2} & \mathbf{0} \\ \mathbf{0} & \mathbf{0} & \mathbf{B}_{d,3} & \mathbf{0} & \mathbf{0} & \mathbf{0} \end{bmatrix},$$

$$\bar{\mathbf{B}}_2(2) = \begin{bmatrix} \mathbf{0} & \mathbf{0} & \mathbf{0} & \mathbf{B}_{d,1} & \mathbf{0} & \mathbf{0} \end{bmatrix},$$

$$\bar{\mathbf{B}}_2(3) = \begin{bmatrix} \mathbf{0} & \mathbf{0} & \mathbf{0} & \mathbf{B}_{d,2} & \mathbf{0} & \mathbf{0} \end{bmatrix},$$

$$\bar{\mathbf{B}}_2(4) = \begin{bmatrix} \mathbf{0} & \mathbf{0} & \mathbf{0} & \mathbf{0} & \mathbf{B}_{d,1} & \mathbf{0} \end{bmatrix},$$

$$\bar{\mathbf{C}}_2(1) = \begin{bmatrix} \mathbf{0} & \mathbf{0} & \mathbf{0} & \mathbf{0} & \mathbf{0} & \mathbf{C}_{d,1} \\ \mathbf{0} & \mathbf{0} & \mathbf{0} & \mathbf{0} & \mathbf{C}_{d,2} & \mathbf{0} \\ \mathbf{0} & \mathbf{0} & \mathbf{C}_{d,3} & \mathbf{0} & \mathbf{0} & \mathbf{0} \end{bmatrix},$$
$$\bar{\mathbf{C}}_2(2) = \begin{bmatrix} \mathbf{0} & \mathbf{0} & \mathbf{0} & \mathbf{C}_{d,1} & \mathbf{0} & \mathbf{0} \end{bmatrix},$$
$$\bar{\mathbf{C}}_2(3) = \begin{bmatrix} \mathbf{0} & \mathbf{0} & \mathbf{0} & \mathbf{C}_{d,2} & \mathbf{0} & \mathbf{0} \end{bmatrix},$$
$$\bar{\mathbf{C}}_2(4) = \begin{bmatrix} \mathbf{0} & \mathbf{0} & \mathbf{0} & \mathbf{0} & \mathbf{C}_{d,1} & \mathbf{0} \end{bmatrix}.$$

By properly setting the $\mathbf{0}$ *and* $\mathbf{1}$ *block matrices and combining with* $\bar{\mathbf{A}}_{21}(j)$, $\bar{\mathbf{A}}_{22}(j)$, $\bar{\mathbf{B}}_2(j)$, $\bar{\mathbf{C}}_2(j)$, *the parameter matrices* $\mathbf{A}(j)$, $\mathbf{B}(j)$ *and* $\mathbf{C}(j)$ *in (3.12) can thus be determined. Until now, the overall system modeling based on the scheduler shown in Figs. 3.3 and 3.6 is completed.*

3.3 Modeling example on three-tank system

To illustrate the modeling procedure of industrial automatic process, the three-tank system with multi-rate sampling will be utilized. A brief introduction of the three-tank system will be first presented. The three-tank system, which is shown in Fig. 3.7, includes three plexiglas tanks, which are interconnected in series by two pipes. The liquid is injected into tank 1 and tank 2 by two pumps, and is ejected through the outflow pipe of tank 2. The liquid heights of tank 1 and tank 2 are controlled by the two pumps, while the level of tank 3 is uncontrollable, which is decoupled with the levels of tank 1 and tank 2. Each of three tanks is equipped with a piezoresistive pressure transducer to measure the level of the corresponding tank, which should be accurately detected for control purpose. Referring to the structures of centralized and decentralized W-NCSs, each tank is considered as a sub-system and the interactions are caused by the adjacent pipes. The continuous-time model of the three-tank system will be first proposed, then it will be discretized into periodic system based on the multirate sampling.

The continuous-time model of the three-tank system after linearization can be modeled as follows

$$\begin{bmatrix} \dot{x}_1(t) \\ \dot{x}_2(t) \\ \dot{x}_3(t) \end{bmatrix} = \begin{bmatrix} -A_{13} & 0 & A_{13} \\ 0 & -A_2 - A_{32} & A_{32} \\ A_{13} & A_{32} & -A_{32} - A_{13} \end{bmatrix} \begin{bmatrix} x_1(t) \\ x_2(t) \\ x_3(t) \end{bmatrix} + \begin{bmatrix} B_1 & 0 \\ 0 & B_2 \\ 0 & 0 \end{bmatrix} \begin{bmatrix} u_1(t) \\ u_2(t) \end{bmatrix} + \begin{bmatrix} d_1(t) \\ d_2(t) \\ d_3(t) \end{bmatrix}$$

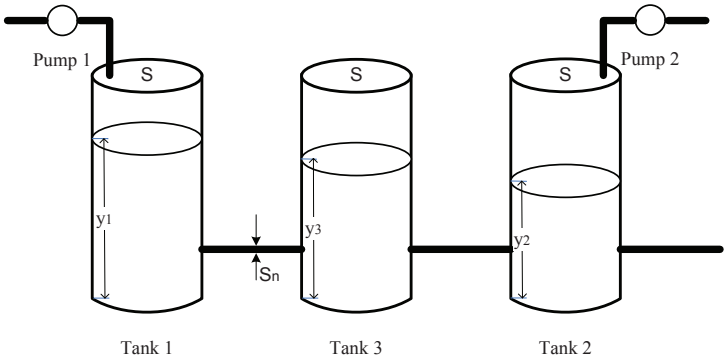

Figure 3.7: Three-tank system setup

$$\begin{bmatrix} y_1(t) \\ y_2(t) \\ y_3(t) \end{bmatrix} = \begin{bmatrix} 1 & 0 & 0 \\ 0 & 1 & 0 \\ 0 & 0 & 1 \end{bmatrix} \begin{bmatrix} x_1(t) \\ x_2(t) \\ x_3(t) \end{bmatrix} + \begin{bmatrix} v_1(t) \\ v_2(t) \\ v_3(t) \end{bmatrix} \tag{3.17}$$

where

$$\begin{aligned} A_{13} &= \frac{1}{S} a_1 s_n \sqrt{\frac{g}{2(x_{10} - x_{30})}},\ A_2 = \frac{1}{S} a_2 s_n \sqrt{\frac{g}{2x_{20}}}, \\ A_{32} &= \frac{1}{S} a_3 s_n \sqrt{\frac{g}{2(x_{30} - x_{20})}},\ B_1 = B_2 = \frac{1}{S} \end{aligned} \tag{3.18}$$

- $x_i(t) = y_i(t),\ i = 1, 2, 3$ is the water level of i-th tank (m);
- $u_i(t),\ i = 1, 2$ is the incoming flow rate of i-th pump (m^3/s);
- S is the cross section area of tanks (m^2);
- $d_i(t),\ i = 1, 2, 3$ is the driving disturbance caused by water surface fluctuation when water is poured into 1-th and 2-th tanks by pumps;
- $v_i(t),\ i = 1, 2, 3$ is the measurement disturbance caused by sensor properties;
- $a_i,\ i = 1, 2, 3$ is the outflow coefficient of the i-th tank;
- s_n is the cross section area of pipes (m^2);
- $x_0 = [x_{10}, x_{20}, x_{30}]^T$ is the operating point. Set $x_{10} = 0.3\mathrm{m},\ x_{20} = 0.2\mathrm{m}$, $x_{30} = 0.25\mathrm{m}$.

Considering that the three sensors are sampled with different sampling rates, the system can be discretized into periodic system. The multirate mechanism here is set to $T_{cyc,1} = 8\text{ms},\ T_{cyc,2} = 12\text{ms},\ T_{cyc,3} = 24\text{ms}$ where $T_{cyc,i},\ i = 1, 2, 3$ are the sampling cycles of i-th sensor, whose definition is equivalent to the cyclic time of the i-th sub-system for three-tank system. The period of whole system T_{period}, $T_{period} = 24\text{ms}$, is the LCM of sensors' sampling cycles.

The scheduler of sensor-to-controller and controller-to-actuator in one T_{period}, which is shown specifically in Fig. 3.8, is presented according to the multirate sampling structure. The control signal is broadcasted after all measurements have been scheduled. The scheduling scenario is under the assumption that the length of each transmission signal doesn't exceed the packet maximal length, which is defined by protocol, so the transmission of every signal can be completed in one time slot. $T_{cyc,min}$ is the GCD of sensors' sampling cycles and is treated as basic process unit. In this case, $T_{cyc,min} = 4\text{ms}$ and the time slot is set to 1ms, which means in every $T_{cyc,min}$, 4 transmission packets can be scheduled. $j,\ j = 0, 1, 2, 3$ is used to denote the arithmetic unit, which is a process unit with transmission tasks of measurements. For the sake of simple notation, $\varsigma_j,\ j = 0, 1, 2, 3$ denotes the time instant of arithmetic unit, which has transmission tasks from beginning of k-th T_{period}. In this case, $\varsigma_0 = 0,\ \varsigma_1 = 2T_{cyc,min},\ \varsigma_2 = 3T_{cyc,min}$ and $\varsigma_3 = 4T_{cyc,min}$.

The periodic system induced by multirate sampling is modeled in k-th main period T_{period} as follows

$$
\begin{aligned}
x_1(kT_{period} + T_{cyc,1}) =& x_1(k, 1) \\
=& A_{d,11}x_1(k, 0) + A_{d,13}x_3(k, 0) \\
&+ B_{d,1}u_1(k, 0) + B_{d,d1}d_1(k, 0), \\
x_2(kT_{period} + T_{cyc,2}) =& x_2(k, 2) \\
=& A_{d,22}x_2(k, 0) + A_{d,23}x_3(k, 0) \\
&+ B_{d,2}u_2(k, 0) + B_{d,d2}d_2(k, 0), \\
x_1(kT_{period} + 2T_{cyc,1}) =& x_1(k, 3) \\
=& A_{d,11}x_1(k, 1) + A_{d,13}x_3(k, 0) \\
&+ B_{d,1}u_1(k, 1) + B_{d,d1}d_1(k, 1), \\
x_1(kT_{period} + 3T_{cyc,1}) =& x_1(k + 1, 0) \\
=& A_{d,11}x_1(k, 3) + A_{d,13}x_3(k, 0) \\
&+ B_{d,1}u_1(k, 3) + B_{d,d1}d_1(k, 3),
\end{aligned}
$$

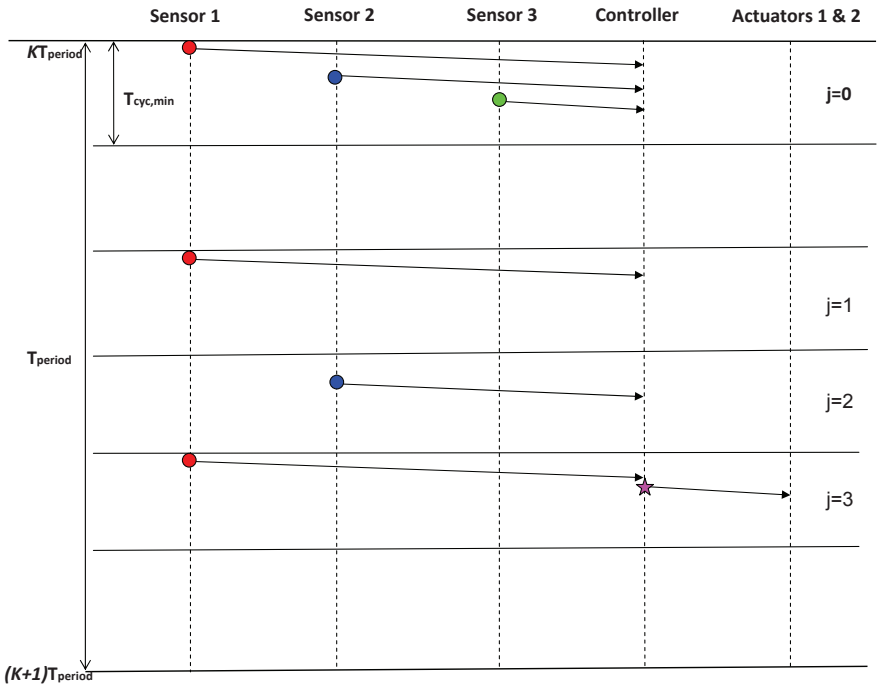

Figure 3.8: Network scheduler of three-tank system based on sampling

$$
\begin{aligned}
x_2(kT_{period}+2T_{cyc,2}) =& x_2(k+1,0)\\
=& A_{d,22}x_2(k,2)+A_{d,23}x_3(k,0)\\
&+B_{d,2}u_2(k,2)+B_{d,d2}d_2(k,2),\\
x_3(kT_{period}+T_{cyc,3}) =& x_3(k+1,0)\\
=& A_{d,33}x_3(k,0)++B_{d,d3}d_3(k,0)\\
&+\begin{bmatrix} A_{d,311} & A_{d,312} & A_{d,313}\end{bmatrix}\begin{bmatrix} x_1(k,0)\\ x_1(k,1)\\ x_1(k,3)\end{bmatrix}\\
&+\begin{bmatrix} A_{d,321} & A_{d,322}\end{bmatrix}\begin{bmatrix} x_2(k,0)\\ x_2(k,2)\end{bmatrix}
\end{aligned}
\tag{3.19}
$$

where

$$
\begin{aligned}
&A_{d,11}=e^{-A_{13}T_{cyc,1}},\ A_{d,22}=e^{-(A_2+A_{32})T_{cyc,2}},\ A_{d,33}=e^{-(A_{32}+A_{13})T_{cyc,3}},\\
&e_{13}=\int_0^{T_{cyc,1}} e^{-A_{13}(T_{cyc,1}-\tau)}d\tau,\ B_{d,1}=e_{13}B_1,\ A_{d,13}=e_{13}A_{13},\\
&e_{23}=\int_0^{T_{cyc,2}} e^{-(A_2+A_{32})(T_{cyc,2}-\tau)}d\tau,\ B_{d,2}=e_{23}B_2,\ A_{d,23}=e_{23}A_{32},
\end{aligned}
$$

$$e_{311} = \int_0^{T_{cyc,1}} e^{-(A_{32}+A_{13})(T_{cyc,3}-\tau)}d\tau,\ A_{d,311} = e_{311}A_{13},$$
$$e_{312} = \int_{T_{cyc,1}}^{2T_{cyc,1}} e^{-(A_{32}+A_{13})(T_{cyc,3}-\tau)}d\tau,\ A_{d,312} = e_{312}A_{13},$$
$$e_{313} = \int_{2T_{cyc,1}}^{T_{cyc,3}} e^{-(A_{32}+A_{13})(T_{cyc,3}-\tau)}d\tau,\ A_{d,313} = e_{313}A_{13},$$
$$e_{321} = \int_0^{T_{cyc,2}} e^{-(A_{32}+A_{13})(T_{cyc,3}-\tau)}d\tau,\ A_{d,321} = e_{321}A_{32},$$
$$e_{322} = \int_{T_{cyc,2}}^{T_{cyc,3}} e^{-(A_{32}+A_{13})(T_{cyc,3}-\tau)}d\tau,\ A_{d,322} = e_{322}A_{32},$$
$$B_{d,d1} = e_{13},\ B_{d,d2} = e_{23},\ B_{d,d3} = \int_0^{T_{cyc,3}} e^{-(A_{32}+A_{13})(T_{cyc,3}-\tau)}d\tau,$$

and $x_i(k,j),\ i=1,2,3,\ j=0,1,2,3$ is the water level of i-th tank at time instant $kT_{period}+\varsigma_j$, $u_i(k,j),\ i=1,2,\ j=0,1,2,3$ is the input flow rates of i-th pump at $kT_{period}+\varsigma_j$, and $d_i(k,j),\ i=1,2,3,\ j=0,1,2,3$ is the driving disturbance of i-th tank at $kT_{period}+\varsigma_j$.

To formulate the discretized model of whole three-tank system, the system states in (3.19), which are updated during one T_{period}, are lifted in accordance with the time sequence as follows

$$\mathbf{x}(k,0) = \begin{bmatrix} x_1(k-1,1) \\ x_2(k-1,2) \\ x_1(k-1,3) \\ x_1(k,0) \\ x_2(k,0) \\ x_3(k,0) \end{bmatrix},\ \mathbf{x}(k,1) = \begin{bmatrix} x_2(k-1,2) \\ x_1(k-1,3) \\ x_1(k,0) \\ x_2(k,0) \\ x_3(k,0) \\ x_1(k,1) \end{bmatrix},$$
$$\mathbf{x}(k,2) = \begin{bmatrix} x_1(k-1,3) \\ x_1(k,0) \\ x_2(k,0) \\ x_3(k,0) \\ x_1(k,1) \\ x_2(k,2) \end{bmatrix},\ \mathbf{x}(k,3) = \begin{bmatrix} x_1(k,0) \\ x_2(k,0) \\ x_3(k,0) \\ x_1(k,1) \\ x_2(k,2) \\ x_1(k,3) \end{bmatrix}.$$

Until now, the three-tank system is described by a periodic model

$$\begin{aligned} \mathbf{x}(k,j+1) &= \mathbf{A}(j)\mathbf{x}(k,j) + \mathbf{B}(j)\mathbf{u}(k,j) + \mathbf{B}_d(j)\mathbf{d}(k,j) \\ \mathbf{y}(k,j) &= \mathbf{C}(j)\mathbf{x}(k,j),\ j=0,1,2,3 \end{aligned} \tag{3.20}$$

where $\mathbf{x}(k,j) \in \mathcal{R}^6$ and $\mathbf{d}(k,j) \in \mathcal{R}^6$ are vectors of state variables and process noises in the time interval $[kT_{period}+\varsigma_j, (k+1)T_{period}+\varsigma_j)$. $\mathbf{u}(k,j)$ is

calculated by PI controller according to the differences between the measurements at kT_{period} and the operating points, so $\mathbf{u}(k,j) = \begin{bmatrix} u_1(k) \\ u_2(k) \end{bmatrix} \in \mathcal{R}^2$ is set to constant during kT_{period}. $\mathbf{y}(k,j)$ is the vector of latest detected water level(s). The dimension of measurement disturbance $\mathbf{v}(k,j)$ is the same as $\mathbf{y}(k,j)$.

The matrices of 4-periodic system are listed as follows

$$\mathbf{A}(0) = \begin{bmatrix} 0 & 1 & 0 & 0 & 0 & 0 \\ 0 & 0 & 1 & 0 & 0 & 0 \\ \vdots & \vdots & \vdots & \vdots & \vdots & \vdots \\ 0 & 0 & 0 & 0 & 0 & 1 \\ 0 & 0 & 0 & A_{d,11} & 0 & A_{d,13} \end{bmatrix}, \quad \mathbf{A}(1) = \begin{bmatrix} 0 & 1 & 0 & 0 & 0 & 0 \\ 0 & 0 & 1 & 0 & 0 & 0 \\ \vdots & \vdots & \vdots & \vdots & \vdots & \vdots \\ 0 & 0 & 0 & 0 & 0 & 1 \\ 0 & 0 & 0 & A_{d,22} & A_{d,23} & 0 \end{bmatrix},$$

$$\mathbf{A}(2) = \begin{bmatrix} 0 & 1 & 0 & 0 & 0 & 0 \\ 0 & 0 & 1 & 0 & 0 & 0 \\ \vdots & \vdots & \vdots & \vdots & \vdots & \vdots \\ 0 & 0 & 0 & 0 & 0 & 1 \\ 0 & 0 & 0 & A_{d,13} & A_{d,11} & 0 \end{bmatrix},$$

$$\mathbf{A}(3) = \begin{bmatrix} 0 & 0 & 0 & 1 & 0 & 0 \\ 0 & 0 & 0 & 0 & 1 & 0 \\ 0 & 0 & 0 & 0 & 0 & 1 \\ 0 & 0 & A_{d,13} & 0 & 0 & A_{d,11} \\ 0 & 0 & A_{d,23} & 0 & A_{d,22} & 0 \\ A_{d,311} & A_{d,321} & A_{d,33} & A_{d,312} & A_{d,322} & A_{d,313} \end{bmatrix},$$

$$\mathbf{B}(0) = \mathbf{B}(2) = \begin{bmatrix} 0 & 0 \\ \vdots & \vdots \\ 0 & 0 \\ B_{d,1} & 0 \end{bmatrix},$$

$$\mathbf{B}(1) = \begin{bmatrix} 0 & 0 \\ \vdots & \vdots \\ 0 & 0 \\ 0 & B_{d,2} \end{bmatrix}, \quad \mathbf{B}(3) = \begin{bmatrix} 0 & 0 \\ 0 & 0 \\ 0 & 0 \\ B_{d,1} & 0 \\ 0 & B_{d,2} \\ 0 & 0 \end{bmatrix},$$

$$\mathbf{B}_d(0) = \begin{bmatrix} 0 & 0 & 0 & 0 & 0 & 0 \\ \vdots & \vdots & \vdots & \vdots & \vdots & \vdots \\ 0 & 0 & 0 & 0 & 0 & 0 \\ 0 & 0 & 0 & B_{d,d1} & 0 & 0 \end{bmatrix}, \quad \mathbf{B}_d(1) = \begin{bmatrix} 0 & 0 & 0 & 0 & 0 & 0 \\ \vdots & \vdots & \vdots & \vdots & \vdots & \vdots \\ 0 & 0 & 0 & 0 & 0 & 0 \\ 0 & 0 & 0 & B_{d,d2} & 0 & 0 \end{bmatrix},$$

$$\mathbf{B}_d(2) = \begin{bmatrix} 0 & 0 & 0 & 0 & 0 & 0 \\ \vdots & \vdots & \vdots & \vdots & \vdots & \vdots \\ 0 & 0 & 0 & 0 & 0 & 0 \\ 0 & 0 & 0 & 0 & B_{d,d1} & 0 \end{bmatrix},$$

$$\mathbf{B}_d(3) = \begin{bmatrix} 0 & 0 & 0 & 0 & 0 & 0 \\ 0 & 0 & 0 & 0 & 0 & 0 \\ 0 & 0 & 0 & 0 & 0 & 0 \\ 0 & 0 & 0 & 0 & 0 & B_{d,d1} \\ 0 & 0 & 0 & 0 & B_{d,d2} & 0 \\ 0 & 0 & B_{d,d3} & 0 & 0 & 0 \end{bmatrix},$$

$$\mathbf{C}(0) = \begin{bmatrix} 0 & 0 & 0 & 1 & 0 & 0 \\ 0 & 0 & 0 & 0 & 1 & 0 \\ 0 & 0 & 0 & 0 & 0 & 1 \end{bmatrix},$$

$$\mathbf{C}(1) = \mathbf{C}(2) = \mathbf{C}(3) = \begin{bmatrix} 0 & 0 & 0 & 0 & 0 & 1 \end{bmatrix}. \tag{3.21}$$

The modeling example of three-tank system with multirate sampling is completed.

3.4 Problem formulation of scheduler and model integration

Considering the wireless communication scheduling, it is designed for every communication task to meet the real-time requirement, i.e., every task must be transmitted under the guidance of scheduler before its deadline. In this section, the modeling of scheduler is based on the premise that the scheduling algorithm is proposed off-line and the scheduler is already known for the communication scheme. The scheduler model can be described in a mathematical way, and further integrated with process model. The model integration is beneficial to the control and FD design issues dealing with imperfect transmission of network.

Consider the W-NCSs with a scheduler represented both by discrete θ-periodic models in Fig. 3.9, where control input $\mathbf{u}(k,j)$ and plant output $\mathbf{y}(k,j)$ are both time driven coordinated by scheduler. $\mathbf{u}_s(k,j)$ and $\mathbf{y}_s(k,j)$ are derived from queueing of $\mathbf{u}(k,j)$ and $\mathbf{y}(k,j)$ through network, respectively. Comparing with the system model (3.12), $\mathbf{u}(k,j)$ is replaced by $\mathbf{u}_s(k,j)$ due to the introduction of scheduler's model. $\mathbf{u}_s(k,j)$ is the actual input of plant and $\mathbf{y}_s(k,j)$ is used as a part of the filter resources. In view of integrated design of the plant and scheduler, $\mathbf{u}(k,j)$ and $\mathbf{y}_s(k,j)$ are

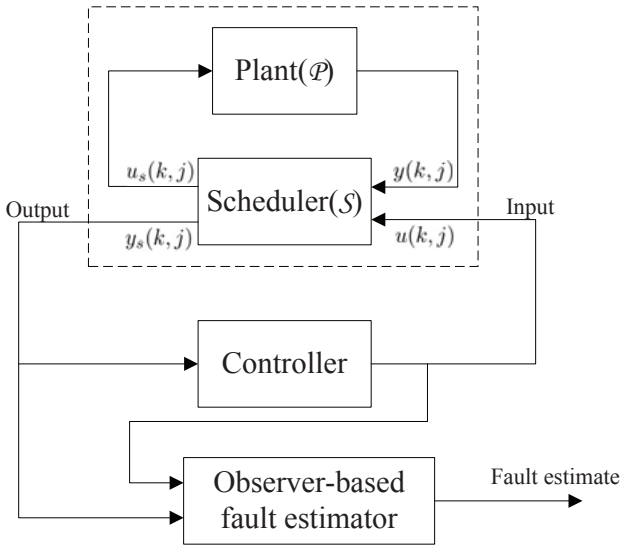

Figure 3.9: Schematic description of W-NCSs with scheduler

the input and output of the integrated model, which is highlighted in the dotted box of Fig. 3.9.

Considering the system model (3.12) with disturbances, the plant $\mathcal{P}$ can be described by the following θ-periodic discrete-time state-space equations,

$$\begin{aligned} \mathbf{x}(k,j+1) &= \mathbf{A}(j)\mathbf{x}(k,j) + \mathbf{B}(j)\mathbf{u}_s(k,j) + \mathbf{B}_d(j)\mathbf{d}(k,j) \\ \mathbf{y}(k,j) &= \mathbf{C}(j)\mathbf{x}(k,j) + \mathbf{v}(k,j),\ j = 0,1,\cdots,\theta-1 \end{aligned} \tag{3.22}$$

where $\mathbf{x}(k,j) \in \mathcal{R}^n$, $\mathbf{u}_s(k,j) \in \mathcal{R}^{q_s(j)}$, and $\mathbf{y}(k,j) \in \mathcal{R}^{m(j)}$ are the plant's state, input and output, respectively. $\mathbf{d}(k,j) \in \mathcal{R}^l$ and $\mathbf{v}(k,j) \in \mathcal{R}^{m(j)}$ are deterministic unknown driving and measurement disturbances. The parameter matrices and vector dimensions are all periodic with appropriate dimensions, that is, for each j,

$$\begin{aligned} &\mathbf{A}(j) = \mathbf{A}(j+\theta),\ \mathbf{B}(j) = \mathbf{B}(j+\theta),\ \mathbf{B}_d(j) = \mathbf{B}_d(j+\theta), \\ &\mathbf{C}(j) = \mathbf{C}(j+\theta),\ q_s(j) = q_s(j+\theta),\ m(j) = m(j+\theta). \end{aligned}$$

To describe the parameterization of the communication scheme, the scheduler $\mathcal{S}$ is also represented by θ-periodic discrete-time state-space equations with inputs $\mathbf{y}(k,j)$ and $\mathbf{u}(k,j)$ as follows,

$$\begin{aligned} \mathbf{x}_s(k,j+1) &= \mathbf{A}_s(j)\mathbf{x}_s(k,j) + \mathbf{B}_{sy}(j)\mathbf{y}(k,j) + \mathbf{B}_{su}(j)\mathbf{u}(k,j) \\ \mathbf{y}_s(k,j) &= \mathbf{C}_{sy}(j)\mathbf{x}_s(k,j) + \mathbf{D}_{sy}(j)\mathbf{y}(k,j) \\ \mathbf{u}_s(k,j) &= \mathbf{C}_{su}(j)\mathbf{x}_s(k,j) + \mathbf{D}_{su}(j)\mathbf{u}(k,j),\ j = 0,1,\cdots,\theta-1 \end{aligned} \tag{3.23}$$

where $\mathbf{x}_s(k,j) \in \mathcal{R}^{n_s}$, $\mathbf{u}(k,j) \in \mathcal{R}^q$, $\mathbf{y}_s(k,j) \in \mathcal{R}^{m_s(j)}$ are the scheduler's state, input and output. All parameter matrices and vector dimensions are periodic with period θ, that is, for each j,

$$\begin{aligned}
&\mathbf{A}_s(j) = \mathbf{A}_s(j+\theta),\ \mathbf{B}_{sy}(j) = \mathbf{B}_{sy}(j+\theta),\ \mathbf{B}_{su}(j) = \mathbf{B}_{su}(j+\theta),\\
&\mathbf{C}_{sy}(j) = \mathbf{C}_{sy}(j+\theta),\ \mathbf{D}_{sy}(j) = \mathbf{D}_{sy}(j+\theta),\ \mathbf{C}_{su}(j) = \mathbf{C}_{su}(j+\theta),\\
&\mathbf{D}_{su}(j) = \mathbf{D}_{su}(j+\theta),\ m_s(j) = m_s(j+\theta).
\end{aligned}$$

Remark 2 *The scheduler is a mathematical way of representing the queueing process imposed on the control input* $\mathbf{u}(k,j)$ *and plant output* $\mathbf{y}(k,j)$. *This queueing process is implemented under the scheduling algorithm, which is proposed to optimize the network real-time performance subject to various constraints, such as limited resources, task priorities [56], deadlines [44] and so on [92]. By properly formulating the parameter matrices* $\mathbf{A}_s(j)$, $\mathbf{B}_{sy}(j)$, $\mathbf{B}_{su}(j)$, $\mathbf{C}_{sy}(j)$, $\mathbf{D}_{sy}(j)$, $\mathbf{C}_{su}(j)$ *and* $\mathbf{D}_{sy}(j)$ *in the form of* $(0,1)$*-matrices, the output* $\mathbf{u}_s(k,j)$ *and* $\mathbf{y}_s(k,j)$ *are composed of ordered elements of* $\mathbf{x}_s(k,j)$, $\mathbf{u}(k,j)$ *and* $\mathbf{y}(k,j)$ *over a set of consecutive time periods. The time period is the time interval unit of single packet transmission, namely time slot, in the schedule.*

Remark 3 *In the heavy load case when the network resource isn't adequate for the scheduling of all transmission tasks, the transmission delay and packet losses are inevitable but still deterministic. The scheduler in this case can also be represented by (3.23). To illustrate the structure of parameter matrices in cases of delay and packet losses, we take the schedule of* $\mathbf{y}(k,j)$ *for example. Suppose the* l*-th element of* $\mathbf{y}(k,j)$, *denoted by* $y_l(k,j)$, *is delayed with* τ, $\tau = 1$. *This delay procedure in the scheduler is finished in two steps. First, by setting the* il*-th element of* $\mathbf{B}_{sy}(j)$ *to 1, where* $i, i \in [1, n_s]$, *is the row number and* l *is the column number of* $\mathbf{B}_{sy}(j)$, $y_l(k,j)$ *is saved in the* i*-th element of* $\mathbf{x}_s(k,j+1)$. *Second, in the next discrete time step, by setting the* ri*-th element of* $\mathbf{C}_{sy}(j+1)$ *to 1,* $y_l(k,j)$ *is scheduled in the* r*-th element of* $\mathbf{y}_s(k,j+1)$, *which means* $y_l(k,j)$ *is allowed to transfer at the* r*-th time slot in the next discrete time step* $(k,j+1)$. *The choices of* i *and* r *are under the consideration of aforementioned constraints. When* $\tau > 1$, *this case can be solved by properly setting* $\mathbf{A}_s(j)$. *Until now, the choice of* n_s *can be easily explained.* $n_s(j)$, $j = 0, 1, \cdots, \theta - 1$ *denotes the sum of dimensions for delayed elements of* $\mathbf{y}(k,j)$ *and* $\mathbf{u}(k,j)$ *in each arithmetic unit.* n_s *is decided by the maximum value of* $n_s(j)$. *For the case that* $y_l(k,j)$ *is lost, it is reachable by setting the* l*-th column of* $\mathbf{D}_{sy}(j)$ *to* $\mathbf{0}$.

In the following parts of this dissertation, the FE approach will be studied. So the additive fault is considered in the process model, (3.22) can be

extended to

$$\begin{aligned}\mathbf{x}(k,j+1) &= \mathbf{A}(j)\mathbf{x}(k,j) + \mathbf{B}(j)\mathbf{u}_s(k,j) + \mathbf{B}_d(j)\mathbf{d}(k,j) + \mathbf{E}_f(j)\mathbf{f}(k,j)\\ \mathbf{y}(k,j) &= \mathbf{C}(j)\mathbf{x}(k,j) + \mathbf{v}(k,j) + \mathbf{F}_f(j)\mathbf{f}(k,j),\ j = 0,1,\cdots,\theta-1\end{aligned} \tag{3.24}$$

where $\mathbf{f}(k,j) \in \mathcal{R}^s$ is the fault to be estimated. $\mathbf{E}_f(j)$ and $\mathbf{F}_f(j)$ are periodic matrices with appropriate dimensions.

By setting

$$\bar{\mathbf{x}}(k,j) = \begin{bmatrix} \mathbf{x}(k,j) \\ \mathbf{x}_s(k,j) \end{bmatrix},\ \mathbf{w}(k,j) = \begin{bmatrix} \mathbf{d}(k,j) \\ \mathbf{v}(k,j) \end{bmatrix}, \tag{3.25}$$

the integrated model of plant and scheduler, denoted by $\mathcal{P}-\mathcal{S}$, is modeled by

$$\begin{aligned}\bar{\mathbf{x}}(k,j+1) &= \bar{\mathbf{A}}(j)\bar{\mathbf{x}}(k,j) + \bar{\mathbf{B}}(j)\mathbf{u}(k,j) + \bar{\mathbf{B}}_d(j)\mathbf{w}(k,j) + \bar{\mathbf{E}}_f(j)\mathbf{f}(k,j)\\ \mathbf{y}_s(k,j) &= \bar{\mathbf{C}}(j)\bar{\mathbf{x}}(k,j) + \bar{\mathbf{D}}_d(j)\mathbf{w}(k,j) + \bar{\mathbf{F}}_f(j)\mathbf{f}(k,j),\ j = 0,1,\cdots,\theta-1\end{aligned} \tag{3.26}$$

where

$$\begin{aligned}\bar{\mathbf{A}}(j) &= \begin{bmatrix} \mathbf{A}(j) & \mathbf{B}(j)\mathbf{C}_{su}(j) \\ \mathbf{B}_{sy}(j)\mathbf{C}(j) & \mathbf{A}_s(j) \end{bmatrix},\\ \bar{\mathbf{B}}(j) &= \begin{bmatrix} \mathbf{B}(j)\mathbf{D}_{su}(j) \\ \mathbf{B}_{su}(j) \end{bmatrix},\ \bar{\mathbf{B}}_d(j) = \begin{bmatrix} \mathbf{B}_d(j) & \mathbf{0} \\ \mathbf{0} & \mathbf{B}_{sy}(j) \end{bmatrix},\\ \bar{\mathbf{C}}(j) &= \begin{bmatrix} \mathbf{D}_{sy}(j)\mathbf{C}(j) & \mathbf{C}_{sy}(j) \end{bmatrix},\ \bar{\mathbf{D}}_d(j) = \begin{bmatrix} \mathbf{0} & \mathbf{D}_{sy}(j) \end{bmatrix},\\ \bar{\mathbf{E}}_f(j) &= \begin{bmatrix} \mathbf{E}_f(j) \\ \mathbf{B}_{sy}(j)\mathbf{F}_f(j) \end{bmatrix},\ \bar{\mathbf{F}}_f(j) = \mathbf{D}_{sy}(j)\mathbf{F}_f(j).\end{aligned}$$

The parameter matrices are also periodic, and are derived from the periodicity of plant's and scheduler's parameter matrices.

3.5 Summary

In this chapter, the communication schemes and system have been modeled both for the centralized and decentralized structures. Considering the industrial automation as applications, there are two characteristics should be sufficiently taken into consideration to generalize the applicability of the model, i.e., to adapt to the real-time communication and coupling relations with multi-sampling measuring. So the communication scheme is modeled

into a sorting process of transmission tasks based on TDMA technique, which can guarantee the successful transmission of deterministic tasks and also the real-time performance. For coupling system with multi-sampling rate, it is modeled into an LP system, which is suitable for both centralized and decentralized systems. At the end of this chapter, the proposed communication tasks sorting process has been described by the state-space equation and the model integration has been finally achieved.

Chapter 4

FE of centralized W-NCSs

This chapter deals with the fault estimation problems of centralized W-NCSs with information scheduler, which is suitable for industrial applications. Considering the periodic integrated model of plant and scheduler (3.26), the basic ideas to develop the FE issue will be presented.

4.1 Performance criterion

As introduced in Section 2.4, FE problem of LP system can be formulated as finding observer gain matrix $\mathbf{L}(j)$ and post-filter $\mathbf{V}(j)$ such that an optimal performance index can be satisfied. Generally, the performance index is represented by an H_∞ norm of transfer function from any input signal with finite energy to the output signal. If the energy level of input is bounded, H_∞ norm can be used to measure the influence of input signal to output signal. The output can be any kind of signal, which depends on the design objectives. To be specific for FE approach design, the H_∞ performance index is proposed to measure the influence of all unknown input signals on the fault estimate error. The following bounded performance index is proposed to limit the influence of all unknown input, i.e., initial state estimate error, driving disturbance, measurement disturbance and fault, on the fault estimate error.

$$\sup_{(\bar{\mathbf{x}}(0,0),\mathbf{w},\mathbf{f})\neq 0} \frac{\|\hat{\mathbf{f}}(k,j)-\mathbf{f}(k,j)\|^2}{\tilde{\bar{\mathbf{x}}}^T(0,0)\mathbf{\Pi}_0^{-1}\tilde{\bar{\mathbf{x}}}(0,0)+\|\mathbf{w}(k,j)\|^2+\|\mathbf{f}(k,j)\|^2} \leq \gamma^2 \qquad (4.1)$$

where $\hat{\mathbf{f}}(k,j)$ is the estimate of $\mathbf{f}(k,j)$, $\tilde{\bar{\mathbf{x}}}(0,0)=\bar{\mathbf{x}}(0,0)-\hat{\bar{\mathbf{x}}}(0,0)$, $0<\gamma<1$ and $\mathbf{\Pi}_0$ is a positive definite matrix, which reflects a priori knowledge of how close the initial state $\bar{\mathbf{x}}(0,0)$ is to the initial state estimate $\hat{\bar{\mathbf{x}}}(0,0)$. Without loss of generality, $\hat{\bar{\mathbf{x}}}(0,0)$ is set to $\mathbf{0}$.

By defining fault estimate error

$$\mathbf{v}_f(k,j) = \hat{\mathbf{f}}(k,j) - \mathbf{f}(k,j),$$

(4.1) is reformulated equivalently into the following quadratic form

$$J = \bar{\mathbf{x}}^T(0,0)\mathbf{\Pi}_0^{-1}\bar{\mathbf{x}}(0,0) + \|\mathbf{w}(k,j)\|^2 + \|\mathbf{f}(k,j)\|^2 - \gamma^{-2}\|\mathbf{v}_f(k,j)\|^2 \geq 0 \quad (4.2)$$

which works as a stationary point and is of great importance for the following FE approach.

4.2 FE of centralized W-NCSs

In this section, the H_∞ fault estimator is designed in terms of solution to a set of Riccati difference equations. H_∞ estimator and recursive computation of the estimator subject to the system state-space model (3.26) will be addressed.

To realize FE of periodic discrete-time W-NCSs, the following lemma solving the FE of finite-horizon time-varying systems is first introduced.

Lemma 1 *[76] Consider a discrete time-varying model*

$$\begin{aligned} \mathbf{x}(k+1) &= \mathbf{A}(k)\mathbf{x}(k) + \mathbf{B}_d(k)\mathbf{d}(k) + \mathbf{E}_f(k)\mathbf{f}(k) \\ \mathbf{y}(k) &= \mathbf{C}(k)\mathbf{x}(k) + \mathbf{v}(k) + \mathbf{F}_f(k)\mathbf{f}(k) \end{aligned} \quad (4.3)$$

The fault estimator $\hat{\mathbf{f}}(k)$ *that satisfies the following performance criterion*

$$\sup_{(\mathbf{x}(0),\mathbf{d},\mathbf{v},\mathbf{f})\neq 0} \frac{\|\hat{\mathbf{f}}(k) - \mathbf{f}(k)\|^2}{\tilde{\mathbf{x}}^T(0)\mathbf{\Pi}_0^{-1}\tilde{\mathbf{x}}(0) + \|\mathbf{d}(k)\|^2 + \|\mathbf{v}(k)\|^2 + \|\mathbf{f}(k)\|^2} \leq \gamma^2 \quad (4.4)$$

where $\tilde{\mathbf{x}}(0) = \mathbf{x}(0) - \hat{\mathbf{x}}(0)$*, exists if and only if*

$$\begin{aligned} \mathbf{\Theta}(k) &:= \mathbf{C}(k)\mathbf{P}(k)\mathbf{C}^T(k) + \mathbf{I} + \mathbf{F}_f(k)\mathbf{F}_f^T(k) > 0 \\ \mathbf{\Xi}(k) &:= (1-\gamma^2)\mathbf{I} - \mathbf{F}_f^T(k)\mathbf{\Theta}^{-1}(k)\mathbf{F}_f(k) < 0 \end{aligned} \quad (4.5)$$

where $\mathbf{P}(k)$ *is recursively calculated by the following equation*

$$\begin{aligned} \mathbf{P}(k+1) = {} & \mathbf{A}(k)\mathbf{P}(k)\mathbf{A}^T(k) + \mathbf{B}_d(k)\mathbf{B}_d^T(k) + \mathbf{E}_f(k)\mathbf{E}_f^T(k) \\ & - \begin{bmatrix} \mathbf{K}(k)\mathbf{\Theta}(k) & \mathbf{E}_f(k) \end{bmatrix} \mathbf{R}^{-1}(k) \begin{bmatrix} \mathbf{K}(k)\mathbf{\Theta}(k) & \mathbf{E}_f(k) \end{bmatrix}^T \end{aligned} \quad (4.6)$$

with initial value $\mathbf{P}(0) = \mathbf{\Pi}_0$, *and*

$$\begin{aligned}\mathbf{K}(k) &= (\mathbf{A}(k)\mathbf{P}(k)\mathbf{C}^T(k) + \mathbf{E}_f(k)\mathbf{F}_f^T(k))\mathbf{\Theta}^{-1}(k)\\ \mathbf{R}(k) &= \begin{bmatrix} \mathbf{\Theta}(k) & \mathbf{F}_f(k) \\ \mathbf{F}_f^T(k) & (1-\gamma^2)\mathbf{I} \end{bmatrix}.\end{aligned} \tag{4.7}$$

The fault estimator is given by

$$\hat{\mathbf{f}}(k) = \mathbf{F}_f^T(k)\mathbf{\Theta}^{-1}(k)(\mathbf{y}(k) - \mathbf{C}(k)\hat{\mathbf{x}}(k|k-1)) \tag{4.8}$$

where $\hat{\mathbf{x}}(k+1|k)$ *is recursively calculated as*

$$\hat{\mathbf{x}}(k+1|k) = \mathbf{A}(k)\hat{\mathbf{x}}(k|k-1) + \mathbf{K}(k)(\mathbf{y}(k) - \mathbf{C}(k)\hat{\mathbf{x}}(k|k-1)) \tag{4.9}$$

with initial value $\hat{\mathbf{x}}(0|-1) = \mathbf{0}$.

Based on the Lemma 1, FE algorithm has been developed for the system with known arbitrary input based on (3.26). Let $\mathbf{x}_d(k,j)$ be the state generated by unknown input $\mathbf{w}(k,j)$ and $\mathbf{f}(k,j)$, and $\mathbf{x}_u(k,j)$ be the state generated by known input $\mathbf{u}(k,j)$. According to the model additivity, it is easy to obtain

$$\begin{aligned}\mathbf{x}_d(k,j+1) &= \bar{\mathbf{A}}(j)\mathbf{x}_d(k,j) + \bar{\mathbf{B}}_d(j)\mathbf{w}(k,j) + \bar{\mathbf{E}}_f(j)\mathbf{f}(k,j)\\ \mathbf{y}_d(k,j) &= \bar{\mathbf{C}}(j)\mathbf{x}_d(k,j) + \bar{\mathbf{D}}_d(j)\mathbf{w}(k,j) + \bar{\mathbf{F}}_f(j)\mathbf{f}(k,j)\end{aligned} \tag{4.10}$$

$$\begin{aligned}\mathbf{x}_u(k,j+1) &= \bar{\mathbf{A}}(j)\mathbf{x}_u(k,j) + \bar{\mathbf{B}}(j)\mathbf{u}(k,j)\\ \mathbf{y}_u(k,j) &= \bar{\mathbf{C}}(j)\mathbf{x}_u(k,j)\end{aligned} \tag{4.11}$$

where $\mathbf{x}_d(0,0) = \bar{\mathbf{x}}(0,0)$, $\mathbf{x}_u(0,0) = \mathbf{0}$ and $j = 0, 1, \cdots, \theta - 1$.

By adding (4.10) and (4.11), it gives (3.26) where

$$\begin{aligned}\bar{\mathbf{x}}(k,j) &= \mathbf{x}_d(k,j) + \mathbf{x}_u(k,j)\\ \mathbf{y}_s(k,j) &= \mathbf{y}_d(k,j) + \mathbf{y}_u(k,j)\end{aligned}$$

It is obvious from (4.11) that $\mathbf{y}_u(k,j)$ is only related with the known input $\mathbf{u}(k,j)$, so $\mathbf{y}_u(k,j)$ can be calculated in every discrete time step.

Consider (4.10) with $\mathbf{y}_d(k,j) = \mathbf{y}_s(k,j) - \mathbf{y}_u(k,j)$ and the following associated stochastic system in Krein space

$$\begin{aligned}\mathbf{x}_k(k,j+1) &= \bar{\mathbf{A}}(j)\mathbf{x}_k(k,j) + \bar{\mathbf{B}}_d(j)\mathbf{w}_k(k,j) + \bar{\mathbf{E}}_f(j)\mathbf{f}_k(k,j)\\ \mathbf{y}_k(k,j) &= \bar{\mathbf{C}}(j)\mathbf{x}_k(k,j) + \bar{\mathbf{D}}_d(j)\mathbf{w}_k(k,j) + \bar{\mathbf{F}}_f(j)\mathbf{f}_k(k,j)\\ \hat{\mathbf{f}}_k(k,j) &= \mathbf{f}_k(k,j) + \mathbf{v}_{fk}(k,j)\end{aligned} \tag{4.12}$$

where $\mathbf{x}_k(k,j)$, $\mathbf{w}_k(k,j)$, $\mathbf{f}_k(k,j)$, $\hat{\mathbf{f}}_k(k,j)$, $\mathbf{v}_{fk}(k,j)$ are Krein-space variables with the following variances

$$\left\langle \begin{bmatrix} \mathbf{x}_k(k,0) \\ \mathbf{w}_k(k,j) \\ \mathbf{f}_k(k,j) \\ \mathbf{v}_{fk}(k,j) \end{bmatrix}, \begin{bmatrix} \mathbf{x}_k(k,0) \\ \mathbf{w}_k(k,i) \\ \mathbf{f}_k(k,i) \\ \mathbf{v}_{fk}(k,i) \end{bmatrix} \right\rangle = \begin{bmatrix} \mathbf{\Pi}_0 & \mathbf{0} & \mathbf{0} & \mathbf{0} \\ \mathbf{0} & \delta_{ji}\mathbf{I} & \mathbf{0} & \mathbf{0} \\ \mathbf{0} & \mathbf{0} & \delta_{ji}\mathbf{I} & \mathbf{0} \\ \mathbf{0} & \mathbf{0} & \mathbf{0} & -\gamma^2\delta_{ji}\mathbf{I} \end{bmatrix}.$$

Here $i,j \in [0,(\theta-1)]$, $\delta_{ji}=0$ when $j\neq i$ and $\delta_{jj}=1$.

By setting $\mathbf{y}_{rk}(k,j) = \begin{bmatrix} \mathbf{y}_k(k,j) \\ \hat{\mathbf{f}}_k(k,j) \end{bmatrix}$, from (4.12) it is easy to obtain that

$$\mathbf{y}_{rk}(k,j) = \mathbf{C}_r(j)\mathbf{x}_k(k,j) + \mathbf{D}_{dr}(j)\mathbf{w}_{fk}(k,j) + \mathbf{F}_{fr}(j)\mathbf{f}_k(k,j) \tag{4.13}$$

where

$$\mathbf{w}_{fk}(k,j) = \begin{bmatrix} \mathbf{w}_k(k,j) \\ \mathbf{v}_{fk}(k,j) \end{bmatrix},\ \mathbf{C}_r(j) = \begin{bmatrix} \bar{\mathbf{C}}(j) \\ \mathbf{0} \end{bmatrix},$$
$$\mathbf{D}_{dr}(j) = \begin{bmatrix} \bar{\mathbf{D}}_d(j) & \mathbf{0} \\ \mathbf{0} & \mathbf{I} \end{bmatrix},\ \mathbf{F}_{fr}(j) = \begin{bmatrix} \bar{\mathbf{F}}_f(j) \\ \mathbf{I} \end{bmatrix}.$$

The estimate of $\mathbf{x}_k(k,j)$ is denoted by $\hat{\mathbf{x}}(k,j|j-1)$, and the state error $\mathbf{e}(k,j)$ and residual $\tilde{\mathbf{y}}_r(k,j)$ are stated as follows

$$\begin{aligned} \mathbf{e}(k,j) &= \mathbf{x}_k(k,j) - \hat{\mathbf{x}}(k,j|j-1) \\ \tilde{\mathbf{y}}_r(k,j) &= \mathbf{y}_{rk}(k,j) - \mathbf{C}_r(j)\hat{\mathbf{x}}(k,j|j-1) \end{aligned} \tag{4.14}$$

The inner product of $\tilde{\mathbf{y}}_r(k,j)$ can be formulated into

$$\begin{aligned} \mathbf{R}(k,j) =& \langle \tilde{\mathbf{y}}_r(k,j), \tilde{\mathbf{y}}_r(k,j) \rangle \\ =& \mathbf{C}_r(j)\langle \mathbf{e}(k,j), \mathbf{e}(k,j)\rangle \mathbf{C}_r^T(j) + \mathbf{D}_{dr}(j)\langle \mathbf{w}_{fk}(k,j), \mathbf{w}_{fk}(k,j)\rangle \mathbf{D}_{dr}^T(j) \\ &+ \mathbf{F}_{fr}(j)\langle \mathbf{f}_k(k,j), \mathbf{f}_k(k,j)\rangle \mathbf{F}_{fr}^T(j) \\ =& \begin{bmatrix} \bar{\mathbf{C}}(j) \\ \mathbf{0} \end{bmatrix} \mathbf{P}(k,j) \begin{bmatrix} \bar{\mathbf{C}}(j) \\ \mathbf{0} \end{bmatrix}^T + \mathbf{D}_{dr}(j) \begin{bmatrix} \mathbf{I} & \mathbf{0} \\ \mathbf{0} & -\gamma^2\mathbf{I} \end{bmatrix} \mathbf{D}_{dr}^T(j) \\ &+ \begin{bmatrix} \bar{\mathbf{F}}_f(j) \\ \mathbf{I} \end{bmatrix} \begin{bmatrix} \bar{\mathbf{F}}_f(j) \\ \mathbf{I} \end{bmatrix}^T \\ =& \begin{bmatrix} \mathbf{\Theta}(k,j) & \bar{\mathbf{F}}_f(j) \\ \bar{\mathbf{F}}_f^T(j) & (1-\gamma^2)\mathbf{I} \end{bmatrix} \end{aligned} \tag{4.15}$$

where

$$\begin{aligned} \mathbf{P}(k,j) &= \langle \mathbf{e}(k,j), \mathbf{e}(k,j)\rangle \\ \mathbf{\Theta}(k,j) &= \bar{\mathbf{C}}(j)\mathbf{P}(k,j)\bar{\mathbf{C}}^T(j) + \bar{\mathbf{D}}_d(j)\bar{\mathbf{D}}_d^T(j) + \bar{\mathbf{F}}_f(j)\bar{\mathbf{F}}_f^T(j) \end{aligned} \tag{4.16}$$

To hold the recursive computation in Krein space, $\mathbf{R}(k,j)$ is strongly nonsingular [38], so it has the following unique triangular decomposition

$$\mathbf{R}(k,j) = \mathbf{M}(k,j)\mathbf{\Lambda}(k,j)\mathbf{M}^T(k,j)$$

where

$$\mathbf{M}(k,j) = \begin{bmatrix} \mathbf{I} & \mathbf{0} \\ -\bar{\mathbf{F}}_f^T(j)\mathbf{\Theta}^{-1}(k,j) & \mathbf{I} \end{bmatrix},\ \mathbf{\Lambda}(k,j) = \begin{bmatrix} \mathbf{\Theta}(k,j) & \mathbf{0} \\ \mathbf{0} & \mathbf{\Xi}(k,j) \end{bmatrix}$$

According to lemmas 7 and 10 in [38], the minimum of J in (4.2) can be obtained with the association of Krein space model (4.12) as follows

$$\begin{aligned} \min J &= \sum_{j=0}^{\theta-1} \tilde{\mathbf{y}}_r^T(k,j)\mathbf{R}^{-1}(k,j)\tilde{\mathbf{y}}_r(k,j) \\ &= \sum_{j=0}^{\theta-1} \tilde{\mathbf{y}}_r^T(k,j)\mathbf{Q}^T(k,j)\mathbf{\Lambda}^{-1}(k,j)\mathbf{Q}(k,j)\tilde{\mathbf{y}}_r(k,j) \\ &= \sum_{j=0}^{\theta-1} \tilde{\mathbf{y}}^T(k,j)\mathbf{\Theta}^{-1}(k,j)\tilde{\mathbf{y}}(k,j) + \sum_{j=0}^{\theta-1} \tilde{\mathbf{r}}^T(k,j)\mathbf{\Xi}^{-1}(k,j)\tilde{\mathbf{r}}(k,j) \end{aligned}$$

where $\tilde{\mathbf{y}}_r(k,j) = \begin{bmatrix} \tilde{\mathbf{y}}(k,j) \\ \mathbf{v}_f(k,j) \end{bmatrix}$, $\mathbf{Q}(k,j) = \begin{bmatrix} \mathbf{I} & \mathbf{0} \\ \bar{\mathbf{F}}_f^T(j)\mathbf{\Theta}^{-1}(k,j) & \mathbf{I} \end{bmatrix}$,

$$\tilde{\mathbf{y}}(k,j) = \mathbf{y}_d(k,j) - \bar{\mathbf{C}}(j)\hat{\mathbf{x}}(k,j|j-1) \tag{4.17}$$

and

$$\begin{aligned} \tilde{\mathbf{r}}(k,j) &= \hat{\mathbf{f}}(k,j) - \bar{\mathbf{F}}_f^T(j)\mathbf{\Theta}(k,j)^{-1}\tilde{\mathbf{y}}(k,j), \\ \mathbf{\Xi}(k,j) &= (1-\gamma^2)\mathbf{I} - \bar{\mathbf{F}}_f^T(j)\mathbf{\Theta}^{-1}(k,j)\bar{\mathbf{F}}_f(j) \end{aligned} \tag{4.18}$$

To solve $\min J$, fault estimator $\hat{\mathbf{f}}(k,j)$ is selected as follows

$$\hat{\mathbf{f}}(k,j) = \bar{\mathbf{F}}_f^T(j)\mathbf{\Theta}^{-1}(k,j)\tilde{\mathbf{y}}(k,j) \tag{4.19}$$

To design the recursive state observer, the following derivation is obtained

based on the definition of $\hat{\mathbf{x}}(k,j|j-1)$

$$\begin{aligned}
\hat{\mathbf{x}}(k,j+1|j) =& \sum_{i=0}^{j}\langle \mathbf{x}_k(k,j+1),\tilde{\mathbf{y}}_r(k,i)\rangle \mathbf{R}^{-1}(k,i)\tilde{\mathbf{y}}_r(k,i) \\
=& \sum_{i=0}^{j-1}\langle \mathbf{x}_k(k,j+1),\tilde{\mathbf{y}}_r(k,i)\rangle \mathbf{R}^{-1}(k,i)\tilde{\mathbf{y}}_r(k,i) \\
&+ \langle \mathbf{x}_k(k,j+1),\tilde{\mathbf{y}}_r(k,j)\rangle \mathbf{R}^{-1}(k,j)\tilde{\mathbf{y}}_r(k,j) \\
=& \bar{\mathbf{A}}(j)\sum_{i=0}^{j-1}\langle \mathbf{x}_k(k,j),\tilde{\mathbf{y}}_r(k,i)\rangle \mathbf{R}^{-1}(k,i)\tilde{\mathbf{y}}_r(k,i) \\
&+ \mathbf{K}_r(k,j)\mathbf{R}^{-1}(k,j)\tilde{\mathbf{y}}_r(k,j) \\
=& \bar{\mathbf{A}}(j)\hat{\mathbf{x}}(k,j|j-1) + \mathbf{K}_r(k,j)\mathbf{R}^{-1}(k,j)\tilde{\mathbf{y}}_r(k,j) \qquad (4.20)
\end{aligned}$$

where

$$\mathbf{K}_r(k,j) = \bar{\mathbf{A}}(j)\mathbf{P}(k,j)\mathbf{C}_r^T(j) + \bar{\mathbf{B}}_d(j)\mathbf{D}_{dr}^T(j) + \bar{\mathbf{E}}_f(j)\mathbf{F}_{fr}^T(j) \qquad (4.21)$$

The derivation of recursive calculation of $\mathbf{P}(k,j)$ is as follows

$$\begin{aligned}
\mathbf{P}(k,j+1) =& \langle \mathbf{e}(k,j+1),\mathbf{e}(k,j+1)\rangle \\
=& \bar{\mathbf{A}}(j)\mathbf{P}(k,j)\bar{\mathbf{A}}^T(j) + \bar{\mathbf{B}}_d(j)\bar{\mathbf{B}}_d^T(j) \\
&+ \bar{\mathbf{E}}_f(j)\bar{\mathbf{E}}_f^T(j) + \mathbf{K}_r(k,j)\mathbf{R}^{-1}(k,j)\mathbf{K}_r^T(k,j) \\
&- \bar{\mathbf{A}}(j)\langle \mathbf{e}(k,j),\tilde{\mathbf{y}}_r(k,j)\rangle \mathbf{R}^{-1}(k,j)\mathbf{K}_r^T(k,j) \\
&- \bar{\mathbf{B}}_d(j)\langle \mathbf{w}_{fk}(k,j),\tilde{\mathbf{y}}_r(k,j)\rangle \mathbf{R}^{-1}(k,j)\mathbf{K}_r^T(k,j) \\
&- \bar{\mathbf{E}}_f(j)\langle \mathbf{f}_k(k,j),\tilde{\mathbf{y}}_r(k,j)\rangle \mathbf{R}^{-1}(k,j)\mathbf{K}_r^T(k,j) \\
&- \mathbf{K}_r(k,j)\mathbf{R}^{-1}(k,j)\langle \tilde{\mathbf{y}}_r(k,j),\mathbf{e}(k,j)\rangle \bar{\mathbf{A}}^T(j) \\
&- \mathbf{K}_r(k,j)\mathbf{R}^{-1}(k,j)\langle \tilde{\mathbf{y}}_r(k,j),\mathbf{w}_{fk}(k,j)\rangle \bar{\mathbf{B}}_d^T(j) \\
&- \mathbf{K}_r(k,j)\mathbf{R}^{-1}(k,j)\langle \tilde{\mathbf{y}}_r(k,j),\mathbf{f}_k(k,j)\rangle \bar{\mathbf{E}}_f^T(j) \\
=& \bar{\mathbf{A}}(j)\mathbf{P}(k,j)\bar{\mathbf{A}}^T(j) + \bar{\mathbf{B}}_d(j)\bar{\mathbf{B}}_d^T(j) \\
&+ \bar{\mathbf{E}}_f(j)\bar{\mathbf{E}}_f^T(j) - \mathbf{K}_r(k,j)\mathbf{R}^{-1}(k,j)\mathbf{K}_r^T(k,j) \qquad (4.22)
\end{aligned}$$

To simplify the algebraic expression by using the parameters in (3.26) to represent the derivation, (4.20) and (4.22) are further formulated into

$$\hat{\mathbf{x}}(k,j+1|j) = \bar{\mathbf{A}}(j)\hat{\mathbf{x}}(k,j|j-1) + \mathbf{K}(k,j)\tilde{\mathbf{y}}(k,j) \qquad (4.23)$$

$$\begin{aligned}
\mathbf{P}(k,j+1) =& \bar{\mathbf{A}}(j)\mathbf{P}(k,j)\bar{\mathbf{A}}^T(j) + \bar{\mathbf{B}}_d(j)\bar{\mathbf{B}}_d^T(j) + \bar{\mathbf{E}}_f(j)\bar{\mathbf{E}}_f^T(j) \\
&- \begin{bmatrix} \mathbf{K}(k,j)\mathbf{\Theta}(k,j) & \bar{\mathbf{E}}_f(j) \end{bmatrix} \mathbf{R}^{-1}(k,j) \begin{bmatrix} \mathbf{\Theta}(k,j)\mathbf{K}^T(k,j) \\ \bar{\mathbf{E}}_f^T(j) \end{bmatrix} \qquad (4.24)
\end{aligned}$$

where

$$\mathbf{K}(k,j) = (\bar{\mathbf{A}}(j)\mathbf{P}(k,j)\bar{\mathbf{C}}^T(j) + \bar{\mathbf{B}}_d(j)\bar{\mathbf{D}}_d^T(j) + \bar{\mathbf{E}}_f(j)\bar{\mathbf{F}}_f^T(j))\mathbf{\Theta}^{-1}(k,j) \quad (4.25)$$

Algorithm 1 *FE of centralized W-NCSs*

1) *Set the initial value* $\mathbf{P}(0,0) = \mathbf{\Pi}_0$ *and* $\hat{\mathbf{x}}(0,0|-1) = \mathbf{0}$.

2) *Check the necessary and sufficient conditions of the FE algorithm as follows*

$$\begin{aligned} \mathbf{\Theta}(k,j) &> \mathbf{0} \\ \mathbf{\Xi}(k,j) &< \mathbf{0} \end{aligned} \quad (4.26)$$

where the definitions of $\mathbf{\Theta}(k,j)$ *and* $\mathbf{\Xi}(k,j)$ *are given in (4.16) and (4.18), respectively. If the conditions are satisfied, go to next step; otherwise, overflow.*

3) *Calculate* $\mathbf{P}(k,j)$ *recursively as in (4.24), where* $\mathbf{K}(k,j)$ *and* $\mathbf{R}(k,j)$ *are calculated by (4.25) and (4.15), respectively.*

4) *Calculate* $\mathbf{y}_u(k,j)$ *and* $\mathbf{y}_d(k,j)$*, where* $\mathbf{y}_u(k,j)$ *is calculated from (4.11) and* $\mathbf{y}_d(k,j) = \mathbf{y}_s(k,j) - \mathbf{y}_u(k,j)$.

5) *Calculate the state estimation* $\hat{\mathbf{x}}(k,j+1|j)$ *and residual* $\tilde{\mathbf{y}}(k,j)$ *recursively by (4.23) and (4.17).*

6) *Calculate fault estimator* $\hat{\mathbf{f}}(k,j)$ *as in (4.19).*

Remark 4 *The* H_∞ *FE for time-varying system with delayed measurements has been investigated in [76]. We should point out the differences between this algorithm and the one in [76] mainly from three aspects. The first one is Algorithm 1 is developed for the periodic system comparing with the time-varying system on a finite horizon [76]. It makes the* l_2 *norm of signals for the two types of systems different, which is illustrated in Chapter 2. The second difference is that Algorithm 1 concerns the model with arbitrary input by using the model's linearity. The third one is Algorithm 1 deals with the model of different process and measurement noises structure. The plant model (3.22) has the same noise structure as in [76], but after the integration with scheduler, the noises are represented by a unified one, namely*

$$\mathbf{w}(k,j) = \begin{bmatrix} \mathbf{d}(k,j) \\ \mathbf{v}(k,j) \end{bmatrix},$$

is the unified noise of the integrated model of plant and scheduler.

Remark 5 *The scheduler adopted in this thesis is based on the off-line scheduling algorithm, thus those periodic parameters in (3.23) are already decided. Note that the FE performance is not only related with the unknown variables, e.g.,* $\mathbf{w}(k,j)$, $\mathbf{f}(k,j)$, *but also related with the scheduler, which determines the transmission latencies. This implies that the network parameters can be considered as one of the optimal variables for (4.1) to obtain the minimum fault estimation error over unknown input. The specific optimal variables of network parameters depend on the scheduling approaches, such as earliest deadline first (EDF), non-preemptive scheduling. Considering the concrete application background and the corresponding communication structure, a real-time scheduling must be proposed to ensure the security of cyber-physical systems. Thus considering the optimal variable of network parameters* $T_{s,i}$, *which is the scheduled period of i-th sub-system, the FE algorithm involving with complicated scheduling can be found by solving the following optimization problem,*

$$\min T_{s,i} \text{ subject to (4.1) and } T_{s,i} \leq T_{cri,i},\ i = 1, \cdots, N$$

where $T_{cri,i}$ *is the absolute deadline of i-th sub-system, and* N *is the number of sub-systems in the network.*

4.3 Summary

In this chapter, FE of centralized periodic W-NCSs has been studied. The FE algorithm aims at dealing with centralized periodic W-NCSs with scheduler, which is called $\mathcal{P} - \mathcal{S}$ system, and has been developed in terms of solution to a set of Riccati difference equations. By adopting the linearity of state equations, the application of fault estimator has been developed into the model with arbitrary input.

Chapter 5

FE of decentralized W-NCSs

With the rapid development of industrial automation, especially of the large scale industry, the limitation of the plant-wide centralized control approach is more and more evident. First, since MCU needs all information over the whole plant, the cost of information communication could be very high and the network building is very complex. It makes the communication as a potential frequent source of failures and may cause additional expenses by production outage. Second, with the increasing dimensionality, the interaction or coupling between system units can be very complicated. It requires a very high computing capability of MCU and the computing delay may affect greatly the system real-time performance. All these drawbacks lead us to develop the FE issues based on decentralized controller/observer.

This chapter attempts to encompass the development of FE methods for decentralized W-NCSs. The decentralized observers' structures will be first proposed based on the system model in Chapter 3 for two kinds of residual structures, i.e., non-shared and shared residual signals. Next, the observer for integrated model will be presented. The FE algorithm will be proposed under an H_∞ performance index, which optimize the influences of disturbance and variations of fault on the estimate error. To start with, we would like to introduce the basic ideas of observer-based FE for decentralized W-NCSs.

5.1 Decentralized observer design

According to the model of decentralized W-NCSs, the fault filtering scheme and algorithm will be proposed in this section. Since the design issues in the decentralized system are implemented in every CS in the independent way, the corresponding sub-observer, which fits for the decentralized computation, will be proposed.

It's worth mentioning that the structure of sub-observer is proposed in two forms, that are the sub-observer with and without shared residuals of other CSs. Literally speaking, the sub-observer without shared residuals is only related with the local residual, i.e., the residual of i-th sub-system. This form is generally used for many FD and filtering approaches. In the consideration of coupling, the state observer is not only related with its own state estimate, but also with the state estimates of other coupled sub-systems, so apparently the residual signals of coupled sub-systems can affect the accuracy of state estimate in some degree. Based on this reason, the sub-observer with shared residuals, which is the second form, is proposed to improve sub-observer performance. In the communication aspect, the residual signals are broadcasted in the same way as transmission of state estimates. The design of observer with shared residuals is under the assumption that residual is transmitted in the same scheduled time slot of updated state, so the transmission scheme between CSs isn't changed by the introduction of residual transmission. To start with, the system model proposed in Chapter 3 will be first modified considering driving disturbance, measurement disturbance and fault, and the sub-observer structure with shared and non-shared residuals will be presented respectively.

5.1.1 With non-shared residuals

Consider the model of the i-th sub-system with disturbances and fault

$$\begin{aligned}\mathbf{x}_i\left((k+1)T_{cyc,i}\right) =& \mathbf{A}_{d,ii}\mathbf{x}_i(kT_{cyc,i}) + \mathbf{B}_{d,i}\mathbf{u}_i(kT_{cyc,i}) \\ &+ \sum_{j\neq i}^{N}\mathbf{A}_{d,ij}(kT_{cyc,i})\bar{\mathbf{x}}_j(kT_{cyc,i}) \\ &+ \mathbf{B}_{d,di}\mathbf{d}_i(kT_{cyc,i}) + \mathbf{E}_{d,fi}\mathbf{f}_i(kT_{cyc,i}) \\ \mathbf{y}_i\left(kT_{cyc,i}\right) =& \mathbf{C}_{d,i}\mathbf{x}_i(kT_{cyc,i}) + \mathbf{v}_i(kT_{cyc,i}) \\ &+ \mathbf{F}_{d,fi}\mathbf{f}_i(kT_{cyc,i})\end{aligned} \tag{5.1}$$

where $\mathbf{d}_i(kT_{cyc,i}) \in \mathcal{R}^{p_i}$ is the driving disturbance, $\mathbf{v}_i(kT_{cyc,i}) \in \mathcal{R}^{m_i}$ is the measurement disturbance, and $\mathbf{f}_i(kT_{cyc,i}) \in \mathcal{R}^{q_i+m_i}$ is the vector that represents all sensor and actuator faults, and will be zero in the fault-free case. $\mathbf{B}_{d,di}$, $\mathbf{E}_{d,fi}$ and $\mathbf{F}_{d,fi}$ are known matrices of appropriate dimensions.

The observer structure of the i-th sub-system related only with local residual signals, which is embedded in and implemented by the i-th CS, is

constructed as follows

$$\begin{aligned}
\hat{\mathbf{x}}_i\left((k+1)T_{cyc,i}\right) =& \mathbf{A}_{d,ii}\hat{\mathbf{x}}_i\left(kT_{cyc,i}\right) + \mathbf{B}_{d,i}\mathbf{u}_i(kT_{cyc,i}) \\
&+ \sum_{j\neq i}^{N} \mathbf{A}_{d,ij}(kT_{cyc,i})\hat{\bar{\mathbf{x}}}_j(kT_{cyc,i}) \\
&+ \mathbf{E}_{d,fi}\hat{\mathbf{f}}_i(kT_{cyc,i}) + \mathbf{L}_i(kT_{cyc,i})\mathbf{r}_i\left(kT_{cyc,i}\right) \\
\hat{\mathbf{f}}_i\left((k+1)T_{cyc,i}\right) =& \hat{\mathbf{f}}_i(kT_{cyc,i}) + \mathbf{V}_i(kT_{cyc,i})\mathbf{r}_i\left(kT_{cyc,i}\right) \\
\hat{\mathbf{y}}_i\left(kT_{cyc,i}\right) =& \mathbf{C}_{d,i}\hat{\mathbf{x}}_i(kT_{cyc,i}) + \mathbf{F}_{d,fi}\hat{\mathbf{f}}_i(kT_{cyc,i})
\end{aligned} \tag{5.2}$$

where $\mathbf{L}_i(kT_{cyc,i}) \in \mathcal{R}^{n_i\times m_i}$ and $\mathbf{V}_i(kT_{cyc,i}) \in \mathcal{R}^{(q_i+m_i)\times m_i}$ are the observer gain and post-filter matrix to be designed and $\mathbf{r}_i\left(kT_{cyc,i}\right)$ is the residual signal of the i-th sub-system, which is

$$\begin{aligned}
\mathbf{r}_i\left(kT_{cyc,i}\right) &= \mathbf{y}_i\left(kT_{cyc,i}\right) - \mathbf{C}_i\hat{\mathbf{x}}_i\left(kT_{cyc,i}\right) - \mathbf{F}_{d,fi}\hat{\mathbf{f}}_i(kT_{cyc,i}) \\
&= \mathbf{C}_{d,i}\mathbf{e}_{xi}\left(kT_{cyc,i}\right) + \mathbf{F}_{d,fi}\mathbf{e}_{fi}(kT_{cyc,i}) + \mathbf{v}_i(kT_{cyc,i})
\end{aligned} \tag{5.3}$$

where $\mathbf{e}_{xi}\left(kT_{cyc,i}\right) = \mathbf{x}_i\left(kT_{cyc,i}\right) - \hat{\mathbf{x}}_i\left(kT_{cyc,i}\right)$ is the state error, and $\mathbf{e}_{fi}\left(kT_{cyc,i}\right) = \mathbf{f}_i\left(kT_{cyc,i}\right) - \hat{\mathbf{f}}_i\left(kT_{cyc,i}\right)$ is the fault estimate error of i-th sub-system.

Considering the scheduler between CSs, $\hat{\bar{\mathbf{x}}}_j(kT_{cyc,i})$, $j \neq i$, represents the state estimates of CSs, which have updated state estimates during the time interval $[kT_{cyc,i}, (k+1)T_{cyc,i})$.

It follows from the periodic model in (3.16) as well as the observer of the i-th sub-system (3.7), the observer algorithm of decentralized W-NCSs can be written into

$$\begin{aligned}
\hat{\bar{\mathbf{x}}}_j((k+1)T_{period} + \varsigma_j) =& \begin{bmatrix} \bar{\mathbf{A}}_{21}(j) & \bar{\mathbf{A}}_{22}(j) \end{bmatrix} \hat{\mathbf{x}}(k,j) \\
&+ \bar{\mathbf{B}}_2(j)\mathbf{u}(k,j) + \bar{\mathbf{E}}_{f2}(j)\hat{\mathbf{f}}(k,j) \\
&+ \bar{\mathbf{L}}_j((k+1)T_{period} + \varsigma_j)\bar{\mathbf{r}}_j\left((k+1)T_{period} + \varsigma_j\right) \\
\hat{\bar{\mathbf{f}}}_j((k+1)T_{period} + \varsigma_j) =& \bar{\mathbf{A}}_{f2}(j)\hat{\mathbf{f}}(k,j) \\
&+ \bar{\mathbf{V}}_j((k+1)T_{period} + \varsigma_j)\bar{\mathbf{r}}_j\left((k+1)T_{period} + \varsigma_j\right) \\
\hat{\mathbf{y}}(k,j) =& \bar{\mathbf{C}}_2(j)\hat{\mathbf{x}}(k,j) + \bar{\mathbf{F}}_{f2}(j)\hat{\mathbf{f}}(k,j)
\end{aligned} \tag{5.4}$$

$$\bar{\mathbf{r}}_j\left((k+1)T_{period} + \varsigma_j\right) = \begin{bmatrix} \vdots \\ \mathbf{r}_i((k+1)T_{period} + \varsigma_j - T_{cyc,i}) \\ \vdots \end{bmatrix} \tag{5.5}$$

$$\bar{\mathbf{L}}_j((k+1)T_{period}+\varsigma_j)=\begin{bmatrix}\ddots & & 0\\ & \mathbf{L}_i((k+1)T_{period}+\varsigma_j-T_{cyc,i}) & \\ 0 & & \ddots\end{bmatrix} \tag{5.6}$$

$$\bar{\mathbf{V}}_j((k+1)T_{period}+\varsigma_j)=\begin{bmatrix}\ddots & & 0\\ & \mathbf{V}_i((k+1)T_{period}+\varsigma_j-T_{cyc,i}) & \\ 0 & & \ddots\end{bmatrix} \tag{5.7}$$

where $\mathbf{f}(k,j)$ is a lifted vector of all faults in the time interval $[kT_{period}+\varsigma_j,(k+1)T_{period}+\varsigma_j)$, whose definition is similar as $\mathbf{x}(k,j)$. $\hat{\bar{\mathbf{x}}}_j((k+1)T_{period}+\varsigma_j)$, $\hat{\mathbf{x}}(k,j)$, $\hat{\mathbf{f}}(k,j)$ denote the estimates for $\bar{\mathbf{x}}_j((k+1)T_{period}+\varsigma_j)$, $\mathbf{x}(k,j)$, $\mathbf{f}(k,j)$ respectively. $\bar{\mathbf{E}}_{f2}(j)$ and $\bar{\mathbf{F}}_{f2}(j)$ consist of $\mathbf{E}_{d,fi}$, $\mathbf{F}_{d,fi}$ and some zero matrices. $\bar{\mathbf{A}}_{f2}(j)$ is a $(0-1)$ matrix, which organizes the queue of elements in $\hat{\mathbf{f}}(k,j)$, so $\hat{\mathbf{f}}(k,j)$ works like a data buffer of all faults estimates in the last T_{period}. $\mathbf{r}_i((k+1)T_{period}+\varsigma_j-T_{cyc,i})$ is the residual vector generated in the i-th sub-system with $i\in I_{\varsigma_j}$, and $\bar{\mathbf{r}}_j\left((k+1)T_{period}+\varsigma_j\right)$ includes all the residual vectors generated in the sub-systems belonging to I_{ς_j}. Because the state estimates are only concerned with the local residual signals, the observer gains $\bar{\mathbf{L}}_j((k+1)T_{period}+\varsigma_j)$ and $\bar{\mathbf{V}}_j((k+1)T_{period}+\varsigma_j)$ are therefore in the form of diagonal.

Recall the output equation in (3.14), it is easy to obtain

$$\begin{aligned}
&\mathbf{r}_i((k+1)T_{period}+\varsigma_j-T_{cyc,i})\\
=&\mathbf{y}_i((k+1)T_{period}+\varsigma_j-T_{cyc,i})-\mathbf{C}_{d,i}\hat{\mathbf{x}}_i((k+1)T_{period}+\varsigma_j-T_{cyc,i})\\
&-\mathbf{F}_{d,fi}\hat{\mathbf{f}}_i((k+1)T_{period}+\varsigma_j-T_{cyc,i})\\
=&\mathbf{C}_{d,i}\mathbf{e}_{xi}((k+1)T_{period}+\varsigma_j-T_{cyc,i})+\mathbf{F}_{d,fi}\mathbf{e}_{fi}((k+1)T_{period}+\varsigma_j-T_{cyc,i})\\
&+\mathbf{v}_i((k+1)T_{period}+\varsigma_j-T_{cyc,i})
\end{aligned} \tag{5.8}$$

where $\hat{\mathbf{x}}_i((k+1)T_{period}+\varsigma_j-T_{cyc,i})$ is the estimate of $\mathbf{x}_i((k+1)T_{period}+\varsigma_j-T_{cyc,i})$ and $\hat{\mathbf{f}}_i((k+1)T_{period}+\varsigma_j-T_{cyc,i})$ is the estimate of $\mathbf{f}_i((k+1)T_{period}+\varsigma_j-T_{cyc,i})$. $\mathbf{e}_{xi}((k+1)T_{period}+\varsigma_j-T_{cyc,i})$ is the same as $\mathbf{e}_{xi}\left(kT_{cyc,i}\right)$ under the overall schedule structure. Similarly $\mathbf{e}_{fi}((k+1)T_{period}+\varsigma_j-T_{cyc,i})$ is like $\mathbf{e}_{fi}\left(kT_{cyc,i}\right)$ under the overall schedule structure. It is obvious that

$$\begin{aligned}
&\mathbf{e}_{xi}((k+1)T_{period}+\varsigma_j-T_{cyc,i})\\
=&\mathbf{x}_i((k+1)T_{period}+\varsigma_j-T_{cyc,i})-\hat{\mathbf{x}}_i((k+1)T_{period}+\varsigma_j-T_{cyc,i})\\
&\mathbf{e}_{fi}((k+1)T_{period}+\varsigma_j-T_{cyc,i})\\
=&\mathbf{f}_i((k+1)T_{period}+\varsigma_j-T_{cyc,i})-\hat{\mathbf{f}}_i((k+1)T_{period}+\varsigma_j-T_{cyc,i})
\end{aligned}$$

To explore the overall system dynamics and develop the overall observer approach, (5.5) can be further formulated to

$$\begin{aligned}
\hat{\mathbf{x}}(k,j+1) =& \mathbf{A}(j)\hat{\mathbf{x}}(k,j) + \mathbf{B}(j)\mathbf{u}(k,j) + \mathbf{E}_f(j)\hat{\mathbf{f}}(k,j) \\
&+ \mathbf{L}(j)\bar{\mathbf{r}}_j((k+1)T_{period} + \varsigma_j) \\
\hat{\mathbf{f}}(k,j+1) =& \mathbf{A}_f(j)\hat{\mathbf{f}}(k,j) + \mathbf{V}(j)\bar{\mathbf{r}}_j((k+1)T_{period} + \varsigma_j) \\
\hat{\mathbf{y}}(k,j) =& \mathbf{C}(j)\hat{\mathbf{x}}(k,j) + \mathbf{F}_f(j)\hat{\mathbf{f}}(k,j) \\
\mathbf{E}_f(j) =& \begin{bmatrix} \mathbf{0} \\ \bar{\mathbf{E}}_{f2}(j) \end{bmatrix},\ \mathbf{F}_f(j) = \bar{\mathbf{F}}_{f2}(j) \\
\mathbf{L}(j) =& \begin{bmatrix} \mathbf{0} \\ \bar{\mathbf{L}}_j((k+1)T_{period} + \varsigma_j) \end{bmatrix} \\
\mathbf{V}(j) =& \begin{bmatrix} \mathbf{0} \\ \bar{\mathbf{V}}_j((k+1)T_{period} + \varsigma_j) \end{bmatrix}
\end{aligned} \tag{5.9}$$

whose dynamics is governed by

$$\begin{aligned}
\mathbf{e}_x(k,j+1) =& \mathbf{x}(k,j+1) - \hat{\mathbf{x}}(k,j+1) \\
=& \left(\begin{bmatrix} \mathbf{0} & \mathbf{I} \\ \bar{\mathbf{A}}_{21}(j) & \bar{\mathbf{A}}_{22}(j) \end{bmatrix} - \begin{bmatrix} \mathbf{0} \\ \bar{\mathbf{L}}_j((k+1)T_{period} + \varsigma_j) \end{bmatrix} \mathbf{C}(j) \right) \mathbf{e}_x(k,j) \\
&+ \left(\begin{bmatrix} \mathbf{0} \\ \bar{\mathbf{E}}_{f2}(j) \end{bmatrix} - \begin{bmatrix} \mathbf{0} \\ \bar{\mathbf{L}}_j((k+1)T_{period} + \varsigma_j) \end{bmatrix} \mathbf{F}_f(j) \right) \mathbf{e}_f(k,j) \\
&+ \begin{bmatrix} \mathbf{0} \\ \bar{\mathbf{B}}_{d2}(j) \end{bmatrix} \mathbf{d}(k,j) - \begin{bmatrix} \mathbf{0} \\ \bar{\mathbf{L}}_j((k+1)T_{period} + \varsigma_j) \end{bmatrix} \mathbf{v}(k,j)
\end{aligned}$$

$$\begin{aligned}
\mathbf{e}_f(k,j+1) =& \mathbf{f}(k,j+1) - \hat{\mathbf{f}}(k,j+1) \\
=& \mathbf{f}(k,j+1) - \mathbf{A}_f(j)\mathbf{f}(k,j) + \mathbf{A}_f(j)\mathbf{f}(k,j) \\
&- \mathbf{A}_f(j)\hat{\mathbf{f}}(k,j) - \mathbf{V}(j)\bar{\mathbf{r}}_j((k+1)T_{period} + \varsigma_j) \\
=& \Delta\mathbf{f}(k,j) + \mathbf{A}_f(j)\mathbf{e}_f(k,j) \\
&- \mathbf{F}(j)\mathbf{C}(j)\mathbf{e}_x(k,j) - \mathbf{V}(j)\mathbf{F}_f(j)\mathbf{e}_f(k,j) - \mathbf{V}(j)\mathbf{v}(k,j) \\
=& \Delta\mathbf{f}(k,j) + \left(\mathbf{A}_f(j) - \mathbf{V}(j)\mathbf{F}_f(j)\right)\mathbf{e}_f(k,j) \\
&- \mathbf{V}(j)\mathbf{C}(j)\mathbf{e}_x(k,j) - \mathbf{V}(j)\mathbf{v}(k,j) \\
=& \left(\mathbf{A}_f(j) - \begin{bmatrix} \mathbf{0} \\ \bar{\mathbf{V}}_j((k+1)T_{period} + \varsigma_j) \end{bmatrix} \mathbf{F}_f(j) \right) \mathbf{e}_f(k,j) \\
&- \begin{bmatrix} \mathbf{0} \\ \bar{\mathbf{V}}_j((k+1)T_{period} + \varsigma_j) \end{bmatrix} \mathbf{C}(j)\mathbf{e}_x(k,j) \\
&+ \Delta\mathbf{f}(k,j) - \begin{bmatrix} \mathbf{0} \\ \bar{\mathbf{V}}_j((k+1)T_{period} + \varsigma_j) \end{bmatrix} \mathbf{v}(k,j)
\end{aligned} \tag{5.10}$$

$$\bar{\mathbf{r}}_j(kT_{cyc,i}) = \begin{cases} \mathbf{r}_j(\zeta_{ij}(kT_{cyc,i})), \text{ no update of } j\text{-th sub-system in} \\ \qquad [kT_{cyc,i}, (k+1)T_{cyc,i}) ; \\ \begin{bmatrix} \mathbf{r}_j(\zeta_{ij}(kT_{cyc,i})) \\ \mathbf{r}_j(kT_{cyc,i} + t_{ij,1}(k)) \\ \vdots \\ \mathbf{r}_j(kT_{cyc,i} + t_{ij,\kappa}(k)) \end{bmatrix}, \text{update(s) of } j\text{-th sub-system in} \\ \qquad [kT_{cyc,i}, (k+1)T_{cyc,i}) \end{cases} \tag{5.12}$$

---

where $\bar{\mathbf{B}}_{d2}(j)$ consists of $\mathbf{B}_{d,di}$ and some zero matrices. $\mathbf{d}(k,j)$ and $\mathbf{v}(k,j)$ are the lifted vectors of driving disturbance and measurement disturbance respectively in the time interval $[kT_{period}+\varsigma_j, (k+1)T_{period}+\varsigma_j)$. $\Delta\mathbf{f}(k,j) = \mathbf{f}(k,j+1) - \mathbf{A}_f(j)\mathbf{f}(k,j)$ is the fault increment.

5.1.2 With shared residuals

Recall the sub-observer structure (5.2) of the i-th sub-system without residual sharing and the coupling relations between CSs, the i-th sub-observer can be extended into the form involving with residual signals of other coupled CSs, which is represented as follows,

$$\begin{aligned} &\hat{\mathbf{x}}_i\left((k+1)T_{cyc,i}\right) \\ &= \mathbf{A}_{d,ii}\hat{\mathbf{x}}_i\left(kT_{cyc,i}\right) + \mathbf{B}_{d,i}\mathbf{u}_i(kT_{cyc,i}) \\ &\quad + \mathbf{E}_{d,fi}\hat{\mathbf{f}}_i(kT_{cyc,i}) + \mathbf{L}_i(kT_{cyc,i})\mathbf{r}_i\left(kT_{cyc,i}\right) \\ &\quad + \sum_{j\neq i}^{N}\left(\mathbf{A}_{d,ij}(kT_{cyc,i})\hat{\bar{\mathbf{x}}}_j(kT_{cyc,i}) + \mathbf{L}_{ij}(kT_{cyc,i})\bar{\mathbf{r}}_j\left(kT_{cyc,i}\right)\right) \end{aligned} \tag{5.11}$$

where $\bar{\mathbf{r}}_j\left(kT_{cyc,i}\right),\ j \neq i$ is a vector whose elements are residual vectors of j-th CS in the period of $[kT_{cyc,i}, (k+1)T_{cyc,i})$, so $\bar{\mathbf{r}}_j\left(kT_{cyc,i}\right)$, which is given in (5.12), has the same structure like $\bar{\mathbf{x}}_j(kT_{cyc,i})$ in (3.9).

It is worth pointing out that the update of the residual vector is accompanied by that of the state estimate, so the transmission of $\mathbf{r}_i(kT_{cyc,i})$ is proposed to be transmitted together with $\hat{\mathbf{x}}_i(kT_{cyc,i})$ in one packet to all the other sub-systems.

To develop the observer with shared residual vectors for system (3.13), it

is easy to deduce

$$\begin{aligned}\hat{\bar{\mathbf{x}}}_j((k+1)T_{period}+\varsigma_j) =& \left[\begin{array}{cc}\bar{\mathbf{A}}_{21}(j) & \bar{\mathbf{A}}_{22}(j)\end{array}\right]\hat{\mathbf{x}}(k,j)+\bar{\mathbf{B}}_2(j)\mathbf{u}(k,j)\\ &+\bar{\mathbf{E}}_{f2}(j)\hat{\mathbf{f}}(k,j)+\bar{\mathbf{L}}_2(j)\mathbf{r}(k,j)\\ \hat{\bar{\mathbf{f}}}_j((k+1)T_{period}+\varsigma_j) =& \bar{\mathbf{A}}_{f2}(j)\hat{\mathbf{f}}(k,j)+\bar{\mathbf{V}}_2(j)\mathbf{r}(k,j)\\ \hat{\mathbf{y}}(k,j) =& \bar{\mathbf{C}}_2(j)\hat{\mathbf{x}}(k,j)+\bar{\mathbf{F}}_{f2}(j)\hat{\mathbf{f}}(k,j)\end{aligned} \tag{5.13}$$

where $\mathbf{r}(k,j)$ is a lifted vector of all residual signals in the time interval $[kT_{period}+\varsigma_j,(k+1)T_{period}+\varsigma_j)$, whose definition is similar as $\mathbf{x}(k,j)$. $\bar{\mathbf{L}}_2(j)$ and $\bar{\mathbf{V}}_2(j)$ are no longer diagonal as $\bar{\mathbf{L}}_j((k+1)T_{period}+\varsigma_j)$ and $\bar{\mathbf{V}}_j((k+1)T_{period}+\varsigma_j)$ respectively in (5.6). Suppose that $I_{\varsigma_j}=\{\cdots,h,\cdots,l,\cdots\}$, $h,\ l\in[1,N]$, $h\neq l$, $\mathbf{r}_h((k+1)T_{period}+\varsigma_j-T_{cyc,h})$ is the m_h-th element of $\mathbf{r}(k,j)$, $\mathbf{r}_l((k+1)T_{period}+\varsigma_j-T_{cyc,l})$ is the m_l-th element of $\mathbf{r}(k,j)$, the entry of m_h-th row and m_l-th column of $\bar{\mathbf{L}}_2(j)$ is $\mathbf{L}_{hl}((k+1)T_{period}+\varsigma_j-T_{cyc,h})$, and the entry of m_l-th row and m_h-th column of $\bar{\mathbf{L}}_2(j)$ is $\mathbf{L}_{lh}((k+1)T_{period}+\varsigma_j-T_{cyc,l})$. $\bar{\mathbf{L}}_2(j)$ can be represented as follows

$$\bar{\mathbf{L}}_2(j)=\left[\begin{array}{ccccc}\ddots & \vdots & & \vdots & \\ \cdots & \mathbf{L}_h & \cdots & \mathbf{L}_{hl} & \cdots\\ & \vdots & \ddots & \vdots & \\ \cdots & \mathbf{L}_{lh} & \cdots & \mathbf{L}_l & \cdots\\ & \vdots & & \vdots & \ddots\end{array}\right] \tag{5.14}$$

where $\mathbf{L}_h$ represents $\mathbf{L}_h((k+1)T_{period}+\varsigma_j-T_{cyc,h})$, $\mathbf{L}_l$ represents $\mathbf{L}_l((k+1)T_{period}+\varsigma_j-T_{cyc,l})$, $\mathbf{L}_{hl}$ represents $\mathbf{L}_{hl}((k+1)T_{period}+\varsigma_j-T_{cyc,h})$ and $\mathbf{L}_{lh}$ represents $\mathbf{L}_{lh}((k+1)T_{period}+\varsigma_j-T_{cyc,l})$.

Similarly, $\bar{\mathbf{V}}_2(j)$ can also be reformulated into the structure as $\bar{\mathbf{L}}_2(j)$

$$\bar{\mathbf{V}}_2(j)=\left[\begin{array}{ccccc}\ddots & \vdots & & \vdots & \\ \cdots & \mathbf{V}_h & \cdots & \mathbf{V}_{hl} & \cdots\\ & \vdots & \ddots & \vdots & \\ \cdots & \mathbf{V}_{lh} & \cdots & \mathbf{V}_l & \cdots\\ & \vdots & & \vdots & \ddots\end{array}\right] \tag{5.15}$$

where $\mathbf{V}_h$ represents $\mathbf{V}_h((k+1)T_{period}+\varsigma_j-T_{cyc,h})$, $\mathbf{V}_l$ represents $\mathbf{V}_l((k+1)T_{period}+\varsigma_j-T_{cyc,l})$, $\mathbf{V}_{hl}$ represents $\mathbf{V}_{hl}((k+1)T_{period}+\varsigma_j-T_{cyc,h})$ and $\mathbf{V}_{lh}$ represents $\mathbf{V}_{lh}((k+1)T_{period}+\varsigma_j-T_{cyc,l})$.

Considering the overall observer based on W-NCSs model (3.12), the

decentralized observer can be further rewritten into the following form

$$\begin{aligned}
\hat{\mathbf{x}}(k,j+1) =& \mathbf{A}(j)\hat{\mathbf{x}}(k,j) + \mathbf{B}(j)\mathbf{u}(k,j) + \mathbf{E}_f(j)\hat{\mathbf{f}}(k,j) \\
&+ \mathbf{L}(j)\mathbf{r}(k,j) \\
\hat{\mathbf{f}}(k,j+1) =& \mathbf{A}_f(j)\hat{\mathbf{f}}(k,j) + \mathbf{V}(j)\mathbf{r}(k,j) \\
\hat{\mathbf{y}}(k,j) =& \mathbf{C}(j)\hat{\mathbf{x}}(k,j) + \mathbf{F}_f(j)\hat{\mathbf{f}}(k,j) \\
\mathbf{L}(j) =& \begin{bmatrix} \mathbf{0} \\ \bar{\mathbf{L}}_2(j) \end{bmatrix},\ \mathbf{V}(j) = \begin{bmatrix} \mathbf{0} \\ \bar{\mathbf{V}}_2(j) \end{bmatrix}
\end{aligned} \tag{5.16}$$

whose dynamics is governed by

$$\begin{aligned}
&\mathbf{e}_x(k,j+1) \\
=& \left(\begin{bmatrix} \mathbf{0} & \mathbf{I} \\ \bar{\mathbf{A}}_{21}(j) & \bar{\mathbf{A}}_{22}(j) \end{bmatrix} - \begin{bmatrix} \mathbf{0} \\ \bar{\mathbf{L}}_2(j) \end{bmatrix} \mathbf{C}(j) \right) \mathbf{e}_x(k,j) \\
&+ \left(\begin{bmatrix} \mathbf{0} \\ \bar{\mathbf{E}}_{f2}(j) \end{bmatrix} - \begin{bmatrix} \mathbf{0} \\ \bar{\mathbf{L}}_2(j) \end{bmatrix} \mathbf{F}_f(j) \right) \mathbf{e}_f(k,j) \\
&+ \begin{bmatrix} \mathbf{0} \\ \bar{\mathbf{B}}_{d2}(j) \end{bmatrix} \mathbf{d}(k,j) - \begin{bmatrix} \mathbf{0} \\ \bar{\mathbf{L}}_2(j) \end{bmatrix} \mathbf{v}(k,j) \\
&\mathbf{e}_f(k,j+1) \\
=& \left(\mathbf{A}_f(j) - \begin{bmatrix} \mathbf{0} \\ \bar{\mathbf{V}}_2(j) \end{bmatrix} \mathbf{F}_f(j) \right) \mathbf{e}_f(k,j) \\
&- \begin{bmatrix} \mathbf{0} \\ \bar{\mathbf{V}}_2(j) \end{bmatrix} \mathbf{C}(j)\mathbf{e}_x(k,j) \\
&+ \Delta\mathbf{f}(k,j) - \begin{bmatrix} \mathbf{0} \\ \bar{\mathbf{V}}_2(j) \end{bmatrix} \mathbf{v}(k,j)
\end{aligned} \tag{5.17}$$

It follows directly from (5.12) that by selecting $\mathbf{L}_{ij}(kT_{cyc,i})$ suitably, the coupling expressed by $\mathbf{A}_{d,ij}(kT_{cyc,i}) - \mathbf{L}_{ij}(kT_{cyc,i})\bar{\mathbf{C}}_j$ can be remarkably reduced. In the context of the overall observer design, i.e., in (5.13), the extension means relaxing the diagonal structure of the observer gain matrices into the structure (5.14) and (5.15), and it also means relaxing the condition of solving the FE algorithm.

As pointed out in Remark 1, when designing the decentralized observer with shared residuals, $\mathbf{y}(k,j)$ in (3.16) includes all output in the time interval $[kT_{period} + \varsigma_j, (k+1)T_{period} + \varsigma_j)$ corresponding with $\mathbf{r}(k,j)$ in (5.13).

5.1.3 Observer development on integrated system

As illustrated in Section 3.2.1, the communication scheme of decentralized W-NCSs includes two types, i.e., in a sub-system and between sub-systems.

The scheme is a hierarchical structure, in which communication between sub-systems is at a top level. The sub-systems broadcast their state estimates with each other every cycle. It is obvious that the information at the top level is more important and the demand of communication rate is much lower that the ground level. So the following research is based on the assumption that the wireless network resource is adequate to ensure the real-time transmission between sub-systems, in other words, no imperfect communication of state estimates will be taken into consideration. While in the ground layer, because of the high uncertainty and complexity, the communication is controlled by the scheduler and formulated for the integration.

Considering the integrated model presented in (3.26), the observer approaches and their dynamics are developed based on the assumption that the data transmission is executed strictly according to the scheduler, and any error characteristic in communication channel, such as unexpected interference, jitter and so on, will not be considered. So the values of data through network under the guidance of scheduler will not change. Accordingly no observer would be designed for scheduler model (3.23), and the observer approaches of integrated model are based on (5.9) and (5.16), respectively. To simplify the notation, $I_{s\varsigma_j}$ is used to denote the set of all those sub-systems, which are scheduled for data transmission between sub-systems at the time instant $kT_{period} + \varsigma_j$.

With non-shared residuals

The observer of integrated system (3.26) with non-shared residuals can be developed as follows

$$\begin{aligned}
\hat{\bar{\mathbf{x}}}(k, j+1) =& \bar{\mathbf{A}}(j)\hat{\bar{\mathbf{x}}}(k, j) + \bar{\mathbf{B}}(j)\mathbf{u}(k, j) + \bar{\mathbf{E}}_f(j)\hat{\mathbf{f}}(k, j) \\
&+ \bar{\mathbf{L}}_s(j)\bar{\mathbf{r}}_{sj}((k+1)T_{period} + \varsigma_j) \\
\hat{\mathbf{f}}(k, j+1) =& \mathbf{A}_f(j)\hat{\mathbf{f}}(k, j) + \bar{\mathbf{V}}_s(j)\bar{\mathbf{r}}_{sj}((k+1)T_{period} + \varsigma_j) \\
\hat{\mathbf{y}}_s(k, j) =& \bar{\mathbf{C}}(j)\hat{\bar{\mathbf{x}}}(k, j) + \bar{\mathbf{F}}_f(j)\hat{\mathbf{f}}(k, j)
\end{aligned} \tag{5.18}$$

where

$$\begin{aligned}
\bar{\mathbf{r}}_{sj}((k+1)T_{period} + \varsigma_j) &= \mathbf{y}_s(k, j) - \hat{\mathbf{y}}_s(k, j) \\
\bar{\mathbf{L}}_s(j) &= \begin{bmatrix} \mathbf{L}_s(j) \\ \mathbf{0} \end{bmatrix} \\
\bar{\mathbf{V}}_s(j) &= \begin{bmatrix} \mathbf{V}_s(j) \\ \mathbf{0} \end{bmatrix}
\end{aligned} \tag{5.19}$$

and $\mathbf{L}_s(j)$, $\mathbf{V}_s(j)$ are diagonal matrices in which the diagonal entries are $\mathbf{L}_{si}((k+1)T_{period}+\varsigma_j-T_{cyc,i})$, $\mathbf{V}_{si}((k+1)T_{period}+\varsigma_j-T_{cyc,i})$, $i \in I_{s\varsigma_j}$, respectively.

The system dynamics is governed by

$$\begin{aligned}
&\bar{\mathbf{e}}_x(k,j+1)\\
=&\bar{\mathbf{x}}(k,j+1)-\hat{\bar{\mathbf{x}}}(k,j+1)\\
=&(\bar{\mathbf{A}}(j)-\bar{\mathbf{L}}_s(j)\bar{\mathbf{C}}(j))\bar{\mathbf{e}}_x(k,j)\\
&+(\bar{\mathbf{E}}_f(j)-\bar{\mathbf{L}}_s(j)\bar{\mathbf{F}}_f(j))\bar{\mathbf{e}}_f(k,j)\\
&+(\bar{\mathbf{B}}_d(j)-\bar{\mathbf{L}}_s(j)\bar{\mathbf{D}}_d(j))\mathbf{w}(k,j)\\
&\bar{\mathbf{e}}_f(k,j+1)\\
=&\mathbf{f}(k,j+1)-\hat{\mathbf{f}}(k,j+1)\\
=&\left(\mathbf{A}_f(j)-\bar{\mathbf{V}}_s(j)\bar{\mathbf{F}}_f(j)\right)\bar{\mathbf{e}}_f(k,j)\\
&-\bar{\mathbf{V}}_s(j)\bar{\mathbf{C}}(j)\bar{\mathbf{e}}_x(k,j)\\
&+\Delta\mathbf{f}(k,j)-\bar{\mathbf{V}}_s(j)\bar{\mathbf{D}}_d(j)\mathbf{w}(k,j)
\end{aligned} \tag{5.20}$$

With shared residuals

The observer of integrated system (3.26) with shared residuals can be developed as follows

$$\begin{aligned}
\hat{\bar{\mathbf{x}}}(k,j+1)=&\bar{\mathbf{A}}(j)\hat{\bar{\mathbf{x}}}(k,j)+\bar{\mathbf{B}}(j)\mathbf{u}(k,j)+\bar{\mathbf{E}}_f(j)\hat{\mathbf{f}}(k,j)\\
&+\bar{\mathbf{L}}_s(j)\mathbf{r}(k,j)\\
\hat{\mathbf{f}}(k,j+1)=&\mathbf{A}_f(j)\hat{\mathbf{f}}(k,j)+\bar{\mathbf{V}}_s(j)\mathbf{r}(k,j)\\
\hat{\mathbf{y}}_s(k,j)=&\bar{\mathbf{C}}(j)\hat{\bar{\mathbf{x}}}(k,j)+\bar{\mathbf{F}}_f(j)\hat{\mathbf{f}}(k,j)
\end{aligned} \tag{5.21}$$

where $\mathbf{r}(k,j)$ is the lifted vector of residuals, which are broadcasted by CSs according to the overall scheduler, and the structures of $\bar{\mathbf{L}}_s(j)$, $\bar{\mathbf{V}}_s(j)$ are same as (5.19). Here $\mathbf{L}_s(j)$, $\mathbf{V}_s(j)$ are no longer diagonal. The entries outside of main diagonal corresponding to the coupling positions are nonzero observer gains to be designed. The system dynamics in this case is built same as (5.20).

5.2 FE of decentralized W-NCSs

In this section, FE approaches will be developed in terms of LMI technique based on the system dynamics (5.20) with the purpose of achieving robustness against disturbances and fault increment. To begin with, (5.20) is reformulated into

$$\bar{\mathbf{e}}(k,j+1) = \bar{\mathbf{A}}_e(j)\bar{\mathbf{e}}(k,j) + \bar{\mathbf{B}}_e(j)\bar{\mathbf{w}}(k,j) \tag{5.22}$$
$$\bar{\mathbf{e}}(k,j) = \begin{bmatrix} \bar{\mathbf{e}}_x(k,j) \\ \bar{\mathbf{e}}_f(k,j) \end{bmatrix},\ \bar{\mathbf{w}}(k,j) = \begin{bmatrix} \mathbf{w}(k,j) \\ \Delta\mathbf{f}(k,j) \end{bmatrix}$$
$$\bar{\mathbf{A}}_e(j) = \begin{bmatrix} \bar{\mathbf{A}}(j) - \bar{\mathbf{L}}_s(j)\bar{\mathbf{C}}(j) & \bar{\mathbf{E}}_f(j) - \bar{\mathbf{L}}_s(j)\bar{\mathbf{F}}_f(j) \\ -\bar{\mathbf{V}}_s(j)\bar{\mathbf{C}}(j) & \mathbf{A}_f(j) - \bar{\mathbf{V}}_s(j)\bar{\mathbf{F}}_f(j) \end{bmatrix}$$
$$\bar{\mathbf{B}}_e(j) = \begin{bmatrix} \bar{\mathbf{B}}_d(j) - \bar{\mathbf{L}}_s(j)\bar{\mathbf{D}}_d(j) & \mathbf{0} \\ -\bar{\mathbf{V}}_s(j)\bar{\mathbf{D}}_d(j) & \mathbf{I} \end{bmatrix}$$

Next, Theorem 1 will describe an H_∞ FE design of periodic system (3.26) with only actuator faults that satisfies the following performance index

$$\|\bar{\mathbf{e}}(k,j)\|^2 \le \gamma^2 \|\bar{\mathbf{w}}(k,j)\|^2 \tag{5.23}$$

where γ is called performance level.

Theorem 1 *For the integrated system (3.26) and its observer (5.18), assume that for* $j = 0, 1, \cdots, \theta - 1$

1. $\bar{\mathbf{F}}_f(j) = 0$, $\mathbf{f}_a(k,j) = \mathbf{f}(k,j)$ *is the lifted vector of actuator faults in the time interval* $[kT_{period} + \varsigma_j, (k+1)T_{period} + \varsigma_j)$;
2. *The pair* $\big(\bar{\mathbf{A}}(j),\ \bar{\mathbf{C}}(j)\big)$ *is observable;*
3. *The dimension of* $\mathbf{y}_s(k,j)$ *is greater than or equal to the dimension of updated faults in* $\mathbf{f}_a(k,j+1)$*, which can be represented by* $\bar{\mathbf{f}}_j((k+1)T_{period} + \varsigma_j)$;
4. $\bar{\mathbf{C}}(j)$ *is of full rank and the columns of* $\bar{\mathbf{E}}_f(j)$ *corresponding to the fault* $\mathbf{f}_i((k+1)T_{period} + \varsigma_j - T_{cyc,i})$, $i \in I_{s\varsigma_j}$ *are linearly independent.*

Given a constant $\gamma > 0$*, a closed circular region* $\mathcal{D}(\alpha, \tau)$ *with center* $\alpha + 0j$ *and radius* τ *and* $\bar{\mathbf{x}}(0,0) = \mathbf{0}$*, if there exists* θ*-periodic symmetric positive definite matrices* $\mathbf{P}(j)$ *and* $\mathbf{Q}(j)$ *such that the following LMIs*

$$\begin{bmatrix} \mathbf{P}(j+1) - 2\mathbf{I} & \bar{\mathbf{A}}_{e0}(j) + \mathbf{Q}(j)\bar{\mathbf{A}}_{e1}(j) - \alpha\mathbf{I} \\ * & -\tau^2\mathbf{P}(j) \end{bmatrix} < \mathbf{0} \tag{5.24}$$

$$\begin{bmatrix} \mathbf{P}(j+1) - 2\mathbf{I} & \bar{\mathbf{A}}_{e0}(j) + \mathbf{Q}(j)\bar{\mathbf{A}}_{e1}(j) & \bar{\mathbf{B}}_{e0}(j) + \mathbf{Q}(j)\bar{\mathbf{B}}_{e1}(j) & \mathbf{0} \\ * & -\mathbf{P}(j) & \mathbf{0} & \mathbf{I} \\ * & * & -\gamma\mathbf{I} & \mathbf{0} \\ * & * & * & -\gamma\mathbf{I} \end{bmatrix} < \mathbf{0} \tag{5.25}$$

where $\bar{\mathbf{A}}_{e0}(j) = \begin{bmatrix} \bar{\mathbf{A}}(j) & \bar{\mathbf{E}}_f(j) \\ \mathbf{0} & \mathbf{A}_f(j) \end{bmatrix}$, $\bar{\mathbf{A}}_{e1}(j) = \begin{bmatrix} -\bar{\mathbf{C}}(j) & \mathbf{0} \end{bmatrix}$, $\bar{\mathbf{B}}_{e0}(j) = \begin{bmatrix} \bar{\mathbf{B}}_d(j) & \mathbf{0} \\ \mathbf{0} & \mathbf{I} \end{bmatrix}$, $\bar{\mathbf{B}}_{e1}(j) = \begin{bmatrix} -\bar{\mathbf{D}}_d(j) & \mathbf{0} \end{bmatrix}$ *hold for each* j*. The eigenvalues of* $\bar{\mathbf{A}}_e(j)$ *belong to the region* $\mathcal{D}(\alpha, \tau)$ *and system dynamics (5.22) can satisfy the performance index (5.23). The observer gain matrices are lifted as* $\mathbf{Q}(j) = \begin{bmatrix} \bar{\mathbf{L}}_s(j) \\ \bar{\mathbf{V}}_s(j) \end{bmatrix}$.

Proof 1 *Define Lyapunov function*

$$\mathbf{V}(k,j) = \bar{\mathbf{e}}^T(k,j)\mathbf{P}(j)\bar{\mathbf{e}}(k,j) > \mathbf{0},\ \mathbf{V}(0,0) = \mathbf{0} \tag{5.26}$$

(5.23) can be satisfied if the following inequalities on a finite horizon $[0, T]$ *of* k *are proved to be true*

$$\begin{aligned}
&\sum_{k=0}^{T}\sum_{j=0}^{\theta-1}(\bar{\mathbf{e}}^T(k,j)\bar{\mathbf{e}}(k,j) - \gamma^2\bar{\mathbf{w}}^T(k,j)\bar{\mathbf{w}}(k,j)) < -\mathbf{V}(T,\theta-1) \leftrightarrow \\
&\sum_{k=0}^{T}\sum_{j=0}^{\theta-1}(\bar{\mathbf{e}}^T(k,j)\bar{\mathbf{e}}(k,j) - \gamma^2\bar{\mathbf{w}}^T(k,j)\bar{\mathbf{w}}(k,j)) \\
<& -\mathbf{V}(T,\theta-1) + \mathbf{V}(0,0) - \mathbf{V}(0,0) \leftrightarrow \\
&\sum_{k=0}^{T}\sum_{j=0}^{\theta-1}(\bar{\mathbf{e}}^T(k,j)\bar{\mathbf{e}}(k,j) - \gamma^2\bar{\mathbf{w}}^T(k,j)\bar{\mathbf{w}}(k,j) + \mathbf{V}(k,j+1) - \mathbf{V}(k,j)) \\
<& -\mathbf{V}(0,0) = \mathbf{0}
\end{aligned}$$

To satisfy $\bar{\mathbf{e}}^T(k,j)\bar{\mathbf{e}}(k,j) - \gamma^2\bar{\mathbf{w}}^T(k,j)\bar{\mathbf{w}}(k,j) + \mathbf{V}(k,j+1) - \mathbf{V}(k,j) < \mathbf{0}$*, it is easy to obtain that*

$$\begin{bmatrix} -\mathbf{P}(j+1) & \mathbf{P}(j+1)\bar{\mathbf{A}}_e(j) & \mathbf{P}(j+1)\bar{\mathbf{B}}_e(j) & \mathbf{0} \\ * & -\mathbf{P}(j) & \mathbf{0} & \mathbf{I} \\ * & * & -\gamma\mathbf{I} & \mathbf{0} \\ * & * & * & -\gamma\mathbf{I} \end{bmatrix} < \mathbf{0}$$

Considering $-\mathbf{P}^{-1}(j+1) \leq \mathbf{P}(j+1) - 2\mathbf{I}$*, (5.25) is satisfied by simple matrix manipulation. The proof of system robust stability (5.24) can refer to [95] and is omitted here.*

Remark 6 *Theorem 1 is suitable for the FE design of integrated model (3.26) for the two kinds of residual structures, i.e., non-shared and shared residuals, since the system dynamics can both be presented by (5.20). The*

positions of concrete nonzero elements in $\bar{\mathbf{L}}_s(j)$ *and* $\bar{\mathbf{V}}_s(j)$ *should be pointed out when solving LMIs. Note that* $\bar{\mathbf{L}}_s(j)$ *and* $\bar{\mathbf{V}}_s(j)$ *are different for the two residual structures, and the difference has been represented in the section of observer design.*

In the following, Theorem 2 will solve the H_∞ FE design problem of periodic system (3.26) with only sensor faults considering the same performance index (5.23).

Theorem 2 *For the integrated system (3.26) and its observer (5.18), assume that for* $j = 0, 1, \cdots, \theta - 1$

1. $\bar{\mathbf{E}}_f(j) = 0$, $\mathbf{f}_s(k, j) = \mathbf{f}(k, j)$ *is the lifted vector of all sensor faults in the time interval* $[kT_{period} + \varsigma_j, (k+1)T_{period} + \varsigma_j)$;
2. *The pair* $\left(\bar{\mathbf{A}}(j),\ \bar{\mathbf{C}}(j)\right)$ *is observable;*
3. *The dimension of* $\mathbf{y}_s(k, j)$ *is greater than or equal to the dimension of updated faults in* $\mathbf{f}_s(k, j+1)$*, which can be represented by* $\bar{\mathbf{f}}_j((k+1)T_{period} + \varsigma_j)$;
4. $\bar{\mathbf{C}}(j)$ *is of full rank and the columns of* $\bar{\mathbf{F}}_f(j)$ *corresponding to the fault* $\mathbf{f}_i((k+1)T_{period} + \varsigma_j - T_{cyc,i})$, $i \in I_{s_{\varsigma_j}}$ *are linearly independent.*

Given a constant $\gamma > 0$*, a closed circular region* $\mathcal{D}(\alpha, \tau)$ *with center* $\alpha + 0j$ *and radius* τ *and* $\bar{\mathbf{x}}(0, 0) = 0$*, if there exists* θ*-periodic symmetric positive definite matrices* $\mathbf{P}(j)$ *and* $\mathbf{Q}(j)$ *such that the following LMIs*

$$\begin{bmatrix} \mathbf{P}(j+1) - 2\mathbf{I} & \bar{\mathbf{A}}_{e0}(j) + \mathbf{Q}(j)\bar{\mathbf{A}}_{e1}(j) - \alpha\mathbf{I} \\ * & -\tau^2\mathbf{P}(j) \end{bmatrix} < \mathbf{0} \tag{5.27}$$

$$\begin{bmatrix} \mathbf{P}(j+1) - 2\mathbf{I} & \bar{\mathbf{A}}_{e0}(j) + \mathbf{Q}(j)\bar{\mathbf{A}}_{e1}(j) & \bar{\mathbf{B}}_{e0}(j) + \mathbf{Q}(j)\bar{\mathbf{B}}_{e1}(j) & \mathbf{0} \\ * & -\mathbf{P}(j) & \mathbf{0} & \mathbf{I} \\ * & * & -\gamma\mathbf{I} & \mathbf{0} \\ * & * & * & -\gamma\mathbf{I} \end{bmatrix} < \mathbf{0} \tag{5.28}$$

where $\bar{\mathbf{A}}_{e0}(j) = \begin{bmatrix} \bar{\mathbf{A}}(j) & \mathbf{0} \\ \mathbf{0} & \mathbf{A}_f(j) \end{bmatrix}$, $\bar{\mathbf{A}}_{e1}(j) = \begin{bmatrix} -\bar{\mathbf{C}}(j) & -\bar{\mathbf{F}}_f(j) \end{bmatrix}$, $\bar{\mathbf{B}}_{e0}(j) = \begin{bmatrix} \bar{\mathbf{B}}_d(j) & \mathbf{0} \\ \mathbf{0} & \mathbf{I} \end{bmatrix}$, $\bar{\mathbf{B}}_{e1}(j) = \begin{bmatrix} -\bar{\mathbf{D}}_d(j) & \mathbf{0} \end{bmatrix}$ *hold for each* j*. The eigenvalues of* $\bar{\mathbf{A}}_e(j)$ *belong to the region* $\mathcal{D}(\alpha, \tau)$ *and system dynamics (5.22) can satisfy the performance index (5.23). The observer gain matrices are lifted as* $\mathbf{Q}(j) = \begin{bmatrix} \bar{\mathbf{L}}_s(j) \\ \bar{\mathbf{V}}_s(j) \end{bmatrix}$.

Proof 2 *The proof is similar to the one of Theorem 1 and is thus omitted here.*

Remark 7 *Similarly, Theorem 2 is suitable for the FE design of integrated model (3.26) for non-shared and shared residual structures. The structure restriction of* $\bar{\mathbf{L}}_s(j)$ *and* $\bar{\mathbf{V}}_s(j)$ *should also be noticed when solving LMIs.*

Remark 8 *It is worth mentioning that the using of shared residuals can improve FE robustness against disturbances when the other sub-systems are fault-free. In case of a malfunction of* j*-th sub-system, its residual includes not only the information of disturbance, but also of fault. It could cause the fault estimate distortion of other coupled sub-systems. So Theorems 1 and 2 dealing with the case of shared residuals are feasible when faults of sensors or actuators don't happen simultaneously.*

5.3 Summary

In this chapter, the observer-based FE of decentralized periodic W-NCSs has been studied. The structures of observer gain matrices and post-filters for two kinds of residual structures, i.e., non-shared and shared residuals, have been presented correspondingly. An LMI-based FE algorithms have been proposed with the objective of satisfying an H_∞ performance index against disturbance and variations of fault. The algorithms have been developed for the system with sensor and actuator faults, respectively.

Chapter 6

Application on the WiNC platform

In this chapter, the FE algorithms for the centralized and decentralized system structures will be demonstrated on the experimental WiNC platform with integrated three-tank sub-system. Based on the periodic system model of three-tank system, the FE algorithms will be executed by a remote controller in the way of centralized pattern or simulated decentralized pattern. The schedulers coordinating with this discretized system model are also proposed. The results show the effectiveness of the FE algorithms. To begin with, we would like to introduce the WiNC experimental platform.

6.1 Experimental setup

WiNC platform is constructed to explore the control, FD, FTC and communication issues based on real-time reliable W-NCSs. The whole WiNC includes two well-known laboratory benchmarks as sub-systems, namely the three-tank system and the inverted pendulum system, a remote controller, wireless communication facilities, as well as a protocol optimized for real-time industrial wireless communication. The wireless network supports IEEE 802.11a/b/g standards and provides the possibility of choosing different modulation methods and frequency bands. TDMA medium access method is adopted in WiNC to ensure the deterministic transmission behaviors, which is necessary for the research in this dissertation [17].

To optimize the real-time communication performance, the following technologies have been employed on the WiNC platform.

1) Adopt real-time Linux kernel as operating system kernel. By using this real-time kernel, every operation is expected to be completed within

a certain rigid time period (generally between 1ms and 10ms). When operation with high priority happens, e.g., fault alarm signal broadcasting, a real-time scheduling policy will be executed, which is benefited by the Linux kernel;

2) Design a new MAC protocol optimized for industrial wireless communication. This is accomplished by using SoftMAC, which supports a flexible wireless research platform. The modification are summarized as follows,

a) Reduce the original 802.11 MAC header to only five bytes at the beginning of a packet;

b) Eliminate the transmission of additional packets caused by carrier sensing and backoff, such as automatic ACK and retransmission, request to send/clear to send (RTS/CTS) and so on;

c) Receive all messages that can be decoded by the physical layer, even those contain checksum errors. The errors may be reconstructed by error correction, so that retransmission can be avoided;

3) Optimize transmission scheduler, especially for large-scale networks, to make the best usage of network resources. The scheduling approach for real-time decentralized networks has been reported in [17]. In this thesis, control commands are broadcasted to actuators for real-time purpose.

WiNC is built with open source software, so it is quite accessible for application of new control or FD algorithms. It also provides harmonious graphic user interface (GUI) and configurable parameters setting, e.g., controller parameters, time slot duration, antenna transmission power and so on.

In this chapter, the FE algorithms will be verified on the WiNC platform integrated with three-tank system. The periodic model of three-tank system is built in Section 3.3, and the parameters of three-tank system in (3.18) are listed as follows

$$S = 0.0154\text{m}^2,\ s_{13} = s_{32} = s_{20} = 5 \times 10^{-5}\text{m}^2,$$
$$g = 9.81\text{m/s}^2,\ a_1 = 0.399,\ a_2 = 0.799,\ a_3 = 0.520.$$

The system matrices in (3.21) are

$$A_{d,11} = 0.9999,\ A_{d,22} = 0.9996,$$
$$A_{d,33} = 0.9993,\ A_{d,13} = 0.0001,$$
$$A_{d,311} = A_{d,312} = A_{d,313} = 0.0001,$$

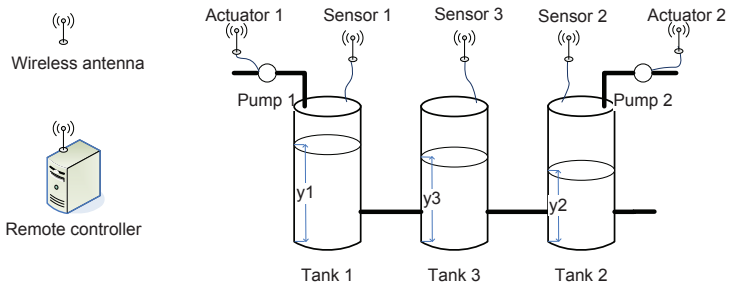

Figure 6.1: WiNC platform with three-tank system

$$A_{d,321} = A_{d,322} = 0.0002,\ A_{d,23} = 0.0002,$$
$$B_{d,1} = 0.5195,\ B_{d,2} = 0.7791,$$
$$B_{d,d1} = 0.0080,\ B_{d,d2} = 0.0120,\ B_{d,d3} = 0.0240.$$

The parameters of PI controller employed are $K_p = 5 \times 10^{-4}$ and $K_i = 0.5 \times 10^{-4}$, where K_p is the proportional gain and K_i is the integral gain. The maximal incoming flow rates of two pumps are $u_{1max} = 1.2417 \times 10^{-4}\mathrm{m}^3/\mathrm{s}$ and $u_{2max} = 1.2188 \times 10^{-4}\mathrm{m}^3/\mathrm{s}$, respectively, so the allowable values of controller's output are limited. Once the calculated control commands exceed $u_{imax}, i = 1, 2$, $u_i(t)$ is limited to be u_{imax}.

The platform structure is shown in Fig. 6.1. As introduced in Section 3.3, the messages from three sensors to the controller, and from the controller to two actuators are exchanged through the wireless network, where every component is assembled with a wireless card. The component medium access behavior is operated under the guidance of scheduler, so the parameter setting of scheduler state-space equation will be presented, which varies from centralized case to decentralized case.

6.2 Implementation of FE on centralized W-NCSs

In this section, the decentralized FE approaches with three kinds of schedulers, i.e., sampling-based scheduler, scheduler with transmission delay and scheduler with packet loss, will be demonstrated on WiNC platform. The experimental implementation is based on the periodic model of three-tank system proposed in Section 3.3. The parameters of respective schedulers are first illustrated. Second, the fault model and the parameters of fault adopted on the platform will be pointed out. At last, the experimental results are analyzed and the results with incomplete information have been compared

with the results based on sampling-based scheduler. To begin with, the fault model employed in this section will be presented.

6.2.1 Fault model

The following sensor faults are considered

$$
\begin{aligned}
f_{s1}(k,j) &= \begin{cases} 0.07, & 8969 \le k \le 13470, \\ 0, & others; \end{cases} \\
f_{s2}(k,j) &= \begin{cases} 0.05, & 10169 \le k \le 14670, \\ 0, & other; \end{cases} \\
f_{s3}(k,j) &= \begin{cases} -0.05, & 11670 \le k \le 15570, \\ 0, & others, \end{cases}
\end{aligned} \tag{6.1}
$$

where $f_{si}(k,j), i = 1,2,3$ represents the sensor fault of i-th water level gauge. Since $T_{period} = 24$ms, the time duration when faults happen, can also be expressed in the continuous time domain as $215.3\text{s} \le t_1 \le 323.3\text{s},\ 244.1\text{s} \le t_2 \le 352.1\text{s},\ 280.1\text{s} \le t_3 \le 373.7\text{s}$ for $f_{si}(k,j), i = 1,2,3$, respectively.

In this thesis, all sensor faults of three water level gauges are considered. The faults are regarded as constant in one period, so a vector denoted as $\mathbf{f}(k,j)$ is used to represent the set of sensor faults, i.e., $\mathbf{f}(k,j) = \mathbf{f}_s(k,j) = \begin{bmatrix} f_{s1}(k,j) & f_{s2}(k,j) & f_{s3}(k,j) \end{bmatrix}^T$. The fault parameters $\mathbf{E}_f(j)$ and $\mathbf{F}_f(j)$ in (3.24) are chosen as

$$
\mathbf{E}_f(j) = 0,\ j = 0,1,2,3,\ \mathbf{F}_f(0) = \begin{bmatrix} 2.5 & 0 & 0 \\ 0 & 2.5 & 0 \\ 0 & 0 & 2.5 \end{bmatrix},
$$

$$
\mathbf{F}_f(1) = \mathbf{F}_f(3) = \begin{bmatrix} 2.5 & 0 & 0 \\ 0 & 0 & 0 \\ 0 & 0 & 0 \end{bmatrix},\ \mathbf{F}_f(2) = \begin{bmatrix} 0 & 0 & 0 \\ 0 & 2.5 & 0 \\ 0 & 0 & 0 \end{bmatrix}.
$$

The initial value of process state estimate is set to

$$
\hat{\mathbf{x}}(0,0|-1) = \begin{bmatrix} 0 & 0 & 0 & 0.02 & 0.03 & 0.03 \end{bmatrix} \tag{6.2}
$$

and $\mathbf{\Pi}_0 = \mathbf{I}_6$. The minimal value of γ is 0.45, which is obtained from simulation result.

6.2.2 FE with sampling-based scheduler

Scheduler model

The scheduler based on the sampling sequences, which is shown in Fig. 3.8, can be expressed as in the state-space model (3.23) and the parameters are

given as follows

$$\mathbf{A}_s(0) = \mathbf{A}_s(1) = \mathbf{A}_s(2) = \mathbf{A}_s(3) = \mathbf{O}_{5\times 5},$$
$$\mathbf{B}_{sy}(1) = \mathbf{B}_{sy}(3) = \begin{bmatrix} 1 & 0 & 0 \\ 0 & 0 & 0 \\ 0 & 0 & 0 \\ 0 & 0 & 0 \\ 0 & 0 & 0 \end{bmatrix},$$
$$\mathbf{B}_{sy}(0) = \begin{bmatrix} 1 & 0 & 0 \\ 0 & 1 & 0 \\ 0 & 0 & 1 \\ 0 & 0 & 0 \\ 0 & 0 & 0 \end{bmatrix},\ \mathbf{B}_{sy}(2) = \begin{bmatrix} 0 & 0 & 0 \\ 1 & 0 & 0 \\ 0 & 0 & 0 \\ 0 & 0 & 0 \\ 0 & 0 & 0 \end{bmatrix},$$
$$\mathbf{B}_{su}(0) = \mathbf{B}_{su}(1) = \mathbf{B}_{su}(2) = \mathbf{O}_{5\times 2},\ \mathbf{B}_{su}(3) = \begin{bmatrix} 0 & 0 \\ 0 & 0 \\ 0 & 0 \\ 1 & 0 \\ 0 & 1 \end{bmatrix},$$
$$\mathbf{C}_{sy}(0) = \mathbf{O}_{3\times 5},\ \mathbf{C}_{sy}(1) = \mathbf{C}_{sy}(2) = \mathbf{C}_{sy}(3) = \mathbf{O}_{1\times 5},$$
$$\mathbf{D}_{sy}(0) = \mathbf{I}_3,\ \mathbf{D}_{sy}(1) = \mathbf{D}_{sy}(2) = \mathbf{D}_{sy}(3) = \mathbf{I}_1,$$
$$\mathbf{C}_{su}(0) = \mathbf{C}_{su}(1) = \mathbf{C}_{su}(2) = \mathbf{C}_{su}(3) = \mathbf{O}_{2\times 5},$$
$$\mathbf{D}_{su}(0) = \mathbf{D}_{su}(1) = \mathbf{D}_{su}(2) = \mathbf{D}_{su}(3) = \mathbf{I}_2. \tag{6.3}$$

Experimental results

The results on WiNC platform corresponding to the sampling-based scheduler are presented in Figs. 6.2, 6.3, 6.4 and 6.5. Fig. 6.2 shows the water levels of three tanks with sensor faults. Figs. 6.3, 6.4 and 6.5 show the FE of each tank, and the estimator has been confirmed to perform well.

From the results, it is easy to calculate the variances of the three water levels at the operating points are $V_1 = 7.2 \times 10^{-7}$, $V_2 = 1.6 \times 10^{-7}$, and $V_3 = 5.6 \times 10^{-8}$ (m^2), respectively, which are mainly caused by the inflow of the pumps. Correspondingly, the variances of error estimates are also related to the variances of water levels, which has been confirmed that the variances of error estimates decrease successively from tank 1 to tank 3. The variation of error estimates during the faulty-free intervals could be caused by system model inaccuracy, e.g., linearization, parameters' uncertainties, and also by some other elements, e.g., sensors' and actuators' calibration inaccuracies, quantization.

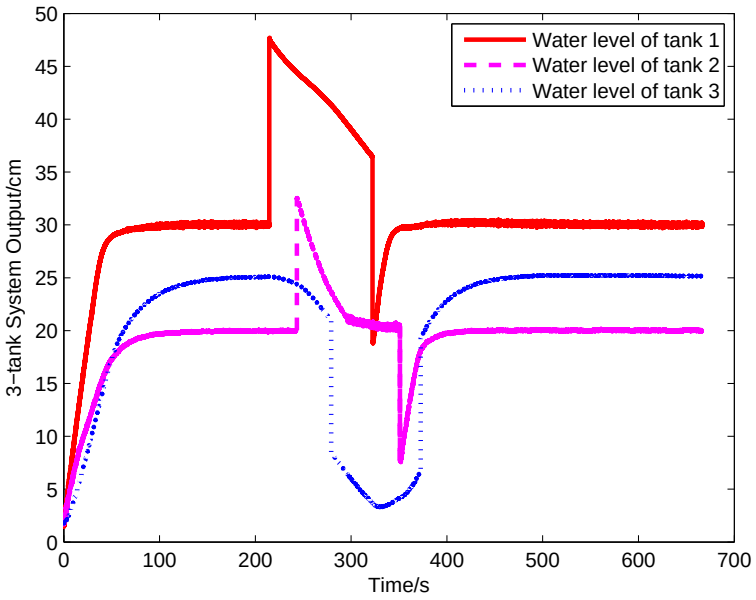

Figure 6.2: Output of 3 tanks of centralized approach

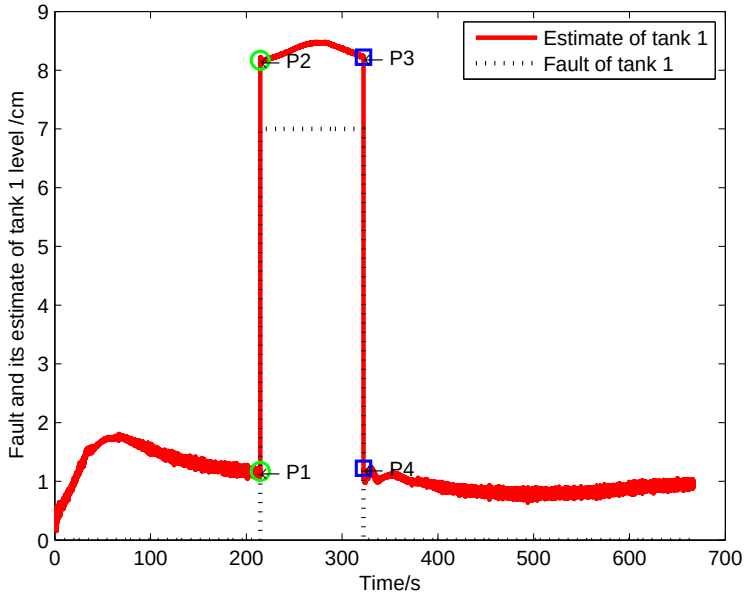

Figure 6.3: Fault and its estimate of tank 1's level of centralized approach

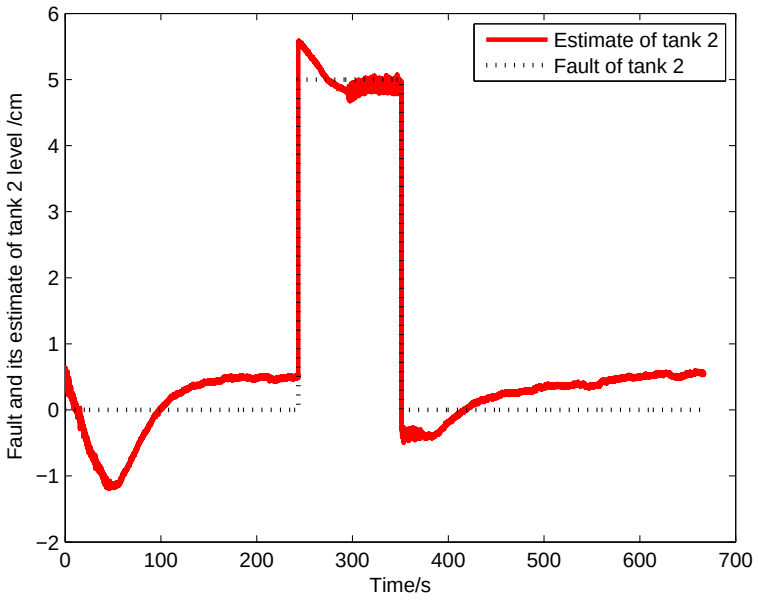

Figure 6.4: Fault and its estimate of tank 2's level of centralized approach

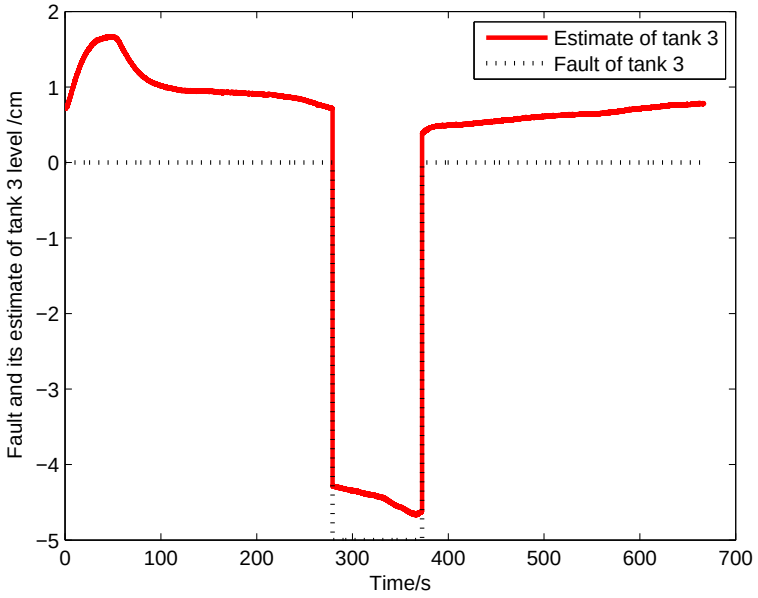

Figure 6.5: Fault and its estimate of tank 3's level of centralized approach

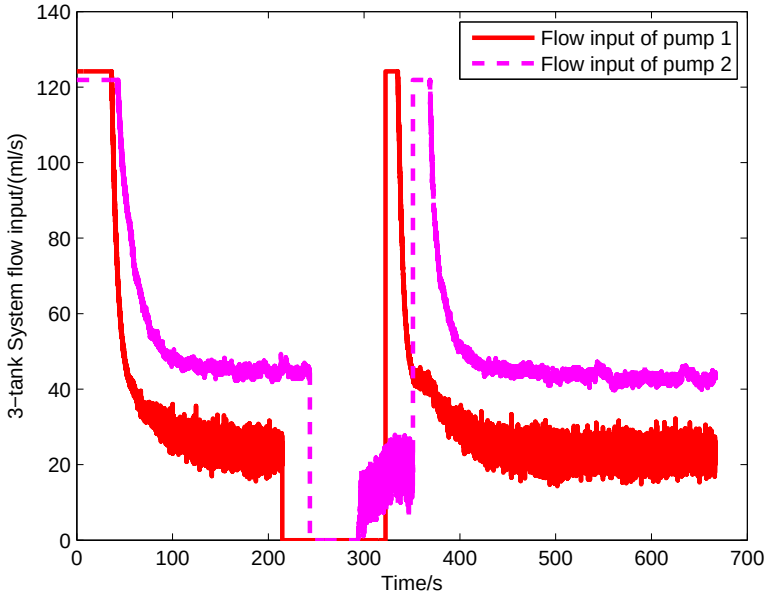

Figure 6.6: Control input of 2 pumps of centralized approach

Take FE of tank 1 in Fig. 6.3 for example to discuss the estimation performance. The sensor error, which is plotted in dotted line, is a rectangular function. Corresponding to the rising edge t_r and falling edge t_f of this rectangular error function, there are 4 points marked in the curve of estimate at the initial time and terminal time of the edges, i.e., P1, P2, P3 and P4. Since the water levels at P1, P2, P3 and P4 are 1.1694, 8.1693, 8.2229 and 1.2232 (cm), respectively, the amplitudes of error estimate at t_r and t_f are 6.9999cm and 6.9997cm, which are very closed to the fault of sensor 1. Similarly, the amplitudes of fault estimates for tank 2 and 3 are also equal to or approximately equal to the relevant faults. It means that the FE algorithm in this case is capable and sensitive to reflect the sensor faults.

The control input calculated by PI controller is shown in Fig. 6.6. Because of the actuator saturation, it is limited between 0 and u_{imax}. When the system has finally reached the steady state in faulty-free case, u_1 ranges from 14.8 to 32.2 (cm^3/s), and u_2 from 39.2 to 47.3 (cm^3/s). When the control input is known for FE algorithm, i.e., $\mathbf{u}_s(k,j) = \mathbf{u}(k,j)$, the value of input will not affect the estimation performance, but when the imperfect transmission of control input is considered, the FE performance will be degraded to some extent.

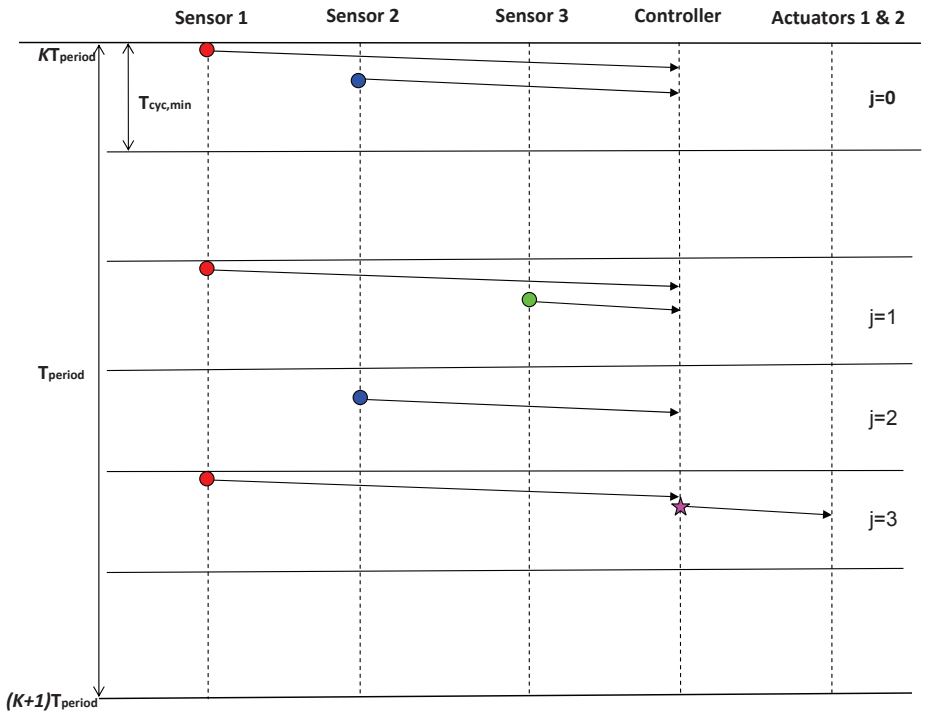

Figure 6.7: Network scheduler of three-tank system with delay

6.2.3 FE with delay scheduler

Scheduler model

Consider the network isn't capable of transmitting all those tasks in time, transmission delays may exist in this case. An example of scheduler with transmission delay of tank 3's measurement periodically is shown in Fig. 6.7, and it makes part of the parameters different from (6.3). Those different parameters of (3.23) are pointed out in the following

$$\mathbf{C}_{sy}(0) = \mathbf{O}_{2\times 5},\ \mathbf{C}_{sy}(1) = \begin{bmatrix} 0 & 0 & 0 & 0 & 0 \\ 0 & 0 & 1 & 0 & 0 \end{bmatrix},$$
$$\mathbf{D}_{sy}(0) = \begin{bmatrix} 1 & 0 & 0 \\ 0 & 1 & 0 \end{bmatrix},\ \mathbf{D}_{sy}(1) = \begin{bmatrix} 1 \\ 0 \end{bmatrix}. \tag{6.4}$$

Experimental results

The results of FE approach with delay scheduler are presented in Figs. 6.8, 6.9 and 6.10.

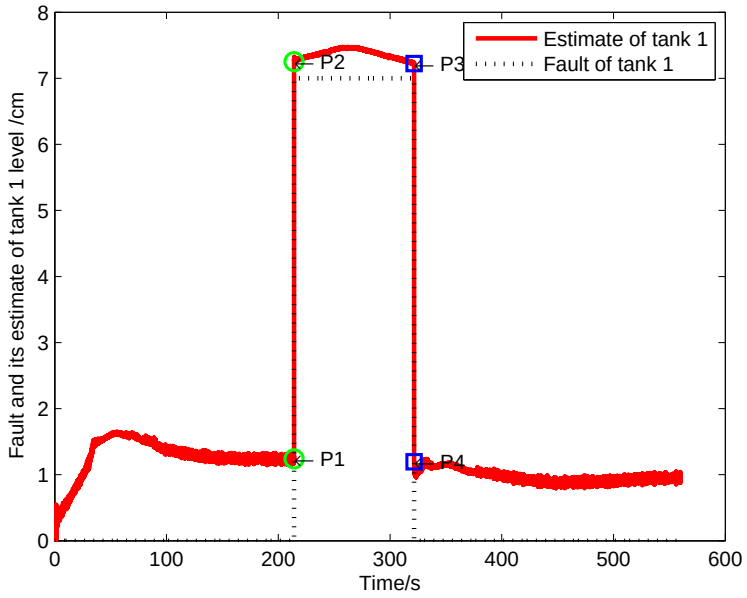

Figure 6.8: Fault and its estimate of tank 1's level with delay of centralized approach

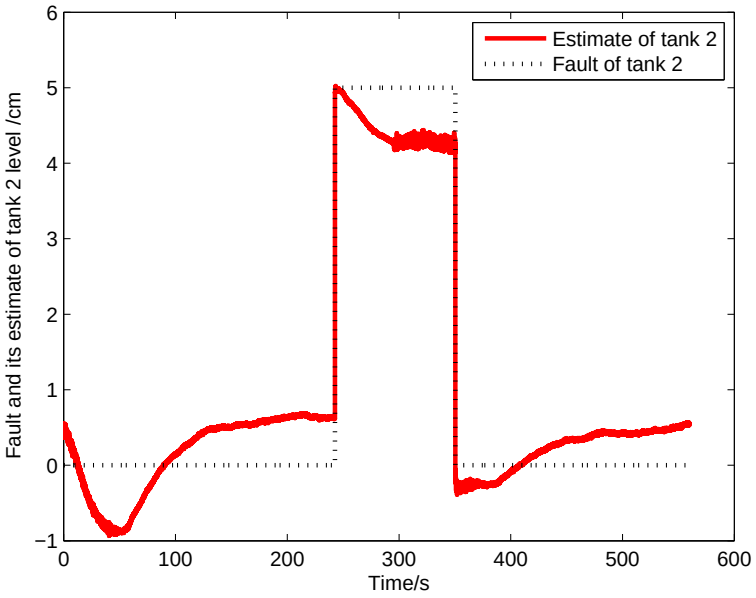

Figure 6.9: Fault and its estimate of tank 2's level with delay of centralized approach

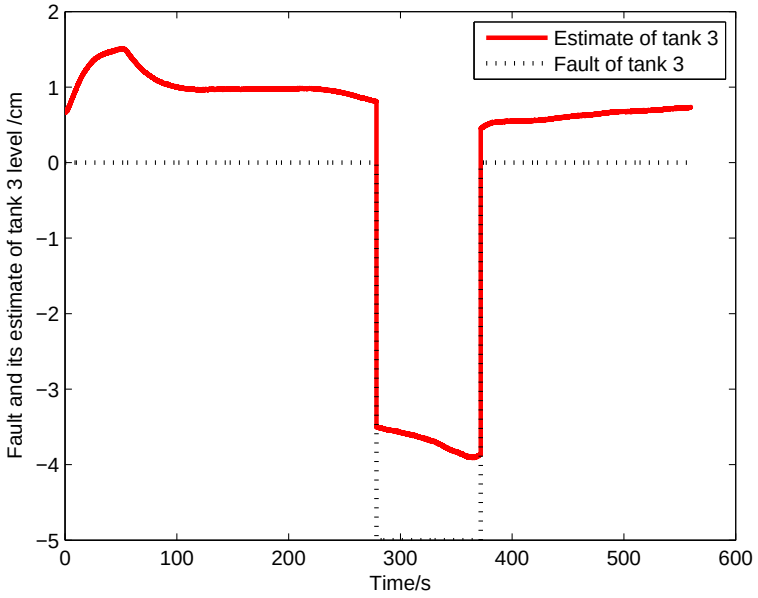

Figure 6.10: Fault and its estimate of tank 3's level with delay of centralized approach

In Fig. 6.8, the water levels at P1, P2, P3 and P4 are 1.2398, 7.2500, 7.2225 and 1.1943 (cm), respectively. The amplitudes of error estimates at the rising edge and falling edge are 6.0102cm and 6.0282cm. Comparing with the results without delay, the FE algorithm performance when dealing with delay scheduler isn't as good as the performance without delay. This conclusion is also appropriate for FE of tank 2 and 3.

6.2.4 FE with packet loss scheduler

Scheduler model

Consider the example that the packet of the second sample of sensor 1 is lost, which is shown in dotted line in Fig. 6.11. It results in that the element of $\mathbf{D}_{sy}(1)$ corresponding to the schedule of $y_1(kT_{period} + 2T_{cyc,1})$ is set to zero. More specifically, the different parameter $\mathbf{D}_{sy}(1)$ from (6.3) is

$$\mathbf{D}_{sy}(1) = 0 \tag{6.5}$$

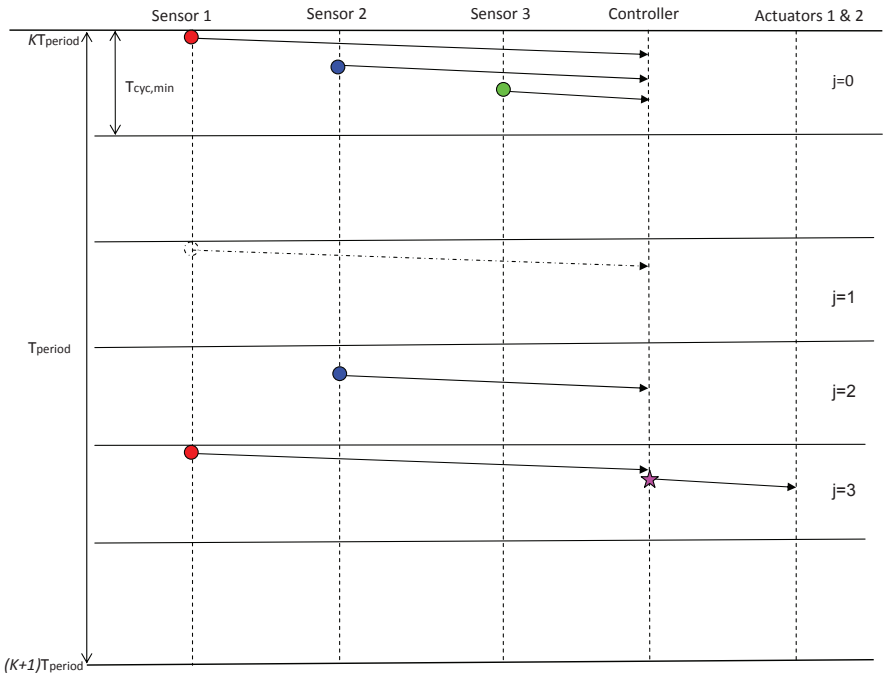

Figure 6.11: Network scheduler of three-tank system with packet loss

Experimental results

The FE results of sensor faults with packet loss scheduler are shown in Figs. 6.12, 6.13 and 6.14. Note that the FE algorithm is also activated when $j = 1$, and the latest measurement of sensor 1 is used.

In Fig. 6.12, the water levels at P1, P2, P3 and P4 are 1.7856, 8.8136, 8.2889 and 1.2822 (cm), respectively. The amplitudes of error estimates at the rising edge and falling edge are 7.0280cm and 7.0067cm. Comparing with the results in Fig. 6.3, the sensitivity of the FE algorithm for this case is still as high as for the case with sampling-based schedule. This conclusion fits also for FE results of tank 2 and 3. It means that the effect of packet loss in transmission on the FE sensitivity isn't so obvious.

While comparing the average values of fault estimates in the faulty-free case, which are calculated from 500s when the water levels have reached the operating points to the end of the detection process, the offset estimate in this case is lager than in the cases with sampling-based schedule and with delay schedule. We can get the conclusion that the existence of packet loss in the transmission scheme will not influence the sensitivity of FE algorithm proposed in this thesis, but it can affect the estimate offset to a relative large

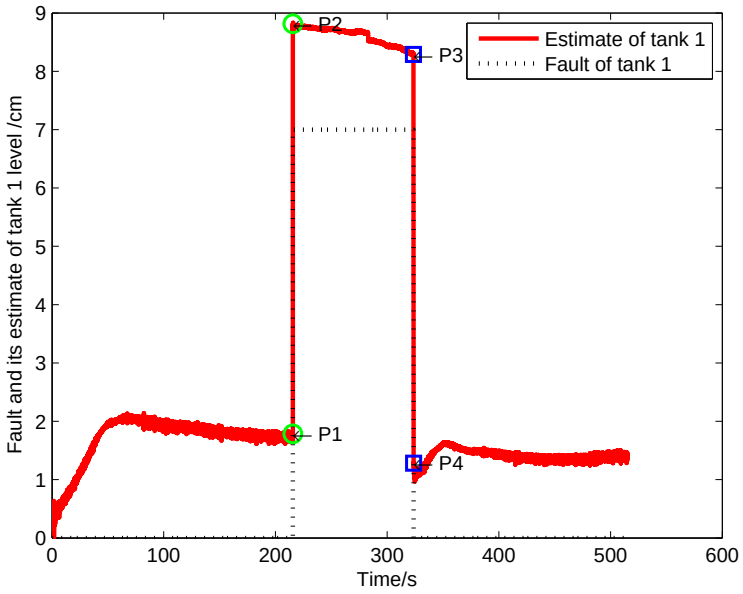

Figure 6.12: Fault and its estimate of tank 1's level with packet loss of centralized approach

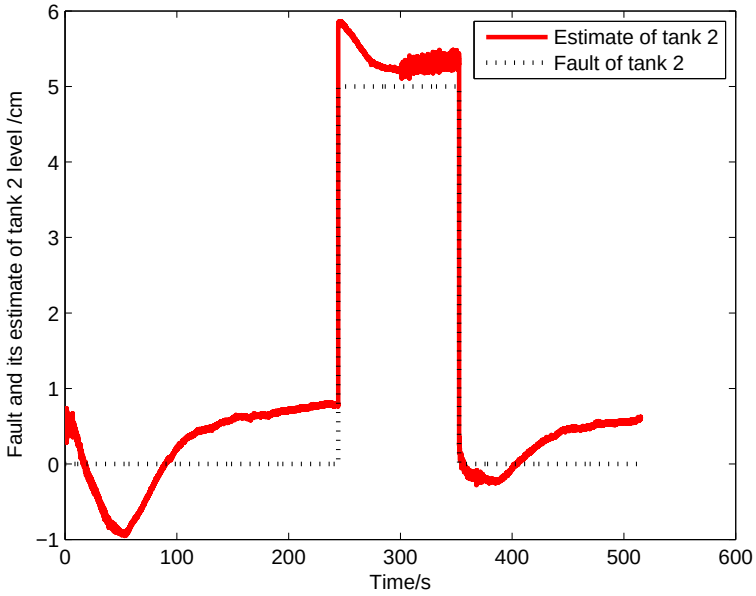

Figure 6.13: Fault and its estimate of tank 2's level with packet loss of centralized approach

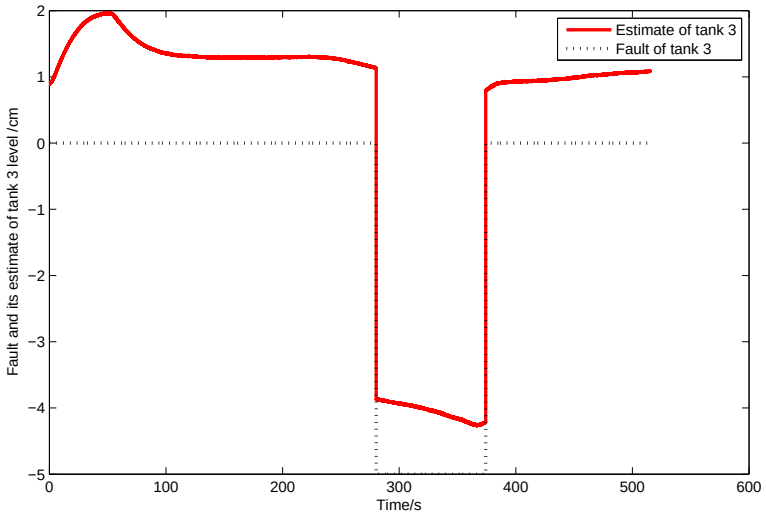

Figure 6.14: Fault and its estimate of tank 3's level with packet loss of centralized approach

degree. Specifically for the three-tank system, since the packet loss happens in tank 1, the offset changes between the case with sampling-based schedule and the case with packet loss schedule reduce successively from tank 1, tank 3 to tank 2 according to the coupling relations of three tanks.

6.3 Implementation of FE on decentralized W-NCSs

In this section, the decentralized FE design will be demonstrated on WiNC platform for the two kinds of residual structures, i.e., the non-shared residuals and shared residuals.

As shown in Fig. 6.1, the remote controller will simulate the operation of decentralized CSs, and the calculation of decentralized FE algorithms will be activated independently whenever its local measurement has reached the CS. The uncertainty of communication between sub-systems still can't be physical tested on the platform. The scheduler adopted here is based on the sampling periods, which is shown in Fig. 3.8. To start with, the experimental results of FE with only sensor faults are presented and discussed.

6.3.1 Sensor FE with non-shared residuals

Fault model

The sensor faults considered here are same as (6.1), and $\mathbf{f}_s(k,j),\ j=0,1,2,3$ is a lifted vector of all sensor faults in one T_{period}, i.e.,

$$\mathbf{f}_s(k,0)=\begin{bmatrix} f_{s1}(k-1,1)\\ f_{s2}(k-1,2)\\ f_{s1}(k-1,3)\\ f_{s1}(k,0)\\ f_{s2}(k,0)\\ f_{s3}(k,0)\end{bmatrix},\ \mathbf{f}_s(k,1)=\begin{bmatrix} f_{s2}(k-1,2)\\ f_{s1}(k-1,3)\\ f_{s1}(k,0)\\ f_{s2}(k,0)\\ f_{s3}(k,0)\\ f_{s1}(k,1)\end{bmatrix},$$

$$\mathbf{f}_s(k,2)=\begin{bmatrix} f_{s1}(k-1,3)\\ f_{s1}(k,0)\\ f_{s2}(k,0)\\ f_{s3}(k,0)\\ f_{s1}(k,1)\\ f_{s2}(k,2)\end{bmatrix},\ \mathbf{f}_s(k,3)=\begin{bmatrix} f_{s1}(k,0)\\ f_{s2}(k,0)\\ f_{s3}(k,0)\\ f_{s1}(k,1)\\ f_{s2}(k,2)\\ f_{s1}(k,3)\end{bmatrix}.$$

The parameters $\mathbf{A}_f(j),\ \mathbf{F}_f(j),\ j=0,1,2,3$ of observer (5.9) are as follows

$$\mathbf{A}_f(0)=\mathbf{A}_f(1)=\begin{bmatrix} 0&1&0&0&0&0\\ 0&0&1&0&0&0\\ \vdots&\vdots&\vdots&\vdots&\vdots&\vdots\\ 0&0&0&0&0&1\\ 0&0&0&1&0&0\end{bmatrix},$$

$$\mathbf{A}_f(2)=\begin{bmatrix} 0&1&0&0&0&0\\ 0&0&1&0&0&0\\ \vdots&\vdots&\vdots&\vdots&\vdots&\vdots\\ 0&0&0&0&0&1\\ 0&0&0&0&1&0\end{bmatrix},\ \mathbf{A}_f(3)=\begin{bmatrix} 0&0&0&1&0&0\\ 0&0&0&0&1&0\\ 0&0&0&0&0&1\\ 0&0&0&0&0&1\\ 0&0&0&0&1&0\\ 0&0&1&0&0&0\end{bmatrix},$$

$$\mathbf{F}_f(0)=\begin{bmatrix} 0&0&0&F_{d,f1}&0&0\\ 0&0&0&0&0&0\\ 0&0&0&0&0&0\end{bmatrix},$$

$$\mathbf{F}_f(1)=\begin{bmatrix} 0&0&0&0&0&0\\ 0&0&0&F_{d,f2}&0&0\\ 0&0&0&0&0&0\end{bmatrix},$$

$$\mathbf{F}_f(2) = \begin{bmatrix} 0 & 0 & 0 & 0 & F_{d,f1} & 0 \\ 0 & 0 & 0 & 0 & 0 & 0 \\ 0 & 0 & 0 & 0 & 0 & 0 \end{bmatrix},$$
$$\mathbf{F}_f(3) = \begin{bmatrix} 0 & 0 & 0 & 0 & 0 & F_{d,f1} \\ 0 & 0 & 0 & 0 & F_{d,f2} & 0 \\ 0 & 0 & F_{d,f3} & 0 & 0 & 0 \end{bmatrix}. \tag{6.6}$$

Observer gain and post-filter

The parameters, including observer gain and post-filter, will be presented. The main differences between the observer design of non-shared residuals and shared residuals exist on the setting of observer gain $\mathbf{L}_s(j)$ and post-filter $\mathbf{V}_s(j)$, which will be listed in the following.

The parameters of system model (3.24) are same as in (3.21), and the parameters of scheduler, which are different from (6.3), are provided as follows

$$\begin{aligned} &\mathbf{C}_{sy}(0) = \mathbf{C}_{sy}(1) = \mathbf{C}_{sy}(2) = \mathbf{O}_{1\times 5},\ \mathbf{C}_{sy}(3) = \mathbf{O}_{3\times 5}, \\ &\mathbf{D}_{sy}(0) = \mathbf{D}_{sy}(2) = \begin{bmatrix} 1 & 0 & 0 \end{bmatrix}, \\ &\mathbf{D}_{sy}(1) = \begin{bmatrix} 0 & 1 & 0 \end{bmatrix},\ \mathbf{D}_{sy}(3) = \mathbf{I}_3 \end{aligned} \tag{6.7}$$

The observer gain matrix $\mathbf{L}_s(j)$ and post-filter $\mathbf{V}_s(j),\ j = 0, 1, 2, 3$ in (5.19) can be obtained

$$\mathbf{L}_s(0) = \begin{bmatrix} 0 \\ \vdots \\ 0 \\ L_1(0) \end{bmatrix},\ \mathbf{L}_s(1) = \begin{bmatrix} 0 \\ \vdots \\ 0 \\ L_2(1) \end{bmatrix},$$
$$\mathbf{L}_s(2) = \begin{bmatrix} 0 \\ \vdots \\ 0 \\ L_1(2) \end{bmatrix},\ \mathbf{L}_s(3) = \begin{bmatrix} 0 & 0 & 0 \\ 0 & 0 & 0 \\ 0 & 0 & 0 \\ L_1(3) & 0 & 0 \\ 0 & L_2(3) & 0 \\ 0 & 0 & L_3(3) \end{bmatrix},$$
$$\mathbf{V}_s(0) = \begin{bmatrix} 0 \\ \vdots \\ 0 \\ V_1(0) \end{bmatrix},\ \mathbf{V}_s(1) = \begin{bmatrix} 0 \\ \vdots \\ 0 \\ V_2(1) \end{bmatrix},$$

$$\mathbf{V}_s(2) = \begin{bmatrix} 0 \\ \vdots \\ 0 \\ V_1(2) \end{bmatrix}, \ \mathbf{V}_s(3) = \begin{bmatrix} 0 & 0 & 0 \\ 0 & 0 & 0 \\ 0 & 0 & 0 \\ V_1(3) & 0 & 0 \\ 0 & V_2(3) & 0 \\ 0 & 0 & V_3(3) \end{bmatrix}. \tag{6.8}$$

In this experiment, assume that the regional pole constraint is $\mathcal{D}(0, 1)$ and $\gamma = 3.18$. The discretized parameter of sensor fault is $F_{d,fi} = 2.5, \ i = 1, 2, 3$. The desired parameters in (6.8) can be obtained as

$$\begin{aligned} &L_1(0) = 0.1505, \ L_2(1) = 0.1400, \ L_1(2) = 0.1378, \\ &L_1(3) = 0.1496, \ L_2(3) = 0.1400, \ L_3(3) = 0.1145, \\ &V_1(0) = 0.3400, \ V_2(1) = 0.3441, \ V_1(2) = 0.3444, \\ &V_1(3) = 0.3394, \ V_2(3) = 0.3441, \ V_3(3) = 0.3544. \end{aligned}$$

Experimental results

The results of sensor fault estimates for each tank are shown in Figs. 6.15, 6.16 and 6.17. The initial and terminal points of the rising and falling edges P1, P2, P3 and P4 are also marked in Fig. 6.15 to analyze the FE performance. The water levels at P1, P2, P3 and P4 are $0.5400, 6.4840, 7.1333$ and 1.1922 (cm), respectively, so the amplitudes of error estimates at t_r and t_f are 5.9340cm and 5.9711cm. Comparing the results of centralized FE algorithm, the performance of decentralized structure is degraded in some degree. This result has proved the analysis mentioned at the beginning of Chapter 3. The results of tank 2 and 3 also support this conclusion.

6.3.2 Sensor FE with shared residuals

Fault model

To compare the FE performance with non-shared residuals, the sensor faults adopted here will not happen at the same time, since the shared residual with information of fault can greatly affect the sensitivity of estimation. List the system parameters, which are specific and different from (3.21) and (6.6) in this case,

$$\mathbf{C}(0) = \mathbf{C}(1) = \mathbf{C}(2) = \mathbf{C}(3) = \mathbf{I}_6,$$

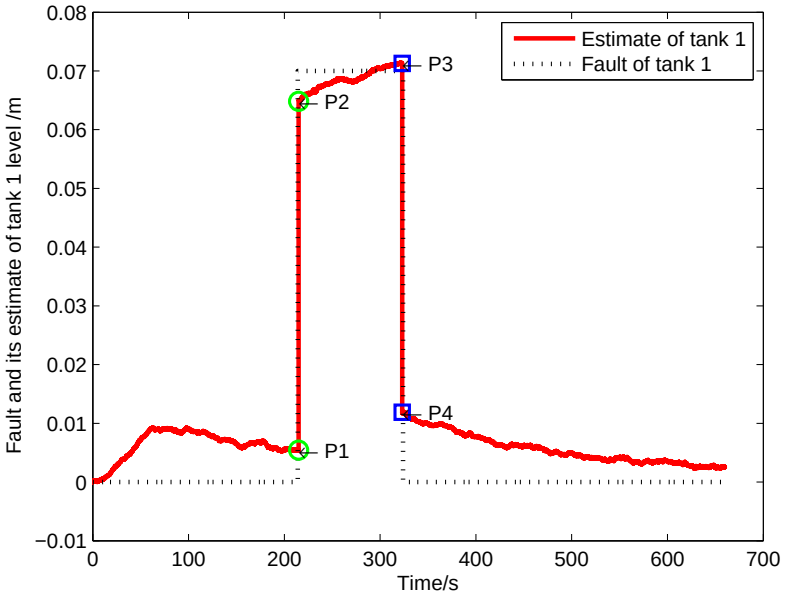

Figure 6.15: Fault and its estimate of tank 1's level with non-shared residuals of decentralized approach

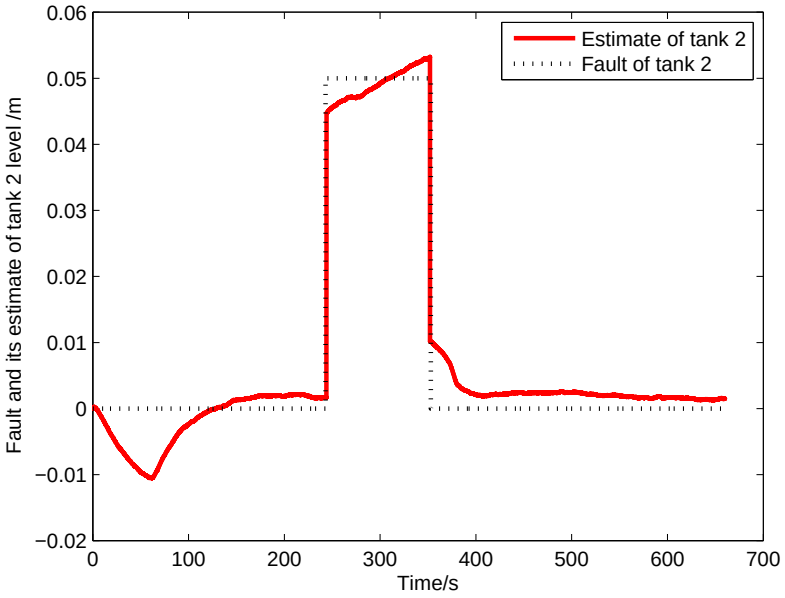

Figure 6.16: Fault and its estimate of tank 2's level with non-shared residuals of decentralized approach

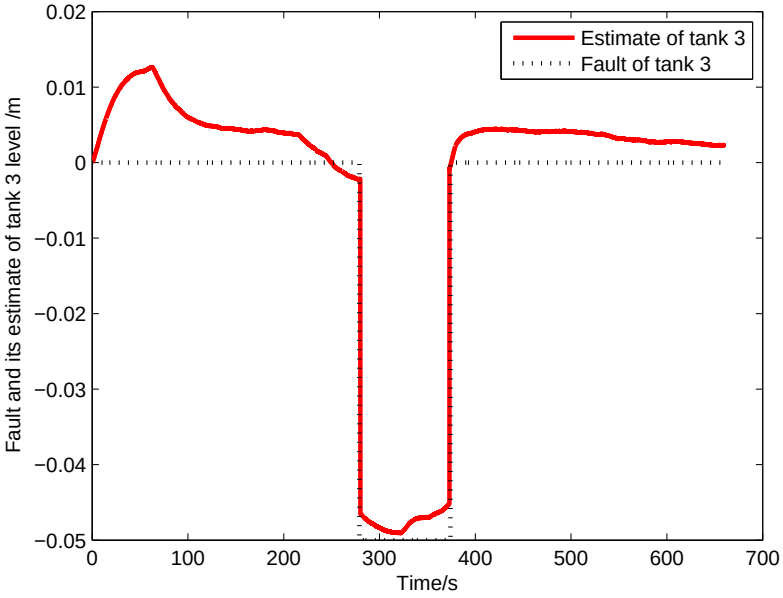

Figure 6.17: Fault and its estimate of tank 3's level with non-shared residuals of decentralized approach

$$\mathbf{F}_f(0) = \begin{bmatrix} 0 & 0 & 0 & 0 & 0 & 0 \\ 0 & 0 & 0 & 0 & 0 & 0 \\ 0 & 0 & 0 & 0 & 0 & 0 \\ 0 & 0 & 0 & F_{d,f1} & 0 & 0 \\ 0 & 0 & 0 & 0 & 0 & 0 \\ 0 & 0 & 0 & 0 & 0 & 0 \end{bmatrix}, \ \mathbf{F}_f(1) = \begin{bmatrix} 0 & 0 & 0 & 0 & 0 & 0 \\ \vdots & \vdots & \vdots & \vdots & \vdots & \vdots \\ 0 & 0 & 0 & 0 & 0 & 0 \\ 0 & 0 & 0 & F_{d,f2} & 0 & 0 \\ 0 & 0 & 0 & 0 & 0 & 0 \end{bmatrix},$$

$$\mathbf{F}_f(2) = \begin{bmatrix} 0 & 0 & 0 & 0 & 0 & 0 \\ \vdots & \vdots & \vdots & \vdots & \vdots & \vdots \\ 0 & 0 & 0 & 0 & 0 & 0 \\ 0 & 0 & 0 & 0 & F_{d,f1} & 0 \\ 0 & 0 & 0 & 0 & 0 & 0 \end{bmatrix}, \ \mathbf{F}_f(3) = \begin{bmatrix} 0 & 0 & 0 & 0 & 0 & 0 \\ 0 & 0 & 0 & 0 & 0 & 0 \\ 0 & 0 & F_{d,f3} & 0 & 0 & 0 \\ 0 & 0 & 0 & 0 & 0 & \\ 0 & 0 & 0 & 0 & F_{d,f2} & 0 \\ 0 & 0 & 0 & 0 & 0 & F_{d,f1} \end{bmatrix}$$

The fault value for i-th sensor is considered in (6.1), but the faults will not happen at the same time, e.g.,

$$f_{s1}(k,j) = \begin{cases} 0.07, & 8969 \leq k \leq 13470, \\ 0, & others, \end{cases}$$
$$f_{s2}(k,j) = 0, \ f_{s3}(k,j) = 0 \tag{6.9}$$

Observer gain and post-filter

The periodic observer gain $\mathbf{L}_s(j)$ and post-filter matrix $\mathbf{V}_s(j)$ with appropriate dimensions are shown

$$\mathbf{L}_s(0) = \begin{bmatrix} 0 & 0 & 0 & 0 & 0 & 0 \\ \vdots & \vdots & \vdots & \vdots & \vdots & \vdots \\ 0 & 0 & 0 & 0 & 0 & 0 \\ 0 & 0 & 0 & L_1(0) & 0 & L_{13}(0) \end{bmatrix},$$

$$\mathbf{L}_s(1) = \begin{bmatrix} 0 & 0 & 0 & 0 & 0 & 0 \\ \vdots & \vdots & \vdots & \vdots & \vdots & \vdots \\ 0 & 0 & 0 & 0 & 0 & 0 \\ 0 & 0 & 0 & L_2(1) & L_{23}(1) & 0 \end{bmatrix},$$

$$\mathbf{L}_s(2) = \begin{bmatrix} 0 & 0 & 0 & 0 & 0 & 0 \\ \vdots & \vdots & \vdots & \vdots & \vdots & \vdots \\ 0 & 0 & 0 & 0 & 0 & 0 \\ 0 & 0 & 0 & L_{13}(2) & L_1(2) & 0 \end{bmatrix},$$

$$\mathbf{L}_s(3) = \begin{bmatrix} 0 & 0 & 0 & 0 & 0 & 0 \\ 0 & 0 & 0 & 0 & 0 & 0 \\ 0 & 0 & 0 & 0 & 0 & 0 \\ 0 & 0 & L_{13}(3) & 0 & 0 & L_1(3) \\ 0 & 0 & L_{23}(3) & 0 & L_2(3) & 0 \\ L_{311}(3) & L_{321}(3) & L_3(3) & L_{312}(3) & L_{322}(3) & L_{313}(3) \end{bmatrix},$$

$$\mathbf{V}_s(0) = \begin{bmatrix} 0 & 0 & 0 & 0 & 0 & 0 \\ \vdots & \vdots & \vdots & \vdots & \vdots & \vdots \\ 0 & 0 & 0 & 0 & 0 & 0 \\ 0 & 0 & 0 & V_1(0) & 0 & V_{13}(0) \end{bmatrix},$$

$$\mathbf{V}_s(1) = \begin{bmatrix} 0 & 0 & 0 & 0 & 0 & 0 \\ \vdots & \vdots & \vdots & \vdots & \vdots & \vdots \\ 0 & 0 & 0 & 0 & 0 & 0 \\ 0 & 0 & 0 & V_2(1) & V_{23}(1) & 0 \end{bmatrix},$$

$$\mathbf{V}_s(2) = \begin{bmatrix} 0 & 0 & 0 & 0 & 0 & 0 \\ \vdots & \vdots & \vdots & \vdots & \vdots & \vdots \\ 0 & 0 & 0 & 0 & 0 & 0 \\ 0 & 0 & 0 & V_{13}(2) & V_1(2) & 0 \end{bmatrix},$$

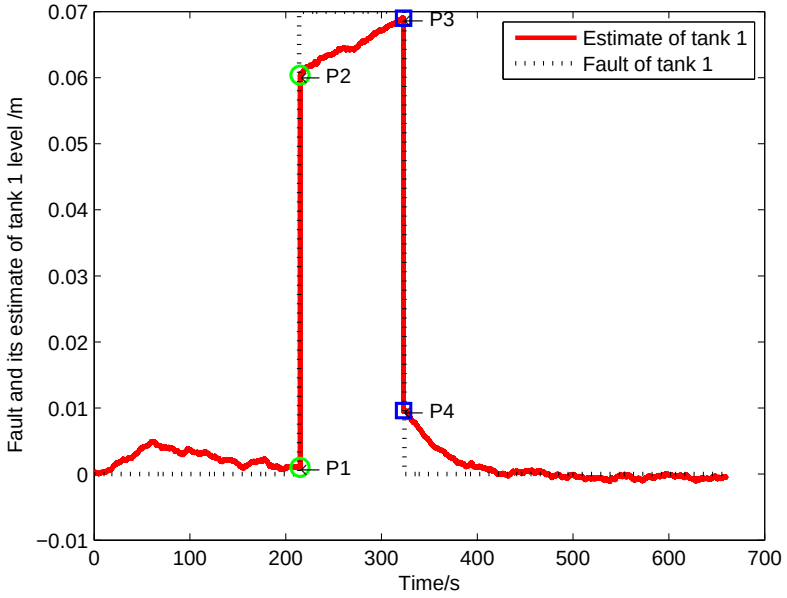

Figure 6.18: Fault and its estimate of tank 1's level with shared residuals of decentralized approach

$$\mathbf{V}_s(3) = \begin{bmatrix} 0 & 0 & 0 & 0 & 0 & 0 \\ 0 & 0 & 0 & 0 & 0 & 0 \\ 0 & 0 & 0 & 0 & 0 & 0 \\ 0 & 0 & V_{13}(3) & 0 & 0 & V_1(3) \\ 0 & 0 & V_{23}(3) & 0 & V_2(3) & 0 \\ V_{311}(3) & V_{321}(3) & V_3(3) & V_{312}(3) & V_{322}(3) & V_{313}(3) \end{bmatrix} \tag{6.10}$$

By solving LMIs in Theorem 2 with $\alpha = 0,\ \tau = 1,\ \gamma = 3.18$, the non-zero desired parameters in (6.10) are listed in the following

$L_1(0) = 0.1505,\ L_{13}(0) = 0.0002,\ L_2(1) = 0.1398,\ L_{23}(1) = 0.0003,$
$L_1(2) = 0.1376,\ L_1(3) = 0.1496,\ L_2(3) = 0.1398,\ L_3(3) = 0.1143,$
$L_{311}(3) = 0.0001,\ L_{312}(3) = 0.0002,\ L_{321}(3) = 0.0002,\ V_1(0) = 0.3400,$
$V_2(1) = 0.3441,\ V_1(2) = 0.3445,\ V_{13}(2) = -0.0001,\ V_1(3) = 0.3394,$
$V_2(3) = 0.3441,\ V_3(3) = 0.3545.$

Experimental results

The results of sensor fault estimates with shared residuals for three tanks are shown in Figs. 6.18, 6.19 and 6.20. The water levels at P1, P2, P3

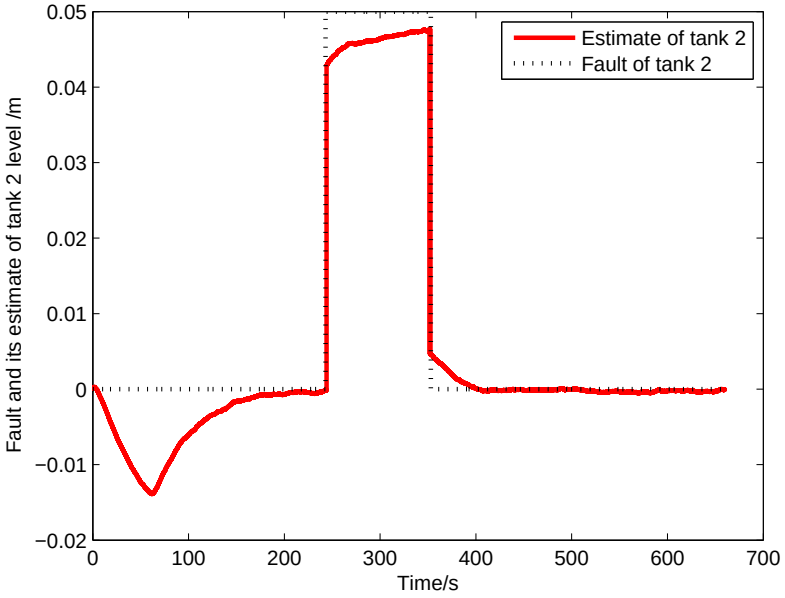

Figure 6.19: Fault and its estimate of tank 2's level with shared residuals of decentralized approach

and P4, which are marked in Fig. 6.18, are $0.1020, 6.0440, 8.1720$ and 2.2312 (cm), respectively, so the amplitudes at t_r and t_f are 5.9420cm and 5.9408cm. Comparing the results of FE with non-shared residuals, the improved performance of sensitivity to faults are not so obvious. But the covariance of fault estimate is smaller and the average value of $\hat{f}_{si}(k,j),\ i=1,2,3$ in fault-free case is closer to zero. It is easy to obtain the conclusion that the robust performance of FE approach with shared residuals is enhanced.

6.3.3 Actuator FE with non-shared residuals

Fault model

The actuator fault $\mathbf{f}_a(k,j),\ j=0,1,2,3$ considered here is a lifted vector of all actuator faults in one T_{period}, i.e.,

$$\mathbf{f}_a(k,0)=\begin{bmatrix} f_{a1}(k-1,1)\\ f_{a2}(k-1,2)\\ f_{a1}(k-1,3)\\ f_{a1}(k,0)\\ f_{a2}(k,0)\end{bmatrix},\ \mathbf{f}_a(k,1)=\begin{bmatrix} f_{a2}(k-1,2)\\ f_{a1}(k-1,3)\\ f_{a1}(k,0)\\ f_{a2}(k,0)\\ f_{a1}(k,1)\end{bmatrix},$$

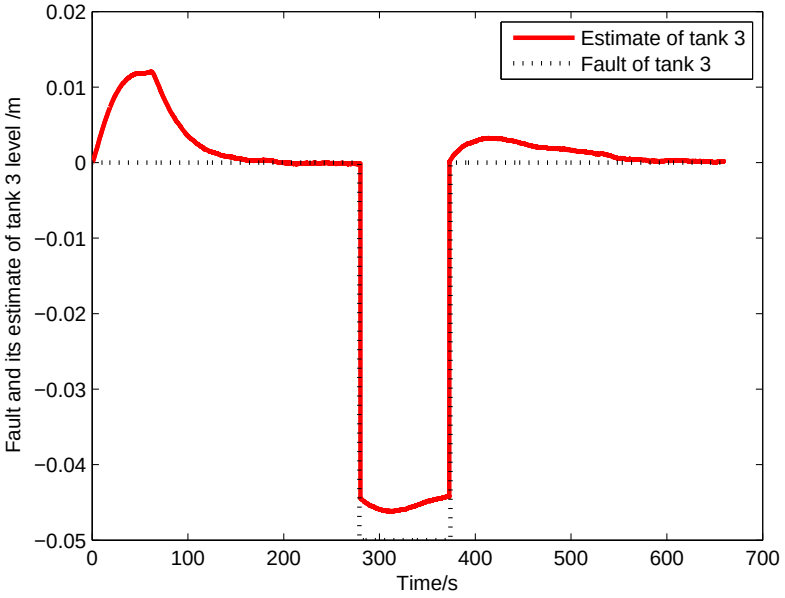

Figure 6.20: Fault and its estimate of tank 3's level with shared residuals of decentralized approach

$$\mathbf{f}_a(k,2) = \begin{bmatrix} f_{a1}(k-1,3) \\ f_{a1}(k,0) \\ f_{a2}(k,0) \\ f_{a1}(k,1) \\ f_{a2}(k,2) \end{bmatrix}, \ \mathbf{f}_a(k,3) = \begin{bmatrix} f_{a1}(k,0) \\ f_{a2}(k,0) \\ f_{a1}(k,1) \\ f_{a2}(k,2) \\ f_{a1}(k,3) \end{bmatrix}.$$

The parameters $\mathbf{A}_f(j),\ \mathbf{E}_f(j),\ j = 0,1,2,3$ of observer (5.9) are as follows

$$\mathbf{A}_f(0) = \mathbf{A}_f(1) = \mathbf{A}_f(2) = \begin{bmatrix} 0 & 1 & 0 & 0 & 0 \\ 0 & 0 & 1 & 0 & 0 \\ \vdots & \vdots & \vdots & \vdots & \vdots \\ 0 & 0 & 0 & 0 & 1 \\ 0 & 0 & 0 & 1 & 0 \end{bmatrix},$$

$$\mathbf{A}_f(3) = \begin{bmatrix} 0 & 0 & 1 & 0 & 0 \\ 0 & 0 & 0 & 1 & 0 \\ 0 & 0 & 0 & 0 & 1 \\ 0 & 0 & 0 & 0 & 1 \\ 0 & 0 & 0 & 1 & 0 \end{bmatrix},$$

$$\mathbf{E}_f(0) = \mathbf{E}_f(2) = \begin{bmatrix} 0 & 0 & 0 & 0 & 0 \\ \vdots & \vdots & \vdots & \vdots & \vdots \\ 0 & 0 & 0 & 0 & 0 \\ 0 & 0 & 0 & E_{d,f1} & 0 \end{bmatrix},$$

$$\mathbf{E}_f(1) = \begin{bmatrix} 0 & 0 & 0 & 0 & 0 \\ \vdots & \vdots & \vdots & \vdots & \vdots \\ 0 & 0 & 0 & 0 & 0 \\ 0 & 0 & 0 & E_{d,f2} & 0 \end{bmatrix},$$

$$\mathbf{E}_f(3) = \begin{bmatrix} 0 & 0 & 0 & 0 & 0 \\ \vdots & \vdots & \vdots & \vdots & \vdots \\ 0 & 0 & 0 & 0 & 0 \\ 0 & 0 & 0 & 0 & E_{d,f1} \\ 0 & 0 & 0 & E_{d,f2} & 0 \\ 0 & 0 & 0 & 0 & 0 \end{bmatrix} \tag{6.11}$$

The discretized parameter of actuator fault is $E_{d,fi} = B_{d,di},\ i = 1, 2$. The actuator faults are as follows

$$f_{a1}(k, j) = \begin{cases} -0.2u_{1max}, & 8969 \leq k \leq 13470, \\ 0, & others; \end{cases} \tag{6.12}$$

$$f_{a2}(k, j) = \begin{cases} -0.3u_{2max}, & 10169 \leq k \leq 14670, \\ 0, & other; \end{cases}$$

Observer gain and post-filter

As discussed in dealing with sensor fault estimation, the observer gain $\mathbf{L}_s(j)$ and post-filter matrix $\mathbf{V}_s(j)$ will be given in details. The parameters of scheduler are shown in (6.7) and other parameters of system model (3.24) are same as in (3.21). The observer gain matrix $\mathbf{L}_s(j)$ is same as (6.8), and $\mathbf{V}_s(j),\ j = 0, 1, 2, 3$ in (5.19) can be obtained as

$$\mathbf{V}_s(0) = \begin{bmatrix} 0 \\ \vdots \\ 0 \\ V_1(0) \end{bmatrix},\ \mathbf{V}_s(1) = \begin{bmatrix} 0 \\ \vdots \\ 0 \\ V_2(1) \end{bmatrix},$$

$$\mathbf{V}_s(2) = \begin{bmatrix} 0 \\ \vdots \\ 0 \\ V_1(2) \end{bmatrix},\ \mathbf{V}_s(3) = \begin{bmatrix} 0 & 0 & 0 \\ 0 & 0 & 0 \\ 0 & 0 & 0 \\ V_1(3) & 0 & 0 \\ 0 & V_2(3) & 0 \end{bmatrix} \tag{6.13}$$

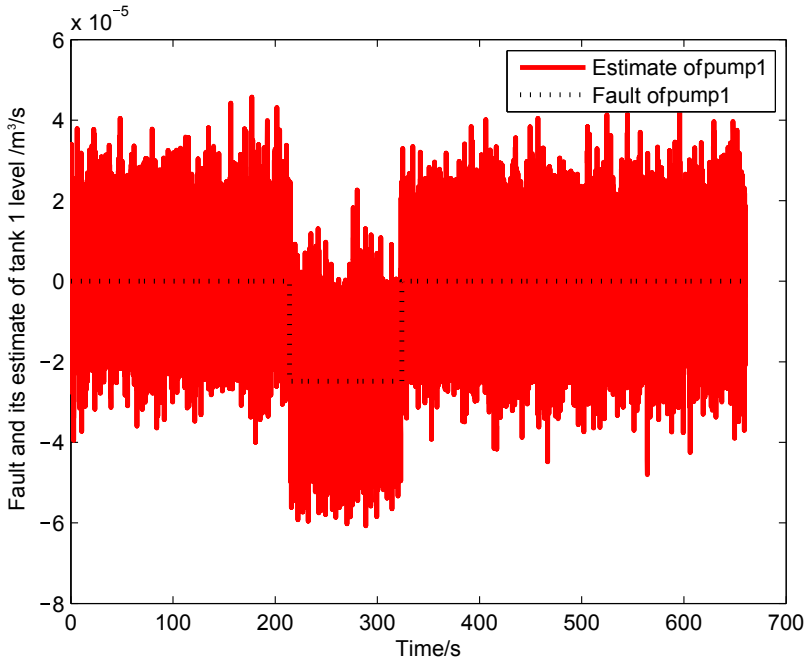

Figure 6.21: Fault and its estimate of pump 1's flow rate with non-shared residuals of decentralized approach

Assume that the regional pole constraint is $\mathcal{D}(0,1)$ and $\gamma = 3.31$. The desired observer parameters in (6.13) can be computed as

$$
\begin{aligned}
&L_1(0) = 1.1710,\ L_2(1) = 1.1984,\\
&L_1(2) = 1.0672,\ L_1(3) = 1.1767,\\
&L_2(3) = 1.1984,\ L_3(3) = 0.9992,\\
&V_1(0) = 0.3294,\ V_2(1) = 0.2538,\\
&V_1(2) = 0.1303,\ V_1(3) = 0.3406,\\
&V_2(3) = 0.2538.
\end{aligned}
$$

Experimental results

The results of actuator fault estimates for each pump are shown in Figs. 6.21 and 6.22.

Since the actuator faults adopted here are very small, the robustness of FE is greatly effected by system disturbances. Even though, the trend of actuator faults can still be estimated.

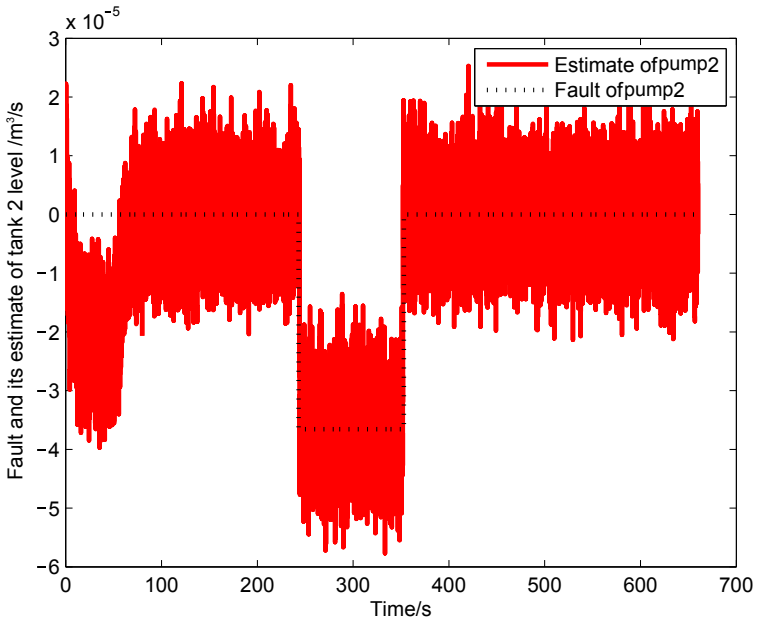

Figure 6.22: Fault and its estimate of pump 2's flow rate with non-shared residuals of decentralized approach

6.3.4 Actuator FE with shared residuals

Observer gain and post-filter

The parameters of scheduler are given in (6.7) and other parameters of system model (3.24) are as in (3.21). The discretized parameter of actuator fault is $E_{d,fi} = B_{d,di},\ i = 1, 2$. The actuator faults are as in (6.12), but the faults will also not happen at the same time. The observer gain matrix $\mathbf{L}_s(j)$ is same as (6.10), and $\mathbf{V}_s(j),\ j = 0, 1, 2, 3$ in (5.19) can be obtained

$$\mathbf{V}_s(0) = \begin{bmatrix} 0 & 0 & 0 & 0 & 0 & 0 \\ \vdots & \vdots & \vdots & \vdots & \vdots & \vdots \\ 0 & 0 & 0 & 0 & 0 & 0 \\ 0 & 0 & 0 & V_1(0) & 0 & V_{13}(0) \end{bmatrix},$$

$$\mathbf{V}_s(1) = \begin{bmatrix} 0 & 0 & 0 & 0 & 0 & 0 \\ \vdots & \vdots & \vdots & \vdots & \vdots & \vdots \\ 0 & 0 & 0 & 0 & 0 & 0 \\ 0 & 0 & 0 & V_2(1) & V_{23}(1) & 0 \end{bmatrix},$$

$$\mathbf{V}_s(2) = \begin{bmatrix} 0 & 0 & 0 & 0 & 0 & 0 \\ \vdots & \vdots & \vdots & \vdots & \vdots & \vdots \\ 0 & 0 & 0 & 0 & 0 & 0 \\ 0 & 0 & 0 & V_{13}(2) & V_1(2) & 0 \end{bmatrix},$$

$$\mathbf{V}_s(3) = \begin{bmatrix} 0 & 0 & 0 & 0 & 0 & 0 \\ 0 & 0 & 0 & 0 & 0 & 0 \\ 0 & 0 & 0 & 0 & 0 & 0 \\ 0 & 0 & V_{13}(3) & 0 & 0 & V_1(3) \\ 0 & 0 & V_{23}(3) & 0 & V_2(3) & 0 \end{bmatrix} \tag{6.14}$$

Assume that the regional pole constraint is $\mathcal{D}(0,1)$ and $\gamma = 3.5$. The non-zero observer parameters in (6.13) can be computed as

$$\begin{aligned} &L_1(0) = 0.1682,\ L_{13}(0) = 0.0001,\ L_2(1) = 1.1778,\ L_{23}(1) = 0.0002, \\ &L_1(2) = 1.0669,\ L_1(3) = 1.1736,\ L_2(3) = 1.1778,\ L_3(3) = 0.9992, \\ &L_{311}(3) = 0.0001,\ L_{312}(3) = 0.0002,\ L_{313}(3) = 0.0001,\ L_{321}(3) = 0.0002, \\ &L_{322}(3) = 0.0001,\ V_1(0) = 0.3250,\ V_2(1) = 0.2232, V_1(2) = 0.1267, \\ &V_1(3) = 0.3354,\ V_2(3) = 0.2232. \end{aligned}$$

Experimental results

The results of actuator fault estimates for each pump are shown in Figs. 6.23 and 6.24. Comparing the results in Figs. 6.21 and 6.22, the variance of fault estimates with shared residuals are smaller that the values with non-shared residuals, especially for the estimate if actuator 2. Again, the conclusion that observer with shared residuals can improve the FE robust performance is proved, even for estimation of small faults.

6.4 Summary

In this chapter, the WiNC platform integrated with three-tank system has first been modeled into the periodic system based on the modeling method proposed in Chapter 3. Second the centralized FE algorithm has been demonstrated on the WiNC platform in the cases of three schedulers, i.e., sampling-based schedule, schedule with transmission delay, schedule with packet loss, respectively. Next the LMI-based FE algorithms of decentralized W-NCSs for two kinds of residual structures, i.e., non-shared and shared residuals, have been applied on the WiNC platform. After results analysis, the FE performance has finally been well demonstrated.

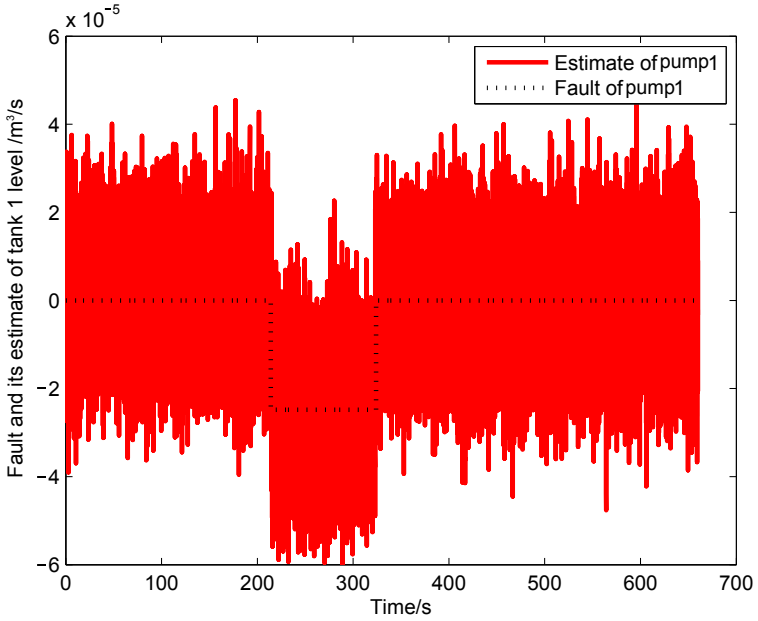

Figure 6.23: Fault and its estimate of pump 1's flow rate with shared residuals of decentralized approach

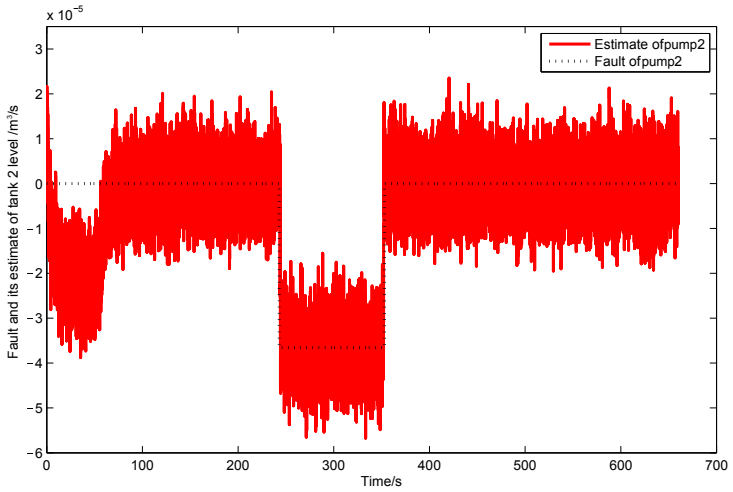

Figure 6.24: Fault and its estimate of pump 2's flow rate with shared residuals of decentralized approach

Chapter 7

Conclusions and further work

The main objective of this thesis is on the investigation of FE research of centralized and decentralized W-NCSs, which are developed for the real-time industrial automatic applications. The characteristics of centralized and decentralized system structures have been first discussed, and it has been found that both structures have some typical advantages that make it suitable for certain types of industrial automation systems. Centralized structure is suitable for a system with very high demands on control performance and resource optimization, while decentralized structure provides more flexibility and autonomy. So the first part of this thesis focuses on developing both centralized and decentralized W-NCSs structures with the objective of building a real-time scheme from the views of modeling of communication and process. From the first view, i.e., communication modeling, a hierarchical communication scheme with deterministic transmission behavior, which fits greatly for the real-time industrial applications, has been established. To be specific, since the transmission tasks of measurements and control commands are normally deterministic over a period of time and the network load only varies in case of faults with a rare probability, the MAC protocol designed for deterministic transmission mechanism can observably improve the effective utilization of network resources and guarantee network QoS. In order to develop the deterministic transmission protocol, TDMA medium access mechanism has been employed, which allows the network sharing by allocating the transmission of signals into different time slots. The network medium resource was thus discretized by TDMA mechanism in the time domain, so the control and measurement signals can be transmitted in the dedicated time slots according with the network scheduler, which can be regarded as a rank of transmission tasks after network resource discretization.

From the process modeling point of view, the overall system has been divided into several sub-systems such that the computation can be more effi-

cient by operation on parallel, which is beneficial to the real-time design. To widen the applicability of the research on industrial automatic application, coupling relations between sub-systems and multi-rate sampling have been considered. The overall system modeling was built based on the lifting of state vectors during one overall period, which is the LCM of all sub-systems' periods. By using the lifted state vector, as well as control input, the overall system model has been established into the form of periodic state-space equation. Considering the network with heavy load, when the scheduling isn't able to sequence all tasks immediately after the signals are generated, it can lead to delay, packet loss and such kind of imperfect transmission, and the system performance can thus be degraded. To overcome this influence, the scheduler has been represented in a mathematical way and further integrated with the periodic model of W-NCSs, so the design issued based on the integrated model can still guarantee the performance considering the network induced effects.

Next the FE scheme for centralized W-NCSs structure has been studied for the periodic integrated model of process and scheduler. An H_∞ filtering approach has been developed with the help of stochastic model in Krein space, which is a solution of the estimate error minimization problem against disturbance and initial state estimate error, and the state estimates were calculated recursively based on the set of observation data. Compared with the general state-space model of this approach, it's worth mentioning that the solution has been developed to solve the model with arbitrary inputs by adopting the linearity of state equations.

To focus on the FE approach of decentralized W-NCSs, the distributed sub-observer has been established for two kinds of residual structures, i.e., non-shared and shared residual signals. The fault estimation has also been designed for the shared and non-shared residuals, respectively. It is easy to obtain that, when the sub-observer is only related with its own residual, the design of state and fault estimation are under the objective of enhancing the robustness against only the local disturbance; when with shared residuals, the sub-observer is designed to be robust against disturbances of all coupled sub-systems. Considering the coupling relation between sub-systems, the state and fault estimation with shared residuals can perform better than the case relating to only local residual. The LMI technique has been adopted as a tool to design the gain matrices.

The FE performances of the centralized and decentralized systems have further been demonstrated on a physical experimental platform WiNC integrated with three-tank system. Based on the communication and process modeling procedures of W-NCSs, the three-tank system has been first formulated into a periodic system. Next, the effectiveness of developed FE al-

gorithm for centralized system with respect to sensor faults has been demonstrated based on three cases of scheduler, i.e., sampling-based scheduler, scheduler with transmission delay, scheduler with packet loss, respectively. Finally, the FE performance for decentralized W-NCSs has also been demonstrated on the WiNC platform, where the sub-observers are operated in simulated mode. The advantage of FE with shared residual has been verified. All in one, the work in this thesis has verified the feasibility of the proposed FE approaches for the centralized and decentralized W-NCSs, which are depicted by a hierarchical framework for industrial automatic applications.

As possible further work, some following concerns should be further considered. First, considering the model complexity of real applications, the FE design can be extended in the presence of model uncertainties. Second, the transmission jitter, bit errors should be considered for the communication modeling so that the scheduler can be represented by state-space equations with transmission disturbances, and it could improve the system performance from the view of confronting network uncertainty.

Bibliography

[1] S.M.M. Alavi and M. Saif. A QFT-based decentralized design approach for integrated fault detection and control. *IEEE Trans. Contr. Syst. T.*, 20(5):1366–1375, 2012.

[2] S.M.M. Alavi and M. Saif. Fault detection in nonlinear stable systems over lossy networks. *IEEE Trans. Contr. Syst. T.*, 21(6):2129–2142, 2013.

[3] P. Antsaklis and J. Baillieul. Guest editorial special issue on networked control systems. *IEEE Trans. Automat. Contr.*, 49(9):1421–1423, Sep. 2004.

[4] M.A. Balley and C.S. Sims. Decentralized reduced-order filters. *IEEE Trans. Aero. Elec. Syst.*, 26(2):254–262, 1990.

[5] A. Benigni, G. D'Antona, U. Ghisla, A. Monti, and F. Ponci. A decentralized observer for ship power system applications: Implementation and experimental validation. *IEEE Trans. Instrum. Meas.*, 59(2):440–449, 2010.

[6] M. Blanke, M. Kinnaert, J. Lunze, M. Staroswiecki, and J. Schröder. *Diagnosis and Fault-Tolerant Control*. Springer-Verlag New York, Inc., 2006.

[7] A. Bonivento, C. Fischione, and A. Sangiovanni-Vincentelli. SERAN: a protocol for clustered WSNs in industrial control and automation. In *Proc. 6th IEEE Communications Society on Sensor, Mesh and Ad Hoc Communications and Networks*, pages 1–3, 2009.

[8] P. Brooks. Ethernet/IP-industrial protocol. In *Proc. 8th IEEE International Conference on Emerging Technologies and Factory Automation*, volume 2, pages 505–514, 2001.

[9] A. Cervin, J. Eker, B. Bernhardsson, and K. Årzén. Feedback-feedforward scheduling of control tasks. *Real-Time Systems*, 23(1-2): 25–53, 2002.

[10] K. Chavan, R.G. Kumar, M.N. Belur, and A. Karandikar. Robust active queue management for wireless networks. *IEEE Trans. Contr. Syst. T.*, 19(6):1630–1638, 2011.

[11] F. Chaves, M. Abbas-Turki, H. Abou-Kandil, and J.M.T. Romano. Transmission power control for opportunistic QoS provision in wireless networks. *IEEE Trans. Contr. Syst. T.*, 21(2):315–331, 2013.

[12] J. Chen and R. J. Patton. *Robust Model-Based Fault Diagnosis for Dynamic Systems*. Kluwer Academic Publishers, Boston, 1999.

[13] J. Chen, X. Cao, P. Cheng, Y. Xiao, and Y. Sun. Distributed collaborative control for industrial automation with wireless sensor and actuator networks. *IEEE Trans. Ind. Electron.*, 57(12):4219–4230, 2010.

[14] T. Chen, T.B. Schön, H. Ohlsson, and L. Ljung. Decentralized particle filter with arbitrary state decomposition. *IEEE Trans. Signal Proces.*, 59(2):465–478, 2011.

[15] C. I. Chihaia. *Active Fault-Tolerance in Wireless Networked Control Systems*. PhD thesis, University of Duisburg-Essen, 2010.

[16] S.X. Ding. *Model-Based Fault Diagnosis Techniques - Design Schemes, Algorithms, and Tools*. Springer-Verlag, 2nd ed. 2013.

[17] S.X. Ding, P. Zhang, S. Yin, and E.L. Ding. An integrated design framework of fault-tolerant wireless networked control systems for industrial automatic control applications. *IEEE Trans. Ind. Inform.*, 9(1):462 – 471, Feb. 2013.

[18] H. Dong, Z. Wang, and H. Gao. Distributed H_∞ filtering for a class of Markovian jump nonlinear time-delay systems over lossy sensor networks. *IEEE Trans. Ind. Electron.*, 60(10):4665–4672, 2013.

[19] L. Dritsas and A. Tzes. Robust stability bounds for networked controlled systems with unknown, bounded and varying delays. *IET Control Theory A.*, 3(3):270–280, Mar. 2009.

[20] H. Fang, H. Ye, and M. Zhong. Fault diagnosis of networked control systems. *Annual Reviews in Control*, 31:55–68, 2007.

[21] H. Ferdowsi, D.L. Raja, and S. Jagannathan. A decentralized fault detection and prediction scheme for nonlinear interconnected continuous-time systems. In *International Joint Conference on Neural Networks(IJCNN)*, pages 1–7, 2012.

[22] R. Ferrari, T. Parisini, and M. Polycarpou. Distributed fault detection and isolation of large-scale discrete-time nonlinear systems: An adaptive approximation approach. *IEEE Trans. Autom. Contr.*, 57(2):275–290, 2012.

[23] P. M. Frank. Fault diagnosis in dynamic systems using analytical and knowledge-based redundancy - a survey. *Automatica*, 26:459–474, 1990.

[24] P. M. Frank. Analytical and qualitative model-based fault diagnosis - a survey and some new results. *European Journal of control*, 2:6–28, 1996.

[25] P. M. Frank and X. Ding. Survey of robust residual generation and evaluation methods in observer-based fault detection systems. *J. Process Contr.*, 7(6):403–424, 1997.

[26] P. M. Frank and X. Ding. Survey of robust residual generation and evaluation methods in observer-based fault detection systems. *J. Process Cont.*, 7(6):403–424, 1997.

[27] F. J. Furrer. *Industrieautomation mit Ethernet-TCP/IP und Web-Technologie*. Hüthig Verlag, 2003.

[28] B. Gaid, A.S. Cela, and Y. Hamam. Optimal real-time scheduling of control tasks with state feedback resource allocation. *IEEE Trans. Contr. Syst. T.*, 17(2):309–326, Mar. 2009.

[29] M. Gaid, A. Cela, and Y. Hamam. Optimal integrated control and scheduling of systems with communication constraints. In *Proc. 44th IEEE Decision and Control, and 2005 European Control Conference*, pages 854–859, Dec. 2005.

[30] M. Gaid, A. Cela, and Y. Hamam. Optimal integrated control and scheduling of networked control systems with communication constraints: Application to a car suspension system. *IEEE Trans. Contr. Syst. T.*, 14(4):776–787, Jul. 2006.

[31] S. Garg. Partitioning of centralized integrated flight/propulsion control design for decentralized implementation. *IEEE Trans. Contr. Syst. T.*, 1(2):93–100, 1993.

[32] J. Gertler. *Fault Detection and Diagnosis in Engineering Systems*. Marcel Dekker, Inc., 1998.

[33] J. Gertler and R. Monajemy. Generating directional residuals with dynamic parity relations. *Automatica*, 31(4):627–635, 1995.

[34] E. Ghahremani and I. Kamwa. Dynamic state estimation in power system by applying the extended Kalman filter with unknown inputs to phasor measurements. *IEEE Trans. Power Syst.*, 26(4):2556–2566, 2011.

[35] M. Grbovic, W. Li, P. Xu, A.K. Usadi, L. Song, and S. Vucetic. Decentralized fault detection and diagnosis via sparse PCA based decomposition and maximum entropy decision fusion. *J. Process Contr.*, 22(4): 738–750, 2012.

[36] C. Hajiyev and H. Soken. Robust adaptive Kalman filter for estimation of UAV dynamics in the presence of sensor/actuator faults. *Aerosp. Sci. Technol.*, 28(1):376–383, 2013.

[37] H. Han, J. Park, and B. Lee. Analysis of thyristor controlled series compensator dynamics using the state variable approach of a periodic system model. *IEEE Trans. Power Delivery*, 12(4):1744–1750, 1997.

[38] B. Hassibi, A.H. Sayed, and T. Kailath. Linear estimation in Krein spaces. I. Theory. *IEEE Trans. Automat. Contr.*, 41(1):18–33, Jan. 1996.

[39] X. He, Z. Wang, Y. Liu, and D.H. Zhou. Least-squares fault detection and diagnosis for networked sensing systems using a direct state estimation approach. *IEEE Trans. Ind. Inform.*, 9(3):1670–1679, 2013.

[40] X. He, Z. Wang, and D. Zhou. Networked fault detection with random communication delays and packet losses. *Int. J. Syst. Sci.*, 39(11):1045–1054, 2008.

[41] M. Hou and P. C. Mueller. Design of a class of luenberger observers for descriptor systems. *IEEE Transactions on Automatic Control*, 40(1): 133–136, 1995.

[42] D. Huang and S. Nguang. Robust fault estimator design for uncertain networked control systems with random time delays: An LMI approach. *Inform. Sciences*, 180(3):465–480, 2010.

[43] W. Huang, X. Cao, B. Wang, and B.J. Wang. An online scheduling algorithm for reconfigurable tasks based on dynamic planning preemptive

threshold. In *International Conference on Computational Intelligence and Software Engineering*, pages 1–4, Dec. 2009.

[44] M. Hwang, P. Kim, and D. Choi. Least slack time rate first: new scheduling algorithm for multi-processor environment. In *International Conference on Complex, Intelligent and Software Intensive Systems(CISIS)*, pages 806–811, Feb. 2010.

[45] S. Ibaraki, S. Suryanarayanan, and M. Tomizuka. Design of Luenberger state observers using fixed-structure H_∞ optimization and its application to fault detection in lane-keeping control of automated vehicles. *IEEE/ASME Trans. Mechatronics*, 10(1):34–42, 2005.

[46] ISA. *ISA-100.11a-2009 Wireless Systems for Industrial Automation: Process Control and Related Applications*. ISA, 2009.

[47] R. Isermann. *Fault-Diagnosis Systems: An Introduction from Fault Detection to Fault Tolerance*. Springer-Verlag Berlin Heidelberg, 2006.

[48] M. Jonsson and K. Kunert. Towards reliable wireless industrial communication with real-time guarantees. *IEEE Trans. Ind. Inform.*, 5: 429–442, 2009.

[49] J. Lavaei. Decentralized implementation of centralized controllers for interconnected systems. *IEEE Trans. Automat. Contr.*, 57(7):1860–1865, 2012.

[50] J. Lavaei and A.G. Aghdam. Decentralized control design for interconnected systems based on a centralized reference controller. In *Proc. 45th IEEE Conference on Decision and Control*, pages 1189–1195, 2006.

[51] H. Li, Z. Sun, H. Liu, and F. Sun. Stabilisation of networked control systems using delay-dependent control gains. *IET Control Theory A.*, 6 (5):698–706, Mar. 2012.

[52] J. Li and G.Y. Tang. Fault diagnosis for networked control systems with delayed measurements and inputs. *IET Control Theory A.*, 4(6): 1047–1054, 2010.

[53] X. Li and S. Sun. H_∞ control for networked systems with random delays and packet dropouts. *Int. J. Control Autom.*, 10(5):1023–1031, Oct. 2012.

[54] X. Li, X. Wu, Z. Xu, and C. Huang. Fault detection observer design for networked control system with long time-delays and data packet dropout. *J. Syst. Eng. Electro.*, 21(5):877–882, 2010.

[55] C. Lien. Robust observer-based control of systems with state perturbations via lmi approach. *IEEE Trans. Autom. Control*, 49(8):1365–1370, 2004.

[56] T.M. Lim, B.S. Lee, and C.K. Yeo. Quantum-based earliest deadline first scheduling for multiservices. *IEEE Trans. Multimedia*, 9(1):157 –168, Jan. 2007.

[57] B. Liu and Y. Xia. Fault detection and compensation for linear systems over networks with random delays and clock asynchronism. *IEEE Trans. Ind. Electron.*, 58(9):4396–4406, 2011.

[58] B. Liu, Y. Xia, Y. Yang, and M. Fu. Robust fault detection of linear systems over networks with bounded packet loss. *J. Franklin I.*, 349(7): 2480–2499, 2012.

[59] Q. Liu, T. Chai, H. Wang, and S.J. Qin. Data-based hybrid tension estimation and fault diagnosis of cold rolling continuous annealing processes. *IEEE Trans. Neural Networ.*, 22(12):2284–2295, 2011.

[60] X. Lu and O. Ozgiiner. Hierarchical task distribution for decentralized subsystem with centralized output. In *Proc. 43rd IEEE Conference on Decision and Control*, volume 2, pages 1715–1720, 2004.

[61] Y. Lv, H. Ma, M. Fu, and C. Yang. Decentralized filtering a multi-agent system with local parametric couplings based on Kalman filter. In *Proc. 25th Chinese Conference on Control and Decision*, pages 101–106, 2013.

[62] N. Meskin and K. Khorasani. Actuator fault detection and isolation for a network of unmanned vehicles. *IEEE Trans. Autom. Contr.*, 54(4): 835–840, 2009.

[63] T. Meurer. On the extended Luenberger-type observer for semilinear distributed-parameter systems. *IEEE Trans. Automa. Control*, 58(7): 1732–1743, 2013.

[64] F.H. Mohamed, G. Salut, G.S. Madan, and T. Andre. Decentralized reduced-order filters. *IEEE Trans. Autom. Contr.*, 23(2):262–268, 1978.

[65] R. Moraes, F. Vasques, and P. Portugal an J. A. Fonseca. VTP-CSMA: A virtual token passing approach for real-time communication in IEEE 802.11 wireless networks. *IEEE Trans. Ind. Informat.*, 3:215–224, 2007.

[66] P. Pangun, C. Fischione, A. Bonivento, K.H. Johansson, and A. Sangiovanni. Breath: An adaptive protocol for industrial control applications using wireless sensor networks. *IEEE Trans. Mobile Comput.*, 10(6): 821–838, 2011.

[67] A. Paoli. *Fault Detection and Fault Tolerant Control for Distributed Systems: A General Framework*. PhD thesis, University of Bologna, 2004.

[68] P. Pedreiras, P. Gai, L. Almeida, and G.C. Buttazzo. FTT-Ethernet: a flexible real-time communication protocol that supports dynamic QoS management on Ethernet-based systems. *IEEE Trans. Ind. Inform.*, 1 (3):162–172, 2005.

[69] C. Peng, T.C. Yang, and E.G. Tian. Brief paper: Robust fault-tolerant control of networked control systems with stochastic actuator failure. *IET Control Theory A.*, 4(12):3003–3011, 2010.

[70] C. Peng, D. Yue, E. Tian, and Z. Gu. Observer-based fault detection for networked control systems with network quality of services. *Appl. Math. Model.*, 34(6):1653–1661, 2010.

[71] V.V. Prabhu. Stable fault adaptation in distributed control of heterarchical manufacturing job shops. *IEEE Trans. Robotic. and Autom.*, 19 (1):142–149, 2003.

[72] K. Ronasi, V.W.S. Wong, and S. Gopalakrishnan. Distributed scheduling in multihop wireless networks with maxmin fairness provisioning. *IEEE Trans. Wirel. Commun.*, 11(5):1753–1763, May 2012.

[73] K. Salahshoor, M. Mosallaei, and M. Bayat. Centralized and decentralized process and sensor fault monitoring using data fusion based on adaptive extended kalman filter algorithm. *Measurement*, 41(10):1059–1076, 2008.

[74] D. Sauter, S. Li, and C. Aubrun. Robust fault diagnosis of networked control systems. *Int. J. Adapt. Control*, 23:722–736, 2009.

[75] R. Sharma and M. Aldeen. Fault and disturbance reconstruction in nonlinear systems using a network of interconnected sliding mode observers. *IET Control Theory Appl.*, 5(6):751–763, 2011.

[76] B. Shen, S.X. Ding, and Z. Wang. Finite-horizon fault estimation for linear discrete time-varying systems with delayed measurements. *Automatica*, 49(1):293–296, 2013.

[77] C. Steiger, H. Walder, and M. Platzner. Operating systems for reconfigurable embedded platforms: online scheduling of real-time tasks. *IEEE Trans. Comput.*, 53(11):1393–1407, Nov. 2004.

[78] H. Sun, S. Li, and C. Sun. Adaptive fault-tolerant controller design for airbreathing hypersonic vehicle with input saturation. *J. Syst. Eng. Electro.*, 24(3):488–499, 2013.

[79] Z. Tang, P. Zeng, and H. Wang. Analysis and design of real-time and reliable industrial wireless control communication network and protocol. In *Proc. 29th Chinese Control Conference*, pages 4157–4163, 2010.

[80] Y. Tian and G. Li. QoC elastic scheduling for real-time control systems. *Real-Time Systems*, 47:534–561, 2011.

[81] Y. Tian, X. Jiang, D.C. Levy, and A. Agrawala. Local adjustment and global adaptation of control periods for QoC management of control systems. *IEEE Trans. Contr. Syst. T.*, 20(3):846–854, May 2012.

[82] X. Wan, H. Fang, and F. Yang. Fault detection for a class of networked nonlinear systems subject to imperfect measurements. *Int. J. Control Autom.*, 10(2):265–274, 2012.

[83] Y. Wang and D. Infield. Supervisory control and data acquisition data-based non-linear state estimation technique for wind turbine gearbox condition monitoring. *IET Renew. Pow. Gen.*, 7(4):350–358, 2013.

[84] Y. Wang, S.X. Ding, H. Ye, and G. Wang. A new fault detection scheme for networked control systems subject to uncertain time-varying delay. *IEEE Trans. Signal Proces.*, 56(10):5258–5268, 2008.

[85] Z. Wang, B. Shen, H. Shu, and G. Wei. Quantized control for nonlinear stochastic time-delay systems with missing measurements. *IEEE Trans. Autom. Control*, 57(6):1431–1444, Jun. 2012.

[86] A. S. Willsky. A survey of design methods for failure detection in dynamic systems. *Automatica*, 12:601–611, 1976.

[87] Y. Xia, M. Fu, and G. Liu. *Analysis and Synthesis of Networked Control Systems*. Springer-Verlag, 2011.

[88] X. Yan and C. Edwards. Robust decentralized actuator fault detection and estimation for large-scale systems using a sliding mode observer. *Int. J. Control*, 81(4):591–606, 2008.

[89] F. Yang and H. Fang. Control structure design of networked control systems based on maximum allowable delay bounds. *J. Franklin I.*, 346 (6):626–635, Aug. 2009.

[90] F. Yang, Z. Wang, Y.S. Hung, and M. Gani. H_∞ control for networked systems with random communication delays. *IEEE Trans. Autom. Control*, 51(3):511–518, Mar. 2006.

[91] W. Yang and H. Shi. Distributed estimation based on LQG control over homogeneous sensor networks. *Int. J. Control Autom.*, 10(6):1173–1181, 2012.

[92] B. Zhang and H.T. Mouftah. Fast bandwidth-constrained shortest path routing algorithm. *IEE P-Commun.*, 153(5):671–674, Oct. 2006.

[93] H. Zhang, Y. Zhang, and X. Ma. Dimensionless approach to multi-parametric stability analysis of nonlinear time-periodic systems: Theory and its applications to switching converters. *IEEE Trans. Circuits and Systems I: Regular Papers*, 60(2):491–504, 2013.

[94] J. Zhang, A.K. Swain, and S. Nguang. Robust sensor fault estimation scheme for satellite attitude control systems. *J. Franklin I.*, 350(9): 2581–2604, 2013.

[95] K. Zhang, B. Jiang, and M. Staroswiecki. Dynamic output feedback-fault tolerant controller design for Takagi-Sugeno fuzzy systems with actuator faults. *IEEE Trans. Fuzzy Syst.*, 18(1):194–201, 2010.

[96] K. Zhang, B. Jiang, and P. Shi. Fault estimation observer design for discrete-time Takagi-Sugeno fuzzy systems based on piecewise Lyapunov functions. *IEEE Trans. Fuzzy Syst.*, 20(1):192–200, 2012.

[97] X. Zhang, M.M. Polycarpou, and T. Parisini. Decentralized fault detection in a class of large-scale nonlinear uncertain systems. In *Proc. 48th IEEE Conference on Decision and Control, held jointly with 28th Chinese Control Conference*, pages 6988–6993, 2009.

[98] Y.M. Zhang, A. Chamseddine, C.A. Rabbath, B.W. Gordon, C.Y. Su, S. Rakheja, C. Fulford, J. Apkarian, and P. Gosselin. Development of advanced FDD and FTC techniques with application to an unmanned quadrotor helicopter testbed. *J. Franklin I.*, 350(9):2396–2422, 2013.